

VITA-SALUTE SAN RAFFAELE UNIVERSITY

International PhD Course in Molecular Medicine
Curriculum in Basic and Applied Immunology and Oncology

**T_{h1}-LIKE HBV-SPECIFIC CD4⁺T CELLS
ARE ABLE TO REVERT THE CD8⁺T
CELL DYSFUNCTION INDUCED BY
HEPATOCELLULAR PRIMING**

Dos: Prof. Matteo Iannacone



Second Supervisor: Dott. Mauro Gaya

PhD Thesis of Valentina Venzin

Registration number 015483

XXXV PhD Cycle

SSD BIO/13

Academic Year 2021/2022

CONSULTAZIONE TESI DI DOTTORATO DI RICERCA

I, the undersigned Valentina Venzin

Registration number 015483

Born in Varese (VA)

On 27/09/1994

Author of the PhD Thesis titled:

“Th1-like HBV-specific CD4⁺T cells are able to revert the CD8⁺T cell dysfunction induced by hepatocellular priming”


DO NOT AUTHORIZE the public release of the thesis for 12 months from the PhD thesis date, specifically from 28/10/2022 to 28/10/2023.

Because:

- The whole project or parts of it may be the subject of a patent application;
- Parts of the thesis have been or are being submitted to a publisher or are in the press;
- The thesis project is financed by external bodies that have rights over it and its publication.

Reproduction of the thesis in whole or in part is forbidden.

Date 26/12/2022

Signature 

DECLARATION

This thesis has been composed by myself and has not been used in any previous application for a degree. Throughout the text I used 'We' interchangeably. This thesis has been written according to the editing guidelines approved by the University. Permission to use images and other material covered by copyright has been sought and obtained.

All the results presented here were obtained by myself, except for:

- 1) *Identification and validation of transgenic Env126 TCR were performed by BioNTech, Mainz, Germany*
- 2) *TCR HB_{S126-138} sequences cloning was performed by Dr. Elisa Bono and Dr. Leonardo Giustini, San Raffaele Scientific Institute, Milan, Italy*
- 3) *Transgenic injection (Pronuclear Injection) was performed by Dr. Lorenza Ronfani in the Core Facility for Conditional Mutagenesis (CFCM Facility), San Raffaele Scientific Institute, Milan, Italy*
- 4) *Serum alanine aminotransferase (sALT) activity was measured by Dr. Raso Michele and Dr. Micol Ravà, Mouse Clinic, San Raffaele Scientific Institute, Milan, Italy.*
- 5) *Liver tissues for immunohistochemistry were processed by Dr. Amleto Fiocchi, Animal Histopathology Facility, San Raffaele Scientific Institute, Milan, Italy.*

All sources of information are acknowledged by means of reference.

ABSTRACT

About 260 million people are chronically infected with hepatitis B virus (HBV), resulting in >700,000 deaths per year from cirrhosis and hepatocellular carcinoma. Despite the availability of prophylactic vaccination, therapeutic approaches for persistent infection are still limited. The immune mechanisms underlying Hepatitis B Virus (HBV) pathogenesis are still not delineated, and while the function and dysfunction of CD8⁺T cells has been deeply investigated, the role of HBV-specific (HBV-sp) CD4⁺T cells has been neglected.

With the aim of studying the role of CD4⁺T cells in the context of HBV pathogenesis, we have generated and tested an HBV-sp CD4⁺TCR transgenic mouse model (Env126), in which all CD4⁺T cells recognize an MHC class II-restricted epitope of the HBV envelope protein.

Here, we used a mouse model of HBV pathogenesis, where adoptively transferred HBV-sp naive CD8⁺T cells recognizing hepatocellular antigens are driven into a state of immune dysfunction. We found that pre-activated Th1-like Env126 CD4⁺T_E cells can revert CD8⁺T cells dysfunctionality after adoptive co-transfer in HBV-replicating mice. With the help of Env126 CD4⁺T_E cells, HBV-sp CD8⁺T cells produce higher levels of IFN γ , TNF α and GrzmB, increase their proliferation capacity and display higher expression levels of activation markers as well as reduction in co-inhibitory molecules. Moreover, we observed that Kupffer cells can ameliorate their cross-presenting capacity and upregulate MHC-I machinery after adoptive transfer of Env126 CD4⁺T_E cells in HBV-Tg mice. Indeed, we confirmed CD4⁺-CD8⁺T cell cooperation is abolished if APCs are not able to interact with Env126 CD4⁺T_E cells in HBV-Tg mice.

These preliminary results show that HBV-sp CD4⁺T cells might have a critical role in defining the course of HBV pathogenesis. As main cooperators of CD8⁺T cells antiviral immunity, HBV-sp CD4⁺T cells spatiotemporal dynamics must be elucidated, helping the design of novel immunotherapeutic strategies aimed at treating HBV infection and its life-threatening complications.

Ai miei genitori e ai miei amici,

*Delle persone incredibilmente speciali
Che sono riuscite a tenermi in piedi
Proprio quando pensavo di non farcela.*

TABLE OF CONTENTS

1.	ACRONYMS AND ABBREVIATIONS	3
2.	LIST OF FIGURES AND TABLES	5
3.	INTRODUCTION	7
3.1.	<i>The liver as an immunological organ</i>	7
3.1.1.	The liver anatomy	7
3.1.2.	Immunological features of the liver.....	10
3.1.3.	The hepatic immune system	12
3.1.4.	The liver immunotolerance.....	14
3.2.	<i>Hepatitis B Virus Infection</i>	16
3.2.1.	Generalities	16
3.2.2.	Structure and replication cycle of HBV	16
3.2.3.	HBV Pathogenesis	20
3.2.4.	HBV Serology	22
3.2.5.	Epidemiology of HBV	23
3.2.6.	Accessible treatments for CHB.....	25
3.2.7.	Available models for the experimental study of HBV pathogenesis..	27
3.3.	<i>T-cell immune responses during HBV infection</i>	29
3.3.1.	Front line offence: CD8 ⁺ T cells in HBV	29
3.3.2.	Back-line defence: CD4 ⁺ T cell responses in HBV.....	33
3.3.3.	CD4 ⁺ -CD8 ⁺ T cell cooperation in HBV infection and beyond.....	35
4.	AIM OF THE WORK	38
5.	RESULTS	39

5.1.	<i>A transgenic HBV-specific TCR mouse model to study antigen-specific CD4⁺T cells in HBV pathogenesis</i>	39
5.1.1.	Generation of Env126 transgenic mouse model.....	39
5.1.2.	Characterization of Env126 transgenic mouse model	42
5.1.3.	Functional testing of Env126 transgenic mouse model.....	46
5.1.4.	Naïve Env126 CD4 ⁺ T response in HBV-Tg mice.....	50
5.2.	<i>Exploring CD8⁺-CD4⁺ T cell cooperation in HBV pathogenesis</i>	56
5.2.1.	Adoptive transfer of naïve Env126 CD4 ⁺ T cells do not impact on CD8 ⁺ T cell response in HBV-Tg mice.....	57
5.2.2.	Pre- <i>in vitro</i> activated Env126 CD4 ⁺ T cells are not able to sustain CD8 ⁺ T cell response in HBV-Tg mice	60
5.2.3.	Generation of T _{h1} -like Env126 CD4 ⁺ T cells.....	64
5.2.4.	Adoptive transfer of T _{h1} -like Env126 CD4 ⁺ T cells improves Env28 CD8 ⁺ T cell proliferation and effector differentiation in HBV-Tg mice.....	67
5.2.5.	T _{h1} -like Env126 CD4 ⁺ T cells help is non-cognate specific	76
5.2.6.	Adoptive transfer of T _{h1} -like Env126 CD4 ⁺ T cells improves the cross-presentation capacity of Kupffer cells in HBV-Tg mice	80
5.2.7.	Env126 CD4 ⁺ T cells help to HBV-sp CD8 ⁺ T cells is mediated by antigen-presenting cells	85
6.	DISCUSSION	90
7.	MATERIALS AND METHODS	103
8.	REFERENCES	113

1. ACRONYMS AND ABBREVIATIONS

Ab Antibody; 27
Ag - Antigen; 44
AHB Acute Hepatitis B; 22
ALT Alanine Transaminase; 23
APC Antigen Presenting Cell; 12
APPs Acute-Phase Proteins; 14
ASO Antisense Oligonucleotides; 27
AST Aspartate Aminotransferase; 23
Bcl-6 B-Cell Lymphoma 6; 53
Ca Calcium; 48
cccDNA Covalently closed circular DNA; 20
CD Cluster Differentiation Antigen; 15
CHB Chronic Hepatitis B; 26
Cor93 Residues 93–100 in the HBV core protein (MGLKFRQL); 78
Co-t Co-transfer; 80
CTL Cytolytic T cell; 66
CTV Cell Trace Violet; 50
CXCR C-X-C motif Receptor; 67
DC Dendritic Cells; 14
DNA Deoxyribonucleic Acid; 27
EDTA EthylenDiaminoTetracetyc Acid; 112
Env28 Residues 28–39 of HBsAg (IPQSLDSWWTSL); 59
ER Endoplasmic Reticulum; 20
FACS Fluorescent Activated Cell Sorter; 112
FBS Fetal Bovine Serum; 112
Foxp3 Forkhead box P3; 53
GrzmB Granzyme B; 64
H&E Haematoxylin And Eosin; 61
HBcAg HBV-Core Antigen; 106
HBeAg HBV "e" Antigen; 107
HBsAg HBV-Surface Antigen; 19
HBSS Hanks' Balanced Salt Solution; 108
HBV Hepatitis B Virus; 18
HBV-sp HBV-specific; 22
HCC Hepatocellular Carcinoma; 18
HCV Hepatitis C Virus; 9
HLA-DR Human Leukocyte Antigen – DR isotype; 34
HSC Hepatic Stellate Cells; 14

IFN Interferon; 35
IHL Intra-hepatic leucocytes; 108
IHL Intra-Hepatic Leucocytes; 14
IL Interleukin; 58
ILC Innate Lymphoid Cell; 14
KC Kupffer Cells; 14
LNPC Liver Non Parenchymal Cell; 109
LSECs Liver Sinusoidal Endothelial Cells; 11
MFI Mean Fluorescent Intensity; 45
MHC Major Histocompatibility Complex; 15
NF- κ B Nuclear Factor Kappa-light-chain-enhancer of activated B cells; 48
NK Natural Killer; 14
NKT Natural Killer T cell; 14
NTCP Sodium taurocholate co-transporting polypeptide; 20
NUCs Nucleotide analog; 27
ORF Open Reading Frame; 20
PBS Phosphate Buffered Saline; 112
PD-1 Programmed Cell Death 1; 71
PDL1 Programmed Death Ligand-1; 27
peg-IFN Pegylated Interferon Alpha; 27
pgRNA pre-genomic RNA; 20
PKC Protein Kinase C; 48
PPR Pattern Recognition Receptor; 22
Rag Recombination-Activating Gene; 75
RBC Red Blood Cell; 109
rcDNA Relaxed circular DNA; 18
RNA Ribonucleic Acid; 27
sALT serum alanine aminotransferase; 24
siRNAs Small-Interfering RNAs; 27
SLOs Secondary Lymphoid Organs; 30
T-bet T-Box Transcription factor TBX21; 53
T_E T effector cell; 73
Tet Tetramer; 44
Th1 T-helper 1; 66
T_N T naive cell; 69
TNF Tumor Necrosis Factor; 68
TNF α Tumor Necrosis Factor Alpha; 48
VSV Vesicular Stomatitis Virus; 66
WT Wild Type; 42

2. LIST OF FIGURES AND TABLES

Figure 1 • Anatomy of murine and human liver compared.	8
Figure 2 • Liver anatomy.	10
Figure 3 • The liver parenchyma.	11
Figure 4 • Viral particle and genomic structure of HBV.	17
Figure 5 • The life cycle of Hepatitis B Virus.	19
Figure 6 • HBV worldwide prevalence.	24
Figure 7 • How CD8⁺T cells keep the liver under surveillance.	31
Figure 8 • CD4⁺T cells in CHB patients.	34
Figure 9 • CD4⁺T cell cooperation with CD8⁺T cells: the three-cell types interaction model.	36
Figure 10 • Identification and validation of functional HBVs epitope.	40
Figure 11 • Constructs design and generation process of Env126 mice.	41
Figure 12 • HBs-sp CD4⁺T cells in Env126 mice.	43
Figure 13 • Env126 Rag1^{-/-} lines generation.	45
Figure 14 • Env126 CD4⁺T cells get activated <i>in vitro</i> after cognate peptide stimulation.	47
Figure 15 • Env126 CD4⁺T cells proliferate and get activated upon HBsAg recognition <i>in vitro</i>.	49
Figure 16 • Naïve Env126 CD4⁺T cells slightly expand, but do not get activated, when transferred into HBV-Tg mice.	52
Figure 17 • Naïve Env126 CD4⁺T cells phenotype is comparable in the spleen of WT and HBV-Tg transferred mice.	54
Figure 18 • Adoptive transfer of naive Env126 CD4⁺T cells do not ameliorate Env28 CD8⁺T cell effector functions in HBV-Tg mice.	58
Figure 19 • Pre-<i>in vitro</i> activation of Env126 CD4⁺T cells.	61
Figure 20 • Adoptive transfer of pre-<i>in vitro</i> activated Env126 CD4⁺T_A do not impact on Env28 CD8⁺T cell responses in HBV-Tg mice.	63
Figure 21 • <i>In vivo</i> differentiation of Env126 CD4⁺T transgenic T cells into T_{h1}-like effector CD4⁺T cells.	65
Figure 22 • Adoptive transfer of T_{h1}-like effector Env126 CD4⁺T cells improves Env28 CD8⁺T cell effector function.	68
Figure 23 • Adoptive transfer of T_{h1}-like effector Env126 CD4⁺T cells improves Env28 CD8⁺T cell proliferation.	70
Figure 24 • Env126 preserve their T_{h1}-like effector phenotype after co-transfer with Env128 in HBV-Tg mice.	72
Figure 25 • Env28 CD8⁺T cells form extravascular clusters when co-transferred with T_{h1}-like CD4⁺T_E Env126.	74

Figure 26 • Adoptive transfer of T_{h1}-like effector Env126 CD4⁺T cells improves Cor93 CD8⁺T cell-mediated liver immunopathology.	77
Figure 27 • Adoptive transfer of T_{h1}-like effector Env126 CD4⁺T cells improves Cor93 CD8⁺T cell effector function.	79
Figure 28 • KCs, but not DCs, ameliorate their cross-presenting capacity after adoptive transfer of Env126 T cells in the liver HBV-Tg mice.	81
Figure 29 • DCs do not ameliorate cross-presenting capacity after adoptive transfer of Env126 T cells in the liver of HBV-Tg mice.	83
Figure 30 • Env126 and Env28 require APCs to cooperate.	86
Figure 31 • Env126 T cells get activate and expand only after interacting with APCs in HBV-Tg mice.	88
Table 1 • Used Antibodies for FACS	109

3. INTRODUCTION

3.1. The liver as an immunological organ

One of the major causes of deaths worldwide is liver disease. Indeed, the sum of annual deceases caused by only the most four common liver diseases such as Hepatitis C Virus (HCV) and Hepatitis B Virus (HBV) infections, Malaria and alcohol-related diseases with their complications, reaches almost 3 million per year (www.who.int/news-room/fact-sheets, Ficht & Iannacone, 2020). The high mortality rate that characterizes liver diseases is direct consequence of the functional, metabolic, and physiological relevance that this peculiar organ holds inside the human body. Indeed, the liver is responsible for more than 500 vital functions: here the energy is stored and converted, microbes and chemicals coming from the gut are detoxicated and neutralized, and the blood is maintained at its homeostasis (Ben-Moshe & Itzkovitz, 2019). In addition to its essential physiological importance, the liver also possesses numerous peculiar characteristics that allow it to be considered also an “immunological organ” (Racanelli & Reherrmann, 2006). The anatomy of this organ shapes the innate and adaptive immune responses in a unique manner and establish one of the most tolerant environments found in the human body; on top of this the liver is also, under physiological conditions, significantly enriched in immune cells (Lucas *et al*, 2017). These abovementioned aspects, that will be in-depth discussed in the following paragraphs, make the hepatic development and resolution of infectious, inflammatory, and neoplastic diseases not always canonical, keeping the study of adaptive immune responses inside the liver a field of significant interest.

3.1.1. The liver anatomy

The structural organization of the liver has fundamental implications for its immune functions and for this reason will be summarily described in this paragraph, to fully understand the uniqueness of this fascinating organ. For our dissertation purposes, it is

important to mention the differences that stand between mouse (**Fig. 1A**) and human (**Fig. 1B**) livers.

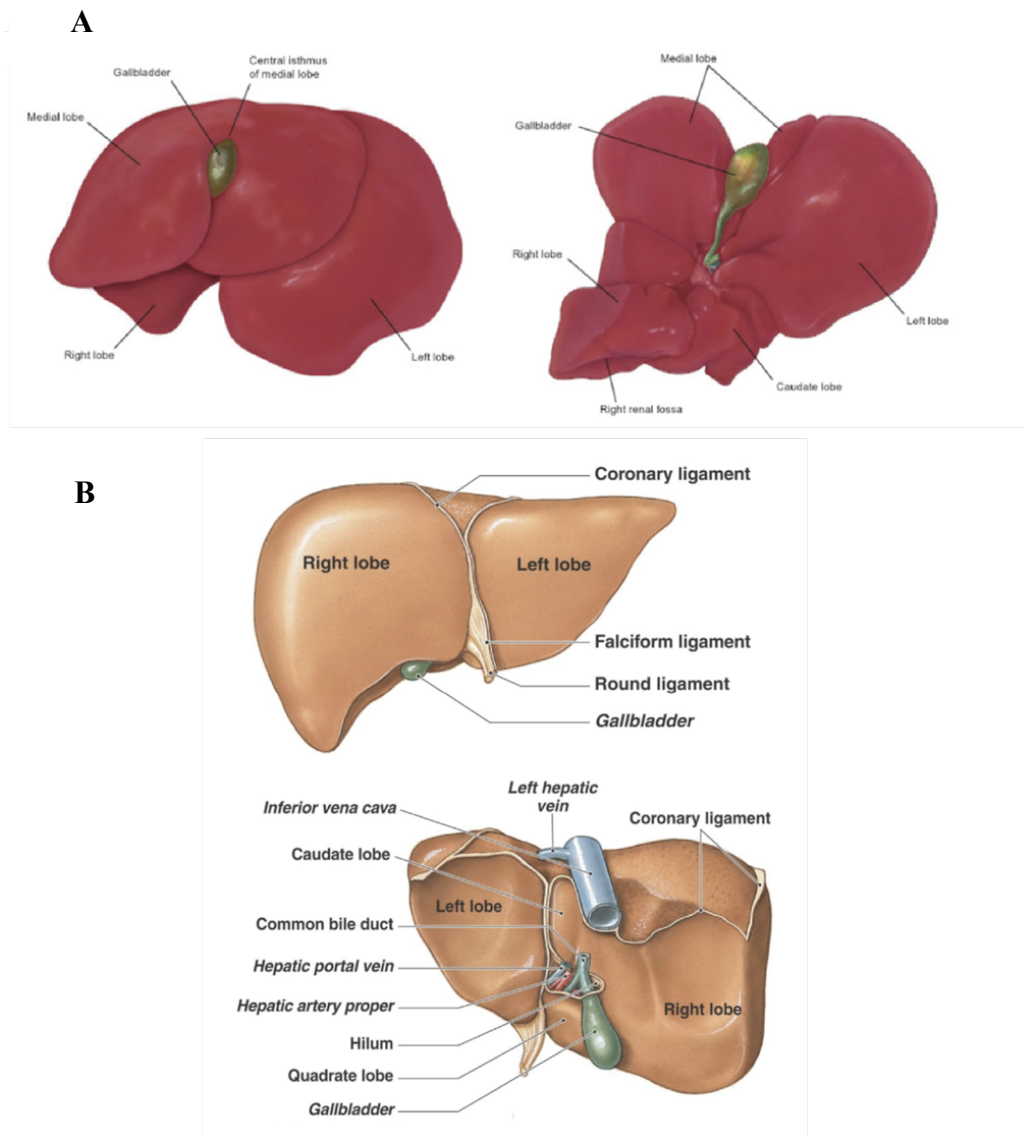


Figure 1 • Anatomy of murine and human liver compared.

(A) Mouse liver is divided into four lobes: left, right (hemisected), medial and caudate. (B) Human liver is divided into four lobes: right, left, caudate and quadrate. From Treuting P. M. & Dintzis, S. M. Comparative anatomy and histology: a mouse and human atlas, 2012, License Number 5415890239127).

From an anatomical point of view, few differences can be identified between the two organisms. The greatest differences are attributable to macroscopic aspects: the human liver occupies the right upper quadrant of the abdominal cavity while instead the murine liver occupies the whole subdiaphragmatic space (**Fig. 1A, B**). Murine liver is also not supported by surface ligaments, that are instead present in the human liver (Kruepunga *et al*, 2019). Despite these divergent characteristics, both human and murine livers do share their microscopical organization and maintain their fundamental and functional unit: the hepatic lobule (**Fig. 2B**).

The hepatic lobule has a hexagonal shape and consists of a set of hepatocytes flanked by portal tracts, which comprise an arteriole, a branch of the portal vein and a tributary of the bile duct; the lobule centre is occupied by the central vein (**Fig. 2B**). This peculiar organization gives to the liver a unique angioarchitecture: it stands at hemodynamic confluence (**Fig. 2A**) (Gershwin, M. Eric, John M. Vierling, 2007). Via the portal vein the nutrient rich blood arrives from the gut: this provides most of the liver blood supply. Instead, the oxygen-rich blood comes to the organ through the hepatic artery and then it gets mixed inside the sinusoids with venous blood. Sinusoids are liver-specific capillary composed by liver sinusoidal endothelial cells (LSECs) and lack a complete basal membrane (**Fig. 3**). Sinusoids contain numerous fenestrae, which give them a peculiar anatomy that permits the exchange of molecules between blood and hepatocytes in a very efficient way that facilitates the basic liver functions. The blood flows then from the portal tract towards the central vein, a path that allow blood plasma to pass from the sinusoids into a sub-endothelial space – called “space of Disse” – where the lymph is collected and sent to the draining lymph nodes (**Fig. 3**) (Ben-Moshe & Itzkovitz, 2019; Ficht & Iannacone, 2020).

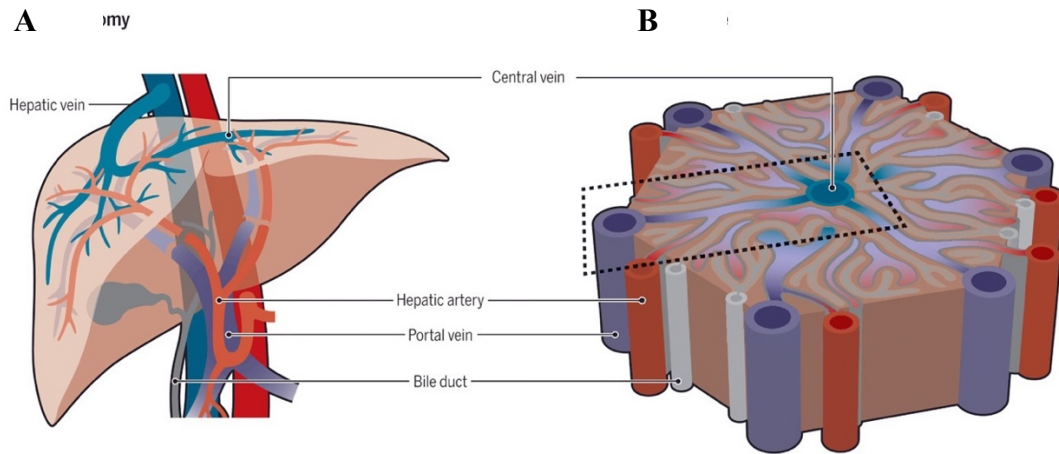


Figure 2 • **Liver anatomy.**

(A) Macro-anatomy of the liver organ. Oxygenated blood enters the liver via the hepatic artery and nutrient-rich blood enter via the portal vein, the blood exits through the hepatic vein. (B) Schematic representations of the liver lobule: each liver lobule has hexagonal shape and is delimited by portal tracts (composed of bile ducts, lymphatics, hepatic artery, and portal veins). The blood flows from the portal tracts towards the central veins by which it exits the organ. From X. Ficht, M. Iannacone, Immune surveillance of the liver by T cells. *Sci. Immunol.* 5, eaba2351 (2020). (Reprinted with permission from AAAS).

3.1.2. Immunological features of the liver

Almost 10^8 peripheral lymphocytes pass through the liver in 24 hours, brought by the great amount of blood that the liver constantly receive from the circulation (Gershwin, M. Eric, John M. Vierling, 2007; Racanelli & Rehermann, 2006).

Among the peculiar immunological characteristics of the liver, one of the most important is the fact that its anatomy and microcirculatory system are able to facilitate the encounter between resident antigen presenting cells (APCs) and blood-borne lymphocytes. Indeed, the arrival and arrest of lymphocytes onto sinusoids is facilitated by the small diameter of these vessels, in which a minimal increase in systemic venous pressure and perturbation of the blood flow result in stasis that can allow the contact between lymphocytes and APCs, facilitating lymphocytes extravasation (Guidotti *et al*, 2015; Piergiovanni *et al*, 2017). The liver favours the encounter between APCs and lymphocytes not only because of its peculiar blood circulation, but also thanks to the

presence of sinusoids fenestrations and the space of Disse (Fig. 3). Lymphocytes, with their 8µm of diameter, just fit the size of the sinusoids and, therefore, the interactions with adhesion molecules and receptors on the surface of sinusoids lining cells are favoured. These interactions are *per se* peculiar: thanks to LSECs arrangement and characteristics, lymphocytes are allowed to access the space of Disse by “touching” the underlying hepatocytes protracting cytoplasmic extensions. (Fig. 3). (Ficht & Iannacone, 2020b; Guidotti *et al*, 2015).

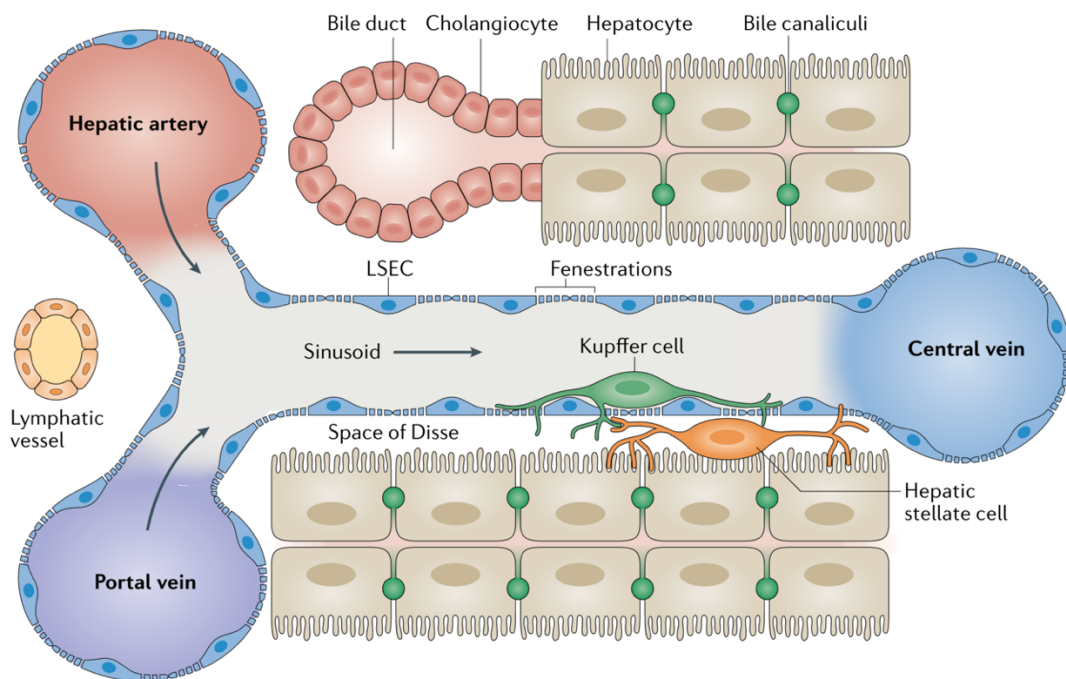


Figure 3 • The liver parenchyma.

Schematic representation of parenchymal organization within the liver. Hepatocytes are arranged in chords surrounded by bile ducts where the bile is collected in the portal tracts; LSECs line all vessels and constitute the specialized liver endothelium which separate hepatocytes from blood flow. HSCs are located within the space of Disse, near to DCs and KCs lined along the endothelium. Arrows indicate the direction of blood flow. (From Iannacone M and Guidotti L, 2022, Licence Number 5415880833783).

Inside liver parenchyma, also hepatocytes play relevant immune functions. Indeed, they constitutively produce and secrete several proteins, relevant for both innate and adaptive branches of the immune system, and of which the production is enhanced during bacterial or viral infections (Zhou *et al*, 2016). Additionally, hepatocytes can receive pathogenic and inflammatory signals and actively respond to them by secreting innate immunity proteins directly into the circulation: these proteins are called acute-phase proteins (APPs) and can directly kill pathogens or instruct the immune system to microbe clearance. Besides hepatocytes, other parenchymal and non-parenchymal cells as cholangiocytes, hepatic stellate cells (HSC) and LSECs can sense and be triggered by immune cells and responses. Unique to the liver is that not only APCs but also LSECs, HSCs and hepatocytes can present antigens to lymphocytes. Of note, all the mentioned cell types are liver-resident cells and are not professionally equipped to migrate and enter the draining lymph nodes (Knolle, 2014).

Finally, the liver is fully populated by a heterogeneous population of both lymphoid and myeloid immune cells, about which will be discussed in the following paragraphs.

3.1.3. The hepatic immune system

The liver houses a large and heterogeneous population of immune cells.

Lymphocytes are distributed throughout the liver parenchyma and around portal tracts (Crispe & Mehal, 1996). Intrahepatic leucocytes (IHL) comprise both conventional and unconventional populations of innate cells (NKT and NK cells) and adaptive immune system cells (CD8⁺ and CD4⁺ T cells and B cells). Other unconventional T cells are present in the liver: ILCs, NK, NKT and $\gamma\delta$ T cells.

The liver also contains different types of resident APCs: Kupffer cells (KCs), LSECs and dendritic cells (DCs). All these types of APCs can capture and present antigens that are passing through the liver sinusoids or that are released by dying hepatocytes (Crispe, 2011). KCs are the most abundant macrophage resident population in total human body and have fundamental functions in the liver. KCs not only scavenge for microbial and

non-pathogenic antigens that arrive in liver from the gut, but they also are equipped for sensing signals of tissue disturbance. Indeed, they keep under control the liver tissue integrity and represent important first actors in initiating or suppressing immune responses (Krenkel & Tacke, 2017; Crispe, 2011). KCs origin from the foetal liver: they stem from erythromyeloid progenitors, and their maintenance mostly depend on local self-renewal (Gomez Perdiguero *et al*, 2015); evidence that KCs can also differentiate from bone-marrow derived monocytes has been also brought up (Scott *et al*, 2016). These cells are mobile, possess phagocytic capacity and express MHC and costimulatory molecules, which render them potential efficient APCs; they also can protrude cell portions into the space of Disse where they are able to contact hepatic stellate cells (HSCs) and hepatocytes. However, their involvement in liver tolerance maintenance and immunosuppression has been already shown (You *et al*, 2008).

Among DCs, in the liver, both plasmacytoid DCs (pDCs) and classical myeloid DCs (mDCs) can be found. Both are endowed with antigen presentation capacity but have been proved to be poor APCs if compared with spleen resident DCs (de Creus *et al*, 2005). Hepatic DCs can migrate from liver parenchyma to portal tracts (Kudo *et al*, 1997) where they are able to interact with T cells, creating a potential priming site of T lymphocytes.

Liver LSECs have also been identified as potential APCs in the liver. Indeed, they were shown to express molecules related to antigen-uptake (mannose and scavenger receptors) (Steffan *et al*, 1986), antigen presentation (MHC machineries) and co-stimulation molecules (CD80, CD86, CD40) (Knolle *et al*, 1999; Lohse *et al*, 1996). Despite their antigen-presentation equipment, T-cell priming by LSECs results in T-cell tolerance (Lohse *et al*, 1996; Knolle *et al*, 1999).

3.1.4. The liver immunotolerance

As anticipated, the liver is a site of immune tolerance.

First demonstration of liver immunotolerance dates back to the 60s, when it was shown that pigs could survive allogeneic liver grafts even in the case of MHC mismatch and with no need of immunosuppression (Calne RY, 1969). Later, confirmations of this phenomenon in other animal species have also been reported (Volker Benseler, 2007; Shigwang Qian *et al*).

All the mechanisms underlying liver-mediated tolerance are still not deeply determined but it is commonly accepted that the combination of the anatomical, biological, molecular, and cellular hepatic characteristics leads to the establishment of a tolerogenic environment (Crispe, 2003; Tiegs & Lohse, 2010). Among the factors that determine this effect, some are worth to be mentioned: i) From the gut, the liver receives blood loaded with pathogens, microbial products, dietary antigens, and toxins, inevitably imposing constraints on immune responses originating in the liver. ii) Vascular organization of the liver facilitates tolerance induction. iii) Resident APCs in the liver are biased towards tolerance. iv) Hepatocytes can present antigens to T cells in the liver.

- i) As previously mentioned, the liver stands between oxygenated blood coming from the arterial system and portal venous blood coming from the intestine. The blood flowing from the gastrointestinal system is inevitably full of both food-derived antigens and bacterial antigens of the intestinal flora. It is clear then, that the possibility of immune activation is higher in the liver than in every other organ. Despite being harmless, food-derived antigens require the generation of tolerance to avoid a constitutive inflammatory state in the liver. Among intestine-derived antigens, as an example, LPS was already shown not able to initiate any kind of immune reaction in the liver (Knolle *et al*, 1995).
- ii) The fenestrae of the sinusoidal endothelium and the absence of a discrete basal membrane, render the sinusoids completely different from every other vascular bed in the body. Indeed, this organization permits the diffusion of metabolites and antigens forward and back from the blood to hepatocytes. This

structure therefore facilitates the easy encounter of naïve or activated T cells with their antigen during their transitions inside sinusoids, directly onto hepatocytes. Since antigen priming of resting naïve T cell is not usually possible in most body tissues, this clearly represents a unique characteristic of liver immunity.

- iii) Rare of the liver is that not only conventional DCs are able to perform antigen-presentation, but also LSECs, KCs and HSC are able to exert the same function. In order to avoid the continuous activation of the adaptive immune system against harmless antigens, antigen-presentation processes that occur in the liver, often lead to T-cell tolerance rather than immune activation. Diverse observations have proved this: DCs rather produce IL-10 than Th-1 cytokines and favour the generation of regulatory T cells (Bamboato *et al*, 2009; Goddard *et al*); KCs contribute to liver tolerance via the production of IL-10 in various conditions (You *et al*, 2008; Knolle *et al*, 1995) and also have been found relevant in liver-mediated tolerance to allogenic grafts (Callery MP *et al*, 1989); LSECs have been found to not being able to properly interact with T cells, rather inducing tolerance during antigen presentation to both CD4⁺ and CD8⁺ T cells (Knolle *et al*, 1999; Limmer *et al*, 2000).
- iv) Hepatocytes are the most abundant parenchymal cells inside the liver. Despite mainly performing metabolic functions, they were proved to be able to act also as APCs in the liver. Indeed, thanks to the absence of a fully formed basal membrane and the lack of tight junctions between LSECs, hepatocytes are able to get in direct contact with circulating T cells (Guidotti *et al*, 2015; Warren *et al*, 2006). Despite the expression of MHC-I and MHC-II during inflammatory processes (Herkel *et al*, 2003), hepatocytes do not express co-stimulatory surface proteins (Lee *et al*, 1999). On the contrary, they are equipped with negative co-stimulatory molecule (Mühlbauer *et al*, 2006), therefore participating in the establishment of a tolerogenic environment in the liver (Holz *et al*, 2010).

The liver immunosuppressive environment can explain the reason why dangerous human pathogens can insinuate in the liver and take advantage of its tolerant habitat

to subvert and muddle immunity responses, eventually establishing persistent infections. Hepatitis B Virus is one of them and will be discussed in the next sections.

3.2. Hepatitis B Virus Infection

3.2.1. Generalities

Hepatitis B is a viral infection caused by Hepatitis B Virus (HBV): it affects the liver and cause both acute and chronic diseases. The WHO estimates that about 1.5 million of people is infected with HBV each year and that 300 million people worldwide were living with chronic HBV infection in 2019. Of these, approximately 900 000 died from its complications: liver failure, cirrhosis, and hepatocellular carcinoma (HCC). Indeed, HBV infection is the one of the most common causes of not only liver disease, but especially liver cancer. Even if not always perceived in developed countries, HBV still represents a major global health problem. Although the existence of a 98% efficient prophylactic vaccination that can prevent the chronic infection, the available therapeutic approaches for the treatment of persistent HBV infection are still very limited and mostly fail to eliminate the virus, mainly due to an incomplete knowledge about all the immune mechanisms underlying HBV pathogenesis.

3.2.2. Structure and replication cycle of HBV

HBV is part of the species of *Orthohepadnavirus* genus and belongs to the *Hepadnaviridae* family (Knipe & Howley, 2013). Ten main genotypes of the virus have been so far identified (A-J) among different regions in the world and has been established by phylogenetic analyses that they differ from each other by ~8% at the nucleotide level. The mature virus carries a partial relaxed double-stranded circular DNA of 3.2 kb in size

(rcDNA) enclosed in an icosahedral nucleocapsid of 42 nm in diameter (**Fig. 4A**) (Venkatakrishnan & Zlotnick, 2016).

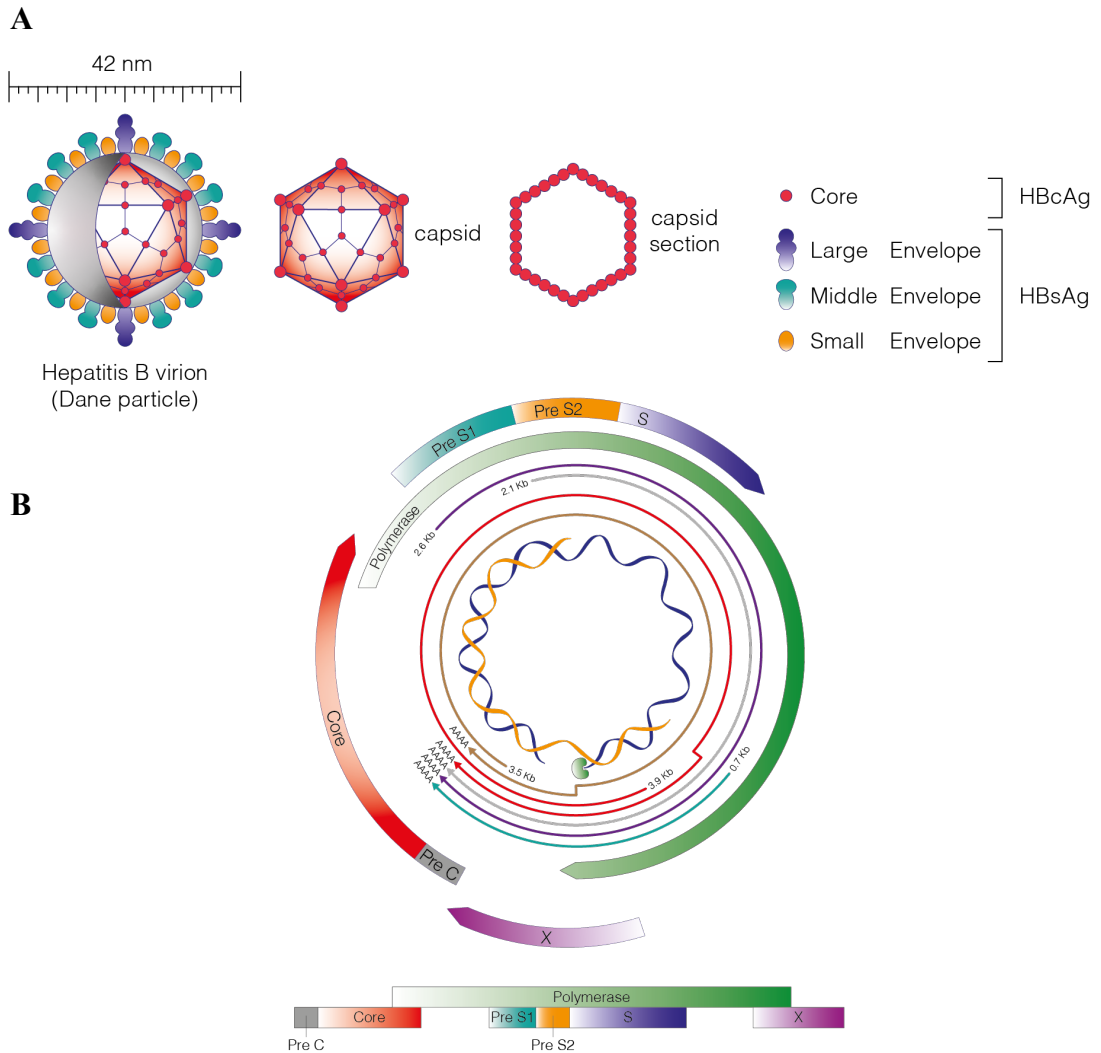


Figure 4 • Viral particle and genomic structure of HBV.

(A) Structural representation of HBV viral particle: HBV virions are ~42nm in diameter, composed by an envelope that contains three different viral genome products called large, middle and small envelope proteins all expressing the determinant of HBsAg. Inside the envelope, HBV possesses a nucleocapsid particle composed by HBcAg homodimers arranged in an icosahedral structure. (B) Outer colour lines represent the translated HBV proteins as a result of the genome translations. Inside, the helixes indicate the rcDNA of HBV and the thin lines depict all the overlapping RNAs produced by HBV genome translation. (From Iannacone M and Guidotti L, 2022, Licence Number 5415880996002)

The HBV double stranded DNA encodes for 7 proteins, has gaps in both strands and carries a reverse transcriptase covalently bound to the 5' end of one strand (**Fig. 4B**). The genome is organized in a positive DNA strand, with variable length in base, and a negative DNA strand which is instead completely circular and forms the outer circle. The genome carries four overlapping genes that comprehend: P for a translating polymerase, PreS1/PreS/S encoding for HBV surface antigen (HBsAg), PreC/C that encode for the core protein of HBV (HBcAg) and X for the HBx protein (**Fig. 4B**). The open reading frames (ORFs) of C and S genes carry extensions at their 5' ends and are called pre-C and pre-S. The region of the pre-S gene in turn divided into two different domains pre-S1 and pre-S2. The translation of the S-ORF thereby results in the production of three different proteins: large (L), medium (M) and small (S) protein of HBV surface protein (**Fig. 4A**). On the other hand, the translation of the pre-C ORF gives rise to the production of two different proteins: the secretory protein of HBV called HBeAg, that represents an accessory protein of the virus strictly required for chronicity establishment, and the core protein HBcAg (**Fig. 4A**). As last, the X protein of HBV (HBx) of which the role is to promote and sustain the efficient replication of HBV, as recently found (Decorsière *et al*, 2016).

The life cycle of HBV begins with the attachment to its unique target: the hepatocyte. The attachment and the viral entry of HBV happens through the interaction between the high affinity membrane receptor NTCP and the HBsAg large protein (**Fig. 5**) (Yan *et al*, 2012; Ni *et al*, 2014). After the attachment and the entry of the virus, the rcDNA is released in the cytoplasm and enters the nucleus through microtubules. Here, it gets transformed into covalently closed circular DNA (cccDNA). This viral strategy leads to the formation of a structure that resemble the one of a small chromosome, that associates with histone and non-histone proteins of the host cell and then serves as transcriptional virus template (Ko *et al*, 2018). From the cccDNA in the nucleus the different HBV subgenomic transcripts are generated and exported into the cytoplasm where they can get translated into the corresponding HBV structure proteins (**Fig. 5**). The results of the transcription of the cccDNA include a pre-genomic RNA (pgRNA) which is transported in the cytoplasm and subjected to reverse transcription: this serves as mRNA for the HBcAg and for the viral polymerase giving rise to the so-called *replication complexes*.

Inside these, the pgRNA is reverse transcribed generating the HBV complete DNA that both replenishes the cccDNA pool and also proceeds for viral packaging.

In the case of productive infection, polymerase and core proteins interact with the pgRNA around which viral capsids are formed. These then bud into the endoplasmic reticulum (ER) and get surrounded by envelope proteins, eventually forming fully mature viruses that are released into the blood stream (**Fig. 5**). Along with complete mature virions, subviral particles are also released into the blood (Knipe & Howley, 2013).

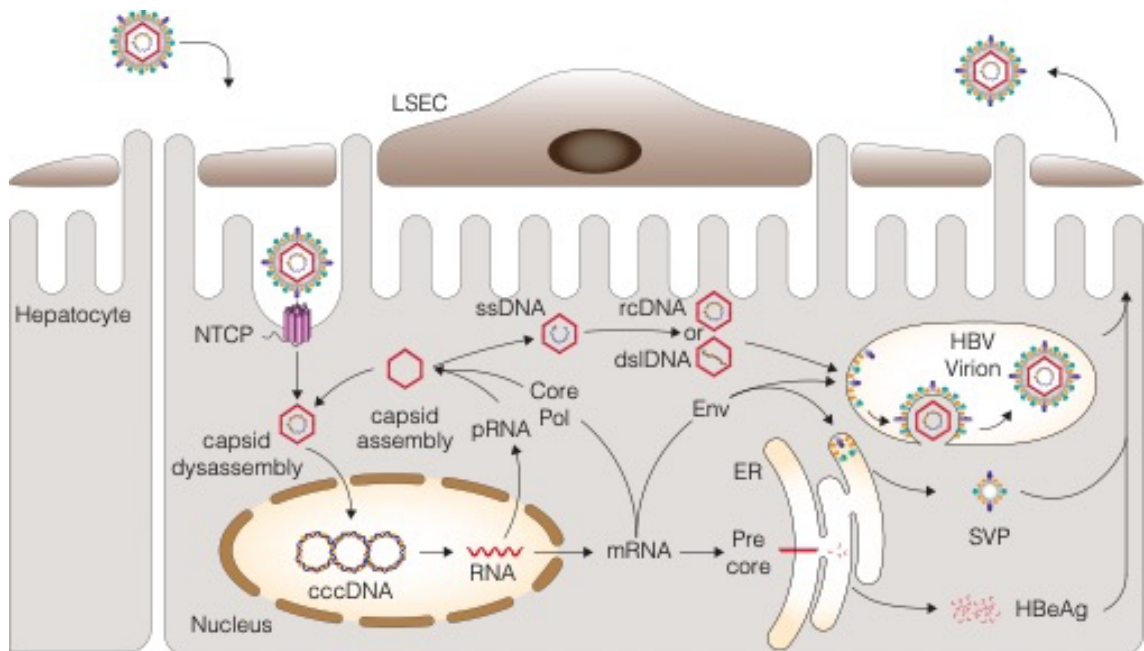


Figure 5 • The life cycle of Hepatitis B Virus.

Circulating HBV virions infect the hepatocyte through the engagement of the NTCP on their surface; this interaction permits viral entry, followed by the transport of the nucleocapsid to the nuclear membrane where it gets disassembled releasing the rcDNA which is internalized into the nucleus. Inside the nucleus the rcDNA is repaired and into the cccDNA which is then ready to function as a template producing all the transcripts necessary for viral replication and virion assembly. HBV exits the cell via budding directly into the bloodstream.

3.2.3. HBV Pathogenesis

HBV is transmitted through horizontal or vertical transmission via the exposure to infected blood and bodily fluids. In the first case, HBV infection can happen after contact with infected blood, saliva, menstrual, vaginal, and seminal fluids; transmission occurs in these cases by sexual intercourse, blood transfusion, percutaneous exposure, needlestick injury, use of contaminated needles or tattooing (Yuen *et al*, 2018). However, especially in highly endemic regions, the most common infection route is the transmission from and infected mother to her child during birth.

After entering the blood circulation, HBV can quickly reach and infect its natural and only target cell: the hepatocyte. After recognizing its receptor and entering the cell, HBV starts its replication cycle and spreading throughout the liver parenchyma. It's important to mention that HBV is a non-cytopathic virus, therefore the infection itself doesn't lead to the death of infected hepatocytes. For this reason, the pathogenesis of HBV-related liver disease is largely due to immune-mediated mechanisms (Guidotti & Chisari, 2006; Iannacone & Guidotti, 2022). During the initial phase, the viral replication strategy permits to HBV to efficiently hide from the innate immune system of hepatocytes. HBV acts in fact as a "stealth" virus and the absence of an early active response of the innate immune system is one of the critical characteristics of its infection process. This innate mimicry mechanism is due to some replication strategies such as the nuclear formation and position of the cccDNA and the production of transcripts equipped with capped and polyadenylated ends that mimic host mRNAs (**Fig. 5**) (Seeger & Mason, 2015). Recent work has supported this hypothesis and shows how HBV is able to become invisible to pattern recognition receptors (PPRs) both in acute and chronic infection contexts (Suslov *et al*, 2018). Thanks to experimental demonstrations coming from past three decades, it was clarified that during HBV infection not only the innate immune responses are weak or totally absent, but that clinical scenarios are totally shaped by adaptive immune responses (Yuen *et al*, 2018). Indeed, clinical outcomes of adult infections are substantially determined by the vigour, kinetics and effectiveness of the response and effector function of HBV-specific (HBV-sp) adaptive immune cells (Guidotti & Chisari, 2006; Bertoletti & Ferrari, 2016; Ferrari, 2015). Among these, CD8⁺T cells take most

responsibility as principal effectors of viral clearance, that is obtained by CD8⁺T-mediated cell killing of infected hepatocytes.

After the initial phase of infection, two possible clinical scenarios can occur: self-limited acute Hepatitis B (AHB) or chronic Hepatitis B (CHB) (T Jake, 2009; Shi & Shi, 2009). The initial phase of HBV pathogenesis is typically asymptomatic. After few weeks, HBV DNA raises and shortly after HBsAg and HBeAg become detectable in the serum, between 4 and 8 weeks post-infection, indicating high presence of HBV replication and high infectivity. Within few weeks, between 10⁹ and 10¹⁰ virions per mL are found in the blood of infected patients, and this correlates with the appearance of liver injury symptoms. T-cell mediated liver injury can be deduced from a rise in serum alanine aminotransferase (ALT) and aspartate aminotransferase (AST) levels in the blood that is usually coupled with a progressive decrease in viral titres both in the blood and in the liver. Antibodies against HBV arise in different patterns: anti-HBc generally appear early before clinical illness while anti-HBe often appear at the peak of clinical illness after that antigen clearance is accomplished. Thus, the loss of HBeAg in parallel with the appearance in the blood of anti-HBe can be considered a favourable serological marker during acute hepatitis B, because indicates healing initiation and the building of a strong adaptive immune response against the virus. Among infected adults, almost 90% can effectively heal and reach the clearance of the virus within 6 months after exposure; the formation of HBV-specific T cells and antibodies is able to maintain a lifelong protective immunity.

However, HBV can also establish chronicity, leading to variable degrees of chronic liver injury that gradually can lead to fibrosis and cirrhosis or late HCC (Farazi & DePinho, 2006; Levrero & Zucman-Rossi, 2016). On the contrary to adults' infection, most of persistent infections have neonatal or perinatal origins. In chronic patients the initial pattern of serological markers is like the acute one. However, HBsAg, HBeAg, and HBV DNA levels in serum remain constantly at high titres, indicating that the viral replication is still ongoing (Shi & Shi, 2009; Mueller & Ahmed). This clinical outcome is generally believed to be dependent on different factors that comprise host characteristics and immune inhibitory mechanisms that overall, render the immunological response to the virus lacking or dysfunctional. This condition, in the absence of a proper

cytotoxic response, able to eradicate infected hepatocytes, can last for years and manifests as an alternation of high or low replicative phases. During these phases fluctuating levels of ALT and HBeAg can be observed, and their duration and frequency can predict and been correlated with the relative risk of developing disease complications. The high replicative phase is instead characterized by an awakening of HBV replication which causes consequently the development of necro inflammatory liver disease.

3.2.4. HBV Serology

The diagnosis of HBV infection and the detection of the precise phase of the disease rely on several clinical, histological, and biochemical aspects but mainly on the detection of HBV antigens and anti-HBV antibodies in the serum of patients (Lampertico *et al*, 2017; T Jake, 2009). Among serological markers relevant to the purpose of this text:

- HBsAg: the presence of the surface antigen of HBV in the serum of infected patients is detectable during both acute and chronic disease. Its levels rise normally between 4- and 8-weeks post infection but can be detected also as early as 1-2 weeks or as late as 11-12 after the virus exposure. Its presence indicates the infectious state of the patients; if persists, chronicity is established.
- HBeAg: the secreted product of the nucleocapsid gene of HBV has similar detection intervals to HBsAg but its presence correlates directly with high levels of HBV replication and high patient infectivity. Its loss is a favourable clinical marker if correlated with the appearance of anti-HBeAg antibodies.
- Serum alanine aminotransferase (sALT): ALT is a transaminase enzyme and an indirect marker of HBV infection and liver health. Since the enzyme is found primarily in the cytosol of healthy hepatocytes, its release and therefore rise in the blood circulation can be indicative of T-cell mediated injury and liver damage. During HBV infection, its levels rise between 4- and 8-weeks post virus exposure.
- Anti-HBsAg antibodies: the presence of antibodies directed against the surface antigen of HBV is interpreted as favourable marker of recovery and persistent

immunity development. Anti-HBs antibodies appear late during infection and recovery after which they persist in the circulation of the patient as indication of resolved infection.

3.2.5. Epidemiology of HBV

The total prevalence of HBV worldwide was estimated to be between 3.4% and 4.6% in 2016. This prevalence, however, significantly varies geographically. Indeed, CHB infections are concentrated and highly endemic in developing regions such as sub-Saharan Africa, Southeast Asia, China, and the Amazon Basin, where the infection can reach high (>8%) prevalence. The prevalence in the Eastern Mediterranean region is intermediate (3.3%) but higher if compared with the one present in South-East Asia regions (2.0%), Europe (1.6%) and both North and South America (0.7%) (**Fig. 6**).

In all the countries where CHB is affecting around or more than the 8% of the population, the infection is being spread through mother-to-child transmission (*vertical* transmission) during the prenatal phase by transplacental transmission in utero or natal transmission during birth. In these cases, when individuals are infected at birth or in early childhood, the chronicity rate is significantly high and can reach the 90%.

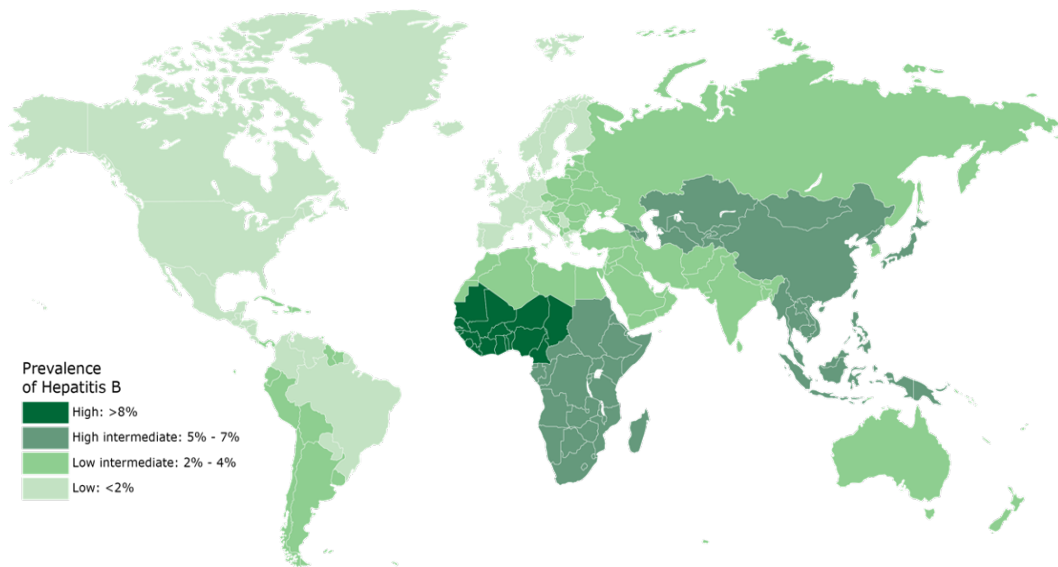


Figure 6 • HBV worldwide prevalence.

Image represents the prevalence of HBV infection worldwide updated to 2019 WHO database. Countries are coloured basing on the prevalence of HBsAg positive cases in the population, broadly classified into high (>8% HBsAg prevalence), high intermediate (5% - 7%), low intermediate (2% - 4%) and low (<2%) prevalence.

HBV epidemiology has positively changed over years and profoundly evolved since the 1980s, mainly thanks to the widely use of the HBV vaccine. The numbers of infected children have indeed declined since the introduction and application of effective vaccine campaigns promoted by the WHO: only the 1.3% of children under 5 years of age were estimated to having developed CHB in 2015 worldwide (Jefferies *et al*, 2018). It is important to mention that infection prevalence has also been influenced by globalization and immigration over the years. Indeed, while the burden of illness is relevant in developing countries, migration of people from high prevalence countries is changing, as a reflection, the disease burden profiles of low-prevalence countries (Sharma *et al*).

On their whole, these considerations can clearly emphasize the key critical burden of HBV diseases worldwide and consequently, the urgent need for appropriate interventions.

3.2.6. Accessible treatments for CHB

The prophylactic anti-HBV vaccines are indispensable and crucial to control HBV spread. HBV vaccines have now been for long available since the 1980s and have been included in immunization programs worldwide. However, and regrettably, the uneven health conditions and accessible health-care resources characterizing many countries and regions of the world, have made the access to the vaccine much more limited and insufficient. Indeed, there are many regions particularly in the Western Pacific region, Africa and Asia where the HBV vaccinal coverage is still very inadequate. In these scenarios, CHB and its life-threatening complications are still an issue: it is precisely in this context that the availability of treatments and cures becomes fundamental.

There is no available cure at the moment in order to completely resolve CHB infection and fully eradicate the virus. However, there are several therapies able to generally improve the patients' quality of life and overall survival, which can be termed as a whole *functional cures*. The available treatments and therapies for HBV infection are aimed at two different purposes: lowering and inhibiting HBV replication and/or boosting adaptive immunity against the virus (Iannacone *et al*, 2022).

Currently available antivirals comprehend nucleoside/nucleotide analogues (NUCs) and pegylated interferon alpha (peg-IFN α). NUCs are primary aimed at inhibiting the viral reverse polymerase (es. Lamivudine, Entecavir, Tenofovir, Adefovir). The treatment with peg-IFN α is thought instead to act on the HBV life cycle directly, inhibiting its replication, transcription, and assembly. Both antivirals represent together the currently approved anti-HBV therapy in single or combined administration (Naggie & Lok, 2021). Unfortunately, these treatments fail to completely clear the virus in most of the cases, making clear the urgent need for new therapeutic strategies. Many laboratories worldwide are currently at work in order to find and develop new effective direct-acting antivirals (Naggie & Lok, 2021; Iannacone *et al*, 2022). Among these, entry inhibitors as well as core protein allosteric modulators, interfering RNAs and cccDNA inhibitors are currently under study (Lee *et al*, 2021).

The other approach towards CHB cure is aimed at boosting HBV-specific adaptive immune responses. The first line of studies is guided by the notion that the persistence of high levels of viral antigens induces progressive T cell dysfunction (Mueller & Ahmed). Several strategies aimed at antigen reduction have consequently been developed and reached the clinic: HBsAg-specific monoclonal antibodies, small-interfering RNAs (siRNAs) or antisense oligonucleotides (ASOs). However, recent observations have outlined that the removal and decrease of HBsAg in the blood circulation is not able alone to impact on disease outcomes (Fumagalli *et al*, 2020; Aliabadi *et al*, 2021; le Bert *et al*, 2020). Among additional approaches that boost HBV immunity there are various therapeutic vaccines and immune-checkpoints inhibitors that are currently being tested in different clinical trials, such as anti-PDL1 monoclonal antibody (Ab). However, it was recently showed by our group that anti-PDL1 treatment is not able to produce a significant impact on antiviral T cells responses in a mouse model of HBV infection (Bénéchet *et al*, 2019) and that instead, the modulation of APCs activity is required. In this sense, it was shown that the therapeutic administration of interleukin 2 (IL-2) (Bénéchet *et al*, 2019; de Simone *et al*, 2021) or an agonizing anti-CD40 antibody (Isogawa *et al*, 2013) are able to boost anti-viral CD8⁺T cells activity and therefore facilitate HBV clearance. Both observations strongly highlight how the activation of dendritic cells and/or Kupffer cells in the liver of HBV-replicating mice, with the consequent improvement of their cross-presentation capacity, may represent significant targets to focus on in further studies.

3.2.7. Available models for the experimental study of HBV pathogenesis

In light of the significant clinical burden of HBV diseases and the urgent need for new therapeutic findings, the availability of experimental models to study this disease become fundamental. As previously said, HBV has a limited tropism for only human and primates. This has been for decades the main obstacle for the study of HBV infection and pathogenesis. The host range of HBV is incredibly restricted and therefore, for many decades there were no available and readily infectable small animal models - with a well-defined immune system - that could be easily employed for research purposes.

Up to now, is beyond the power of the most sophisticated *in vitro* methodology to remotely simulate the reciprocity of all the cellular, physical, and molecular elements that determine the *in vivo* behaviour of immune cells circulating throughout the liver microvasculature during the HBV infection. Likewise, there is no known technology to generate or maintain *in vitro* highly specialized and differentiated cells such as the hepatocytes (Dandri & Lütgehetmann, 2014). However, with the advent of HBV-replication-competent transgenic mice, it has been possible to overcome these limitations (Guidotti *et al*, 1995). Indeed, almost 30 years ago, the first HBV-replication-competent transgenic HBV mouse, named 1.3.32, was generated. In these mice, all hepatocytes can produce and replicate the complete virus genome and its structural proteins at high levels in a non-cytopathic manner.

The 1.3.32 mice were generated by the microinjection of terminally redundant viral DNA construct containing the HBV genome with relative promoters and enhancers: in these mice all four HBV RNAs are produced inside the hepatocytes. HBV replication occurs in viral nucleocapsids inside the cytoplasm of the hepatocytes surrounding the liver central veins (centrilobular hepatocytes) (Guidotti *et al*, 1995; Iannacone & Guidotti, 2015). Hepatocytes are able not only to replicate the virus but also to permit its viral spread because of an efficient viral replication: indeed, in the serum of 1.3.32 mice virions are detectable at levels up to 10^7 - 10^8 virions per mL. Furthermore, 1.3.32 mice are immunologically tolerant to all HBV antigens, therefore providing a good platform to evaluate immunotherapeutic strategies aimed at breaking tolerance and terminate

persistent HBV infection. In addition to 1.3.32 mouse model, MUP core mice also represent an alternative platform to study adaptive immune specific responses against HBV virus. In MUP core mice a non-secretable form of the core protein (HBcAg) is produced thanks to the transcriptional control exerted by the liver-specific mouse urinary promoter (MUP) in 100% liver hepatocytes (Guidotti *et al*, 1994). As for 1.3.32, MUP core mice were generated by microinjection of a subgenomic fragment of HBV genome from the 5' core coding region. However, the absence of total HBV genome does not allow the production of HBV virions or other HBV antigens than HBcAg. The HBV core protein is located preferentially in the nucleus of resting hepatocytes and released in the cytoplasm only during mitosis. Both MUP core and 1.3.32 mice represent useful mouse models to study T cell responses against a nominal antigen of HBV.

3.3. T-cell immune responses during HBV infection

Condensing from previous sections, it is clear that the liver possesses a unique immune microenvironment and is enriched in distinct immune populations which hold paramount importance during hepatotropic infections. These discussed aspects become decisive during HBV infection where, being HBV a non-cytopathic virus that trigger a weak innate response, the adaptive system ultimately determines the outcome of the disease (Bertoletti & Ferrari, 2016; Shuai *et al*, 2016; Chisari & Ferrari, 1995). Within the entire adaptive immune system, CD8⁺T cells have been found to be particularly crucial as the main responsible effectors of viral clearance and liver inflammation during HBV infection. Therefore, HBV research has understandably been focused on CD8⁺T responses against the virus, regrettably leaving the field with a significant lack of data that does persists with respect to the CD4⁺T cells compartment (Gill & McCarthy, 2020).

In the following paragraphs, I will describe the contribution of CD8⁺T cells in HBV immunopathogenesis and, on the other hand, what is known about the CD4⁺T cell responses and their cooperation with CD8⁺T cells, emphasizing the great need for in-depth study of their role and importance in the disease.

3.3.1. Front line offence: CD8⁺T cells in HBV

CD8⁺T cells play a crucial part during HBV infection: They are the main responsible for HBV pathogenesis and virus clearance, achieved by both cytolytic and non-cytolytic mechanisms. Their participation dynamics in HBV disease have been deeply investigated and clarified during the last decades, and the some of the main related discoveries will be summarized in this paragraph.

Naïve CD8⁺T cells are constantly recirculating between the secondary lymphoid organs (SLOs) and the blood in search for cognate Ag-MHCI complexes. The immunological dogma sees naïve CD8⁺T cells encountering the antigen inside SLOs, where presentation of circulating virions and subviral particles by APCs is efficacious in promoting their differentiation into effector cells. This interaction allows their

differentiation into cytolytic CD8⁺T cells (CTLs) that can be recognized by a now well-defined phenotype. CTLs expressions of activation surface markers are enhanced (e.g. CD44, CD25, CD69, CD28, CD27) and in parallel followed by the downregulation of naïve feature markers (e.g. CD62L, CCR7, LFA-1) and the start of production of effector (e.g. IFN γ , TNF α , IL-2) and cytolytic cytokines (e.g. granzymes, perforins) (Kaech & Cui, 2012). After acquiring the proper lineage fate, CTLs can then move to the infection site and kill the infected cells, leading eventually to viral clearance and disease resolution.

However, this is not always the case during hepatotropic infections. Indeed, the unique structural organization, composition and anatomy of the liver permits the direct contact between CD8⁺T cells and unconventional, non-professional APCs (i.e., hepatocytes): the diameter of sinusoids, their lack of a tight continuous basal membrane, the presence of fenestrae, and the slow blood flow circulation that characterize the liver parenchyma together favour T-hepatocyte contacts inside the sinusoids (Warren *et al*, 2006). One of the first evidences of hepatic Ag-recognition dates to the 90s, when it was proved that HBV-specific (hereafter HBV-sp) CD8⁺T cells were selectively causing a liver-restricted necro inflammatory disease in HBV bearing mice (Ando K *et al*, 1994). Shortly thereafter, Bertolino and colleagues confirmed the liver as a feasible priming site for naïve CD8⁺T cells by two different studies (Bertolino *et al*, 2001; Bertolino *et al*, 1995). These observations were later followed by other studies coming from different groups, including ours, that showed how the hepatocellular priming induces more easily tolerance than immunity in HBV-transgenic mice (Bowen *et al*, 2004; Isogawa *et al*, 2013a; Bénéchet *et al*, 2019). However, there have been also contradictory studies that reported an opposite scenario of liver restricted CD8⁺T cells responses (Klein & Crispe, 2006).

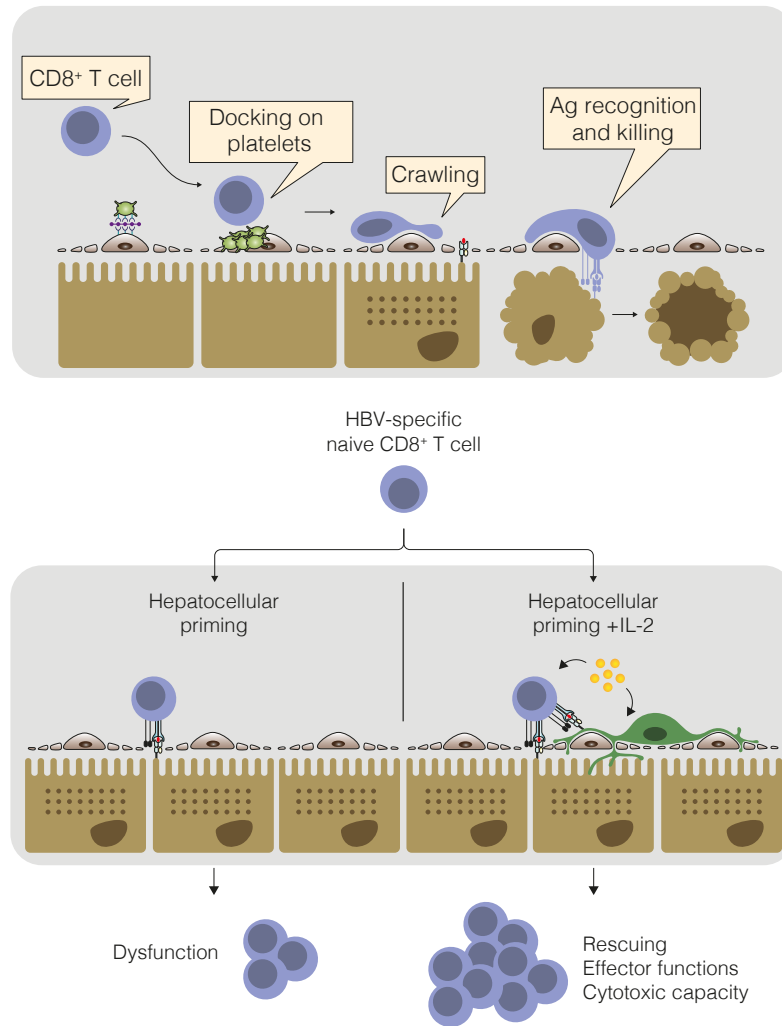


Figure 7 • How CD8⁺T cells keep the liver under surveillance.

(A) Schematic representation of CD8⁺T cells undergoing mouse intrahepatic priming in HBV-Tg mice: after the initial docking within sinusoids onto platelets, CD8⁺T cells start to crawl. The binding to the specific antigen presented on MHC-I by hepatocytes leads to the extension of cellular protrusions, cytokine production and killing of infected cells. (B) Mechanism proposed to describe the dynamics of CD8⁺T cells primed to HBV antigens in the liver. During HBV infection, priming of naïve CD8⁺T cells by hepatocytes leads to dysfunction: HBV-sp CD8⁺T cells proliferate and accumulate in periportal cluster and do not differentiate into effector cytotoxic CD8⁺T cells. The in vivo IL-2 administration is able to overcome the induction of dysfunctionality exerted by hepatocellular priming.

During the last decade, our group deeply investigated the dynamics of CD8⁺T cells Ag recognition in the liver during HBV pathogenesis, and a commonly accepted model has

been proposed (**Fig. 8**). After crawling along liver sinusoids by docking on platelets (Iannacone *et al*, 2005) and interacting with hepatocytes through sinusoidal fenestrae, HBV-sp CD8⁺T cells undergo intrahepatic Ag recognition (Guidotti *et al*, 2015; Inverso & Iannacone, 2016). During acute infection, when Ag-presentation is favourably exerted by professional APCs, intrahepatic priming results in the killing of a good fraction of infected hepatocytes, cytokine production, inflammatory cells recruitment that supports CD8⁺T cell-mediated liver immunopathology and suppression of HBV replication as a result (Bertoletti & Ferrari, 2016; Ferrari *et al*, 1990; Bénéchet *et al*, 2019). On the contrary, CHB is characterized by an inefficient CD8⁺T cell antiviral response. Indeed, it was shown that if their priming happens in the liver of HBV-transgenic mice – a mouse model of neonatal HBV infection (Guidotti *et al*, 1995) - naïve CD8⁺ T cells can only get locally activated and proliferate but cannot differentiate into fully-capable effector and cytotoxic T cells. Rather, genome and transcriptomic analyses revealed that HBV-sp CD8⁺T cells progressively acquire a differentiation program that eventually leads to the establishment of a dysregulated T cell phenotype (Benechet & Iannacone, 2017; Bénéchet *et al*, 2019). Short after, our group also added to this data that the phenotype of liver-primed CD8⁺T cells do not overlap with the one of exhausted T cells pointed out in other viral contexts and indeed, in line with this assertion, hepatocellularly primed CD8⁺T cells are not able to respond to anti-PD-L1 therapy, but instead can be re-invigorated by IL-2 (Bénéchet *et al*, 2019; de Simone *et al*, 2021).

The reason why liver T cell priming range from efficiency to dysfunction and give rise to either AHB or CHB, should be linked to the plethora of variable factors that influence CD8⁺T cell priming: TCR affinity, Ag nature, magnitude of Ag production, and the broad of inflammatory stimuli are only some of the ones that can be involved. Among them maybe also, not to be forgotten, CD4⁺T cell help.

3.3.2. Back-line defence: CD4⁺T cell responses in HBV

Detailed functional dissection of Ag-specific CD4⁺T cells has received little attention in HBV field and this knowledge gap has been recently underlined (Upkar S. Gill & Neil E. McCarthy, 2020). In the above cited editorial article of Journal of Hepatology, Gill and McCarthy point out the significant lack of appreciation that CD4⁺T cells have suffered in HBV basic and applied research during the last decades. By listing and discussing the few results that give hints about HBV-sp CD4⁺T cells relevance in the disease, the authors wanted to open avenues and encourage future studies of these crucial cells. Indeed, CD4⁺T cells are known to be critical components of virus-induced adaptive immune responses in terms of development, maintenance and control of both T-cell and B-cell immunity. CD4⁺T cells are dynamic cells that, after Ag-recognition, can acquire several committed subtypes, each of which exert multiple critical functions during viral immunity (Cohen *et al*, 2014; Kiner *et al*, 2021): they drive and support the activation of APCs, promote antibody production, drive innate cells recruitment, sustain, and maintain CD8⁺T cells antiviral activity (Luckheeram *et al*, 2012a; Zhu *et al*, 2010).

Despite the focus on CD8⁺T cell immune response in HBV, some experimental observations have been made during the last years highlighting CD4⁺T cells' essential role. In 2009, one of the first observation was done in experimentally infected chimpanzees (Asabe *et al*, 2009): Asabe and colleagues showed that if CD4⁺T cells are depleted before inoculating the animals with a normally rapidly controlled inoculum, T cell priming was abolished and caused persistent infection with almost no detectable immunopathology. Short after, in a mouse model of HBV genome plasmid hydrodynamic transfection, CD4⁺T cells were found to have a fundamental role in the induction of an effective CD8⁺T cell-mediated HBV clearance (Yang *et al*, 2010). Despite these critical experimental studies, the deepening of the role of HBV-sp CD4⁺T cells has not proceeded. These few cited experimental data are consistent with first clinical observations in the early 90s, showing that strong HBV-specific CD4⁺T cell responses have been observed in patients with self-limited acute HBV infection (Penna *et al*, 1996; Ferrari *et al*, 1990). Indeed, the number of antigen-specific CD4⁺T cells has been found to be significantly increased in patients with AHB compared to patients with CHB, in which small frequency of circulating HBV-sp CD4⁺T cells was highlighted. Plus, in line

with these data, HLA-DR has been identified as the major locus for susceptibility to HBV-related acute-on-chronic liver failure, clearly indicating a role of CD4⁺T cells in the HBV immunopathogenesis (Tan *et al.*, 2018). This role is also relevant in the context of co-infections (Urbani *et al.*, 2005) as it was observed by Urbani *et al.*, who showed how the lack of HBV-sp CD4⁺T cells is directly correlated with HBV persistence in HBV/HCV co-infected patients despite the presence of detectable HBV-sp CD8⁺T cells. Recently, the importance of the role of these cells in HBV pathogenesis has come from the clinic, underlying the importance of CD4⁺T cells in HBV infected patients (Wang *et al.*, 2020).

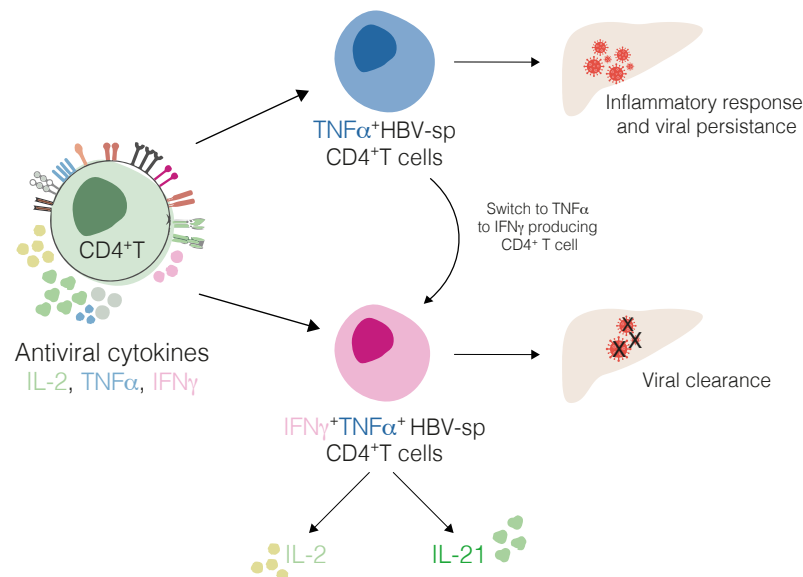


Figure 8 • CD4⁺T cells in CHB patients.

Image depicting the phenotype of CD4 T cells observed in the blood circulation of HBV chronic infected patients. The concomitant production of IFN γ and TNF α , or the switch to single production TNF α to double production of IFN γ and TNF α , may lead to viral clearance.

More in detail, Wang *et al.* performed a deep immunological characterization of HBV-sp CD4⁺T cells in the blood of CHB patients in different stages of the disease. They showed that different types of HBV-sp CD4⁺T cells can be found in chronic patients but that two main subgroups can be identified: single TNF α -producing or IFN γ ⁺TNF α ⁺ double positive HBV-sp CD4⁺T cells (**Fig. 9**). Basing on patients' clinical outcomes, the

authors observed that while $\text{TNF}\alpha^+$ CD4^+ T cells were more representative of patients with high viral titres and persistent infection, double producers CD4^+ T cells were characteristic of patients that approached viral clearance (Fig 9). Of note, $\text{IFN}\gamma^+$ CD4^+ T cells had also a Th1-related phenotype, as they were found to express T-bet and being able to produce IL-2 and IL-21 cytokines (Wang *et al*, 2020). These data are consistent with clinical observations in patients that date back to the 90s (Jung *et al*, 1995; Penna *et al*, 1997), in which a potent and broad multi-specific Th1 CD4^+ T cell response was already hypothesized to be essential to favour a self-limited AHB disease fate.

Despite these observations, is clear that there is still a lot to learn about the specific cellular and molecular mechanisms in which HBV-sp CD4^+ T cells are involved, their transcriptional signature and functional properties in acute and chronic infection and even more, the importance these cells have in disease fate decisions. The deep study of HBV-sp CD4^+ T cells is then required and could shed light on fundamental still open questions in the field, helping the design of novel immunotherapeutic strategies aimed at treating HBV infection and its life-threatening complications.

3.3.3. CD4^+ - CD8^+ T cell cooperation in HBV infection and beyond

The current commonly accepted model of CD4^+ - CD8^+ T cell cooperation is an entangled choreography played by an Ag-specific CD4^+ T cell and a related Ag-specific CD8^+ T cell with the help of an APC, that acts as an interaction platform and “language translator” (Wu & Murphy, 2022).

Even though the three-cells interaction paradigm has changed and evolved during the years, a detailed mechanism can be now outlined, thanks to the multiple discoveries that have been made in diverse infectious and tumoral contexts (Borst *et al*, 2018; Pishesha *et al*, 2022).

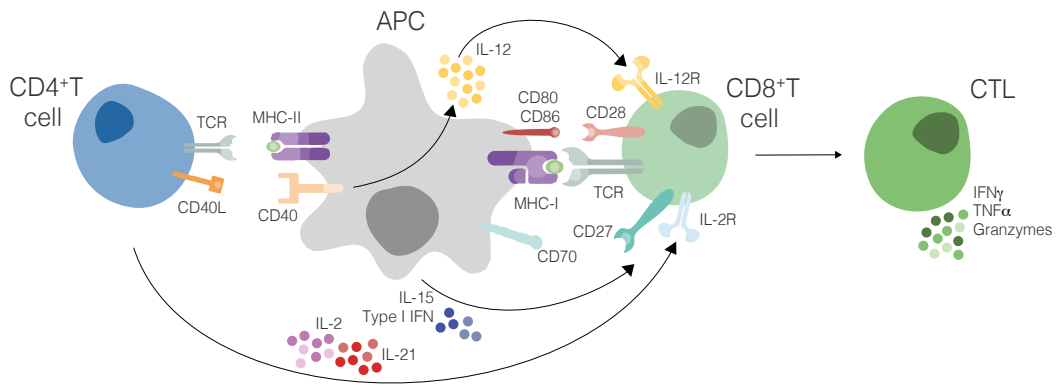


Figure 9 • CD4⁺T cell cooperation with CD8⁺T cells: the three-cell types interaction model.

Schematic representation of the interactions between CD4⁺ and CD8⁺T cells during the second priming phase. The Ag-MHCII interaction between the CD4⁺T cell and the APC leads the latter to ameliorate their cross-presenting capacity and to deliver specific co-stimulatory and cytokines signals that eventually favor the differentiation of the CD8⁺ cell into a CTL.

Fundamental steps of CD4⁺ and CD8⁺ T cooperation (**Fig. 9**) can be summarized as follow in a chronological order:

- i) As first, both Ag-specific CD4⁺ and CD8⁺ T cells are believed to independently encounter their cognate Ag presented on MHC-II and MHC-I molecules on two different specialized APCs.
- ii) The help is then delivered in a second priming phase, in which a CD4⁺ and a CD8⁺ T cell recognize their respective antigens on the same APC.
- iii) The second effective Ag-specific interaction between the CD4⁺T cell and the APC is commonly referred to as “licensing”, is mediated by CD40-CD40L axis and gives rise to diverse effects (Smith *et al*, 2004; Ferris *et al*, 2020). CD40 signalling the APC stimulates the enhancement of cross-presentation, co-stimulatory and secreting capacities. The expression of MHC-I molecules and co-stimulatory molecules such as CD80, CD86 and CD70 is augmented on APC surface (Feau *et al*, 2012) and is followed by an intensified cytokine production of IL-15, IL-12 and Type I IFN (Agarwal *et al*, 2009).
- iv) All described effects are delivered to the CD8⁺ T cell that at the same time, or in a later timeframe, is interacting with the licensed APC. APC signals are

sensed by the CD8⁺ T cell via the respective receptors (e.g., CD28, CD27, IL-12R) and this eventually leads to their differentiation into fully equipped CTLs (Borst *et al*, 2018).

- v) On top of listed mechanisms, it was also shown that CD4⁺T cells can in parallel directly provide supporting signals to CD8⁺ T cells, producing IL-2 and IL-21 (Elsaesser *et al*, 2009).

The ultimate effect of this process is then the promotion of a bigger magnitude and better quality of CTLs responses against the invading pathogen. During infections of intracellular pathogens such as viruses, the involved CD4⁺T cell subtype that delivers help to the CD8⁺ T cell compartment is commonly believed to be a T helper 1 CD4⁺T cell (Tuzlak *et al*, 2021). It is clear that CD4⁺T cell help can reasonably govern the amplitude and magnitude of the CTLs response during their priming phase, and that can consequently be a valuable turning point of overall adaptive immune responses. This leads to think that opportunities may exist to provide these help signals as part of viral or cancer immunotherapy in order to optimize Ag-specific CD8⁺T cell protective responses (Melssen & Slingluff, 2017) and could be exploited to design innovative HBV therapeutic drugs as recently highlighted (Isser *et al*, 2022). Unfortunately, there is currently neither clear experimental evidence of CD4⁺ and CD8⁺ T cooperation in HBV pathogenesis, nor a definite idea of its possible relevance in both disease fate evolution and therapeutic application.

Given this background and these premises, I hope it will be evident how the chance of studying HBV-sp CD4⁺T cell responses in HBV pathogenesis would be an incredible opportunity and could bring scientific advance to a field where, still, there is a lot of progress to make.

4. AIM OF THE WORK

The rationale of this project is then aimed at enlightening the role of Ag-specific CD4⁺T cells in the context of HBV immunopathogenesis. Indeed, the project was born with the realization of the existence of a big scientific gap regarding the spatiotemporal dynamics of HBV-specific CD4⁺T cells in the HBV field.

The overall purpose of the project is to characterize HBV-specific CD4⁺T cell activation and differentiation and explore the extent to which Ag-specific CD4⁺T cells help intrahepatic CD8⁺T cell differentiation. With this project, we took advantage of recent methodological developments, combining imaging techniques with high-dimensional flow cytometry, with dedicated mouse models of HBV pathogenesis to unravel where, when and how HBV-sp CD4⁺T cells are involved in HBV pathogenesis. The ultimate goal of the project is to gather information about this immune population in order to deploy them to their fullest potential in immunotherapeutic strategies.

The aims that were set at the beginning of the projects can be summarized as follow:

- i) Generation and implementation of an *HBV-specific CD4⁺T TCR transgenic mouse* model.
- ii) Characterization of *HBV-sp CD4⁺T cells responses in HBV* pathogenesis.
- iii) Assessment of the *activation dynamics* of HBV-sp CD4⁺T cells.
- iv) Understanding HBV-sp CD4⁺T cells *crosstalk with the CD8⁺T cells compartment* in the context of HBV pathogenesis.

5. RESULTS

5.1. A transgenic HBV-specific TCR mouse model to study antigen-specific CD4⁺T cells in HBV pathogenesis

In order to study the behaviour of Ag-specific CD4⁺T cells in HBV pathogenesis, we generated *ad hoc* for this project a new transgenic mouse model inside which all CD4⁺T cells are able to recognize a specific peptide belonging to the envelope protein of HBV.

Up to now, there is no available *in vitro* methodology to adequately study the *in vivo* behaviour of Ag-sp CD4⁺T cells during HBV pathogenesis. The importance of the generation of this animal model therefore relies on the fact that it allowed us to deeply study for the first time the role and dynamics of HBV-specific (HBV-sp) CD4⁺T cells in the context of HBV pathogenesis. We believe that current immunotherapeutic approaches could strongly benefit from new insights into the molecular and cellular mechanisms of CD4⁺T cells immune responses in HBV infection, supporting the design of avant-garde treatment strategies to cure CHB disease.

5.1.1. Generation of Env126 transgenic mouse model

In order to study the behaviour of Ag-specific CD4⁺T cells in HBV pathogenesis, we generated an HBV-specific CD4⁺ TCR transgenic mouse in which CD4⁺T cells carry a reactive T-cell receptor that is specific for the HBsAg (Env126, C57BL/6N). More precisely in these mice, CD4⁺T cells express the mouse alpha-chain and beta-chain of the TCR that pairs with the CD4 co-receptor and is specific for HBsAg peptide residues 126-138 in the context of I-A^d. The peptide comprising residues 126-138 of HBsAg (RGLYFPAGGSSSG) has been identified among major CD4⁺T cell immunodominant epitopes located in the preS2 region of HBV genome and therefore was selected as election peptide to be tested (Mancini *et al*, 1998).

Env126 transgenic mouse line was generated by a well-established TCR discovery platform. In detail, C57BL/6 wild type (WT) mice were immunized with the HBV peptide HBs₁₂₆₋₁₃₈ (100µg) along with poly(I:C) immune adjuvant at three time points every 7 days before the isolation of splenocytes (**Fig. 10A**). The obtained splenocytes were then *ex vivo* restimulated with the specific HBs₁₂₆₋₁₃₈ peptide *in vitro*. As a control, CD4⁺T cells were in parallel cultured with ovalbumin peptide (OVAII, residues 323-339), functioning as an irrelevant MHCII-restricted Ag, and Concanavalin A (ConA) as control of Ag-independent T cells activation (Palacios, 1982). IFN γ ⁺ CD4⁺T cells were enriched and after 24 hours, single cell sorting was performed to isolate the high IFN γ -producing CD4⁺T cells population (**Fig 10B**). IFN γ -producing cell-sorted CD4⁺T cells were then TCR electroporated allowing TCR sequencing and further functional testing.

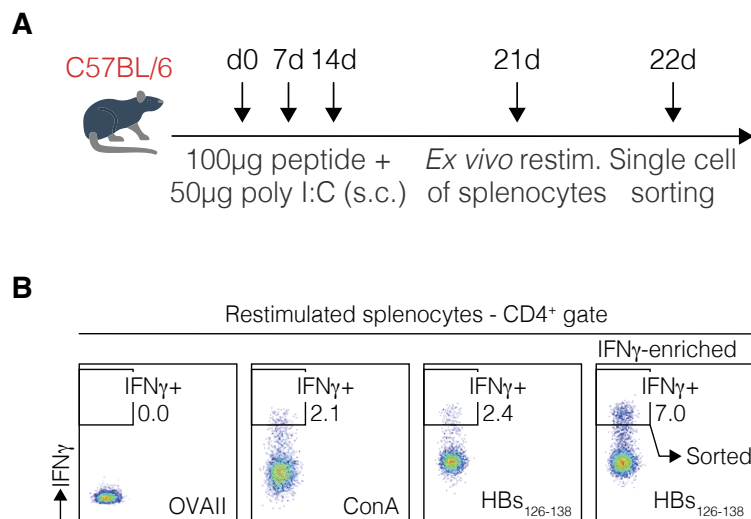


Figure 10 • Identification and validation of functional HBVs epitope.

(A) Schematic representation of the immunization protocol: C57BL/6 mice were injected with HBsAg₁₂₆₋₁₃₈ (100µg) along with poly(I:C) immune adjuvant subcutaneously (s.c.) at three time points every 7 days. At day 21 post immunization, mice were sacrificed, and spleens were collected. Isolated splenocytes were *ex vivo* restimulated with cognate peptide HBsAg₁₂₆₋₁₃₈. As a control, isolated splenocytes were cultured with OVAII peptide (as irrelevant control Ag) and Concanavalin A (ConA). IFN γ ⁺ CD4⁺T cells were enriched via MACS[®] Pre-enrichment kit and after 24 hours single cell sorting of IFN γ -producing CD4⁺T cells population was performed. (B) Representative flow cytometry plots showing the frequency of IFN γ ⁺CD4⁺T cells in HBsAg₁₂₆₋₁₃₈ immunized mice after *in vitro* stimulation in indicated conditions. CD4⁺T were defined as Live⁺CD45⁺CD3⁺CD8⁻CD4⁺.

From these steps, the two sequences of both alpha and beta chain of the HBs₁₂₆₋₁₃₈ reactive TCR have been defined and cloned in Diane Mathis cassette plasmid (**Fig. 11A**) (Kouskoff et al, 1995). After zygote pronuclear injection and implantation in pseudo-pregnant recipient females, two separate transgenic mouse lines were generated, carrying the TCR alpha and beta chains specific for the HBs₁₂₆₋₁₃₈ peptide (called V_{alpha7} and V_{beta7} mouse lines, respectively). These two mouse lines have been then crossed against each other to generate the Env126 transgenic mouse line carrying both transgenes encoding for the two chains, then able to pair with each other to form a stable HBs₁₂₆₋₁₃₈-reactive TCR (**Fig. 11B**).

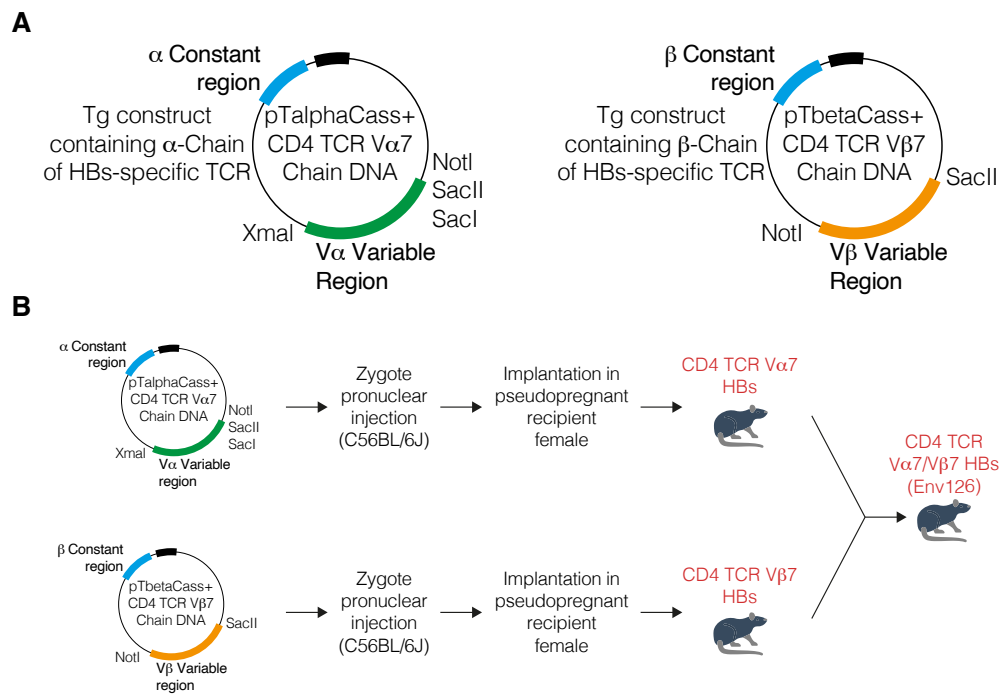


Figure 11 • Constructs design and generation process of Env126 mice.

(A) Schematic representation of the transgenic constructs maps generated after the cloning of the HBs-specific TCR α and β chain sequences into cassette plasmids (Kouskoff et al, 1995). (Left) Plasmid cassette (pTalphaCass) for the expression of TCR α gene comprises the V α (variable alpha region) sequence of the specific HBs₁₂₆₋₁₃₈ TCR (in green), the sequence encoding for the α constant region (in blue) downstream enhancers components (in black) and XmaI, NotI, SacII and SacI unique restriction enzyme sites. (Right) Plasmid cassette (pTbetaCass) for the expression of TCR β gene comprises the V β (variable beta region) sequence of the specific

HBs₁₂₆₋₁₃₈ TCR (in orange), the sequence encoding for the β constant region (in blue) downstream enhancers components (in black), and NotI and SacII unique restriction enzyme sites. **(B)** Schematic representation of the process of generation for Env126 transgenic mice: mouse zygotes were injected with the two transgenic constructs created and then implanted in pseudo-pregnant mouse females generating two first progenies constituting two different mouse lines in which HBs-specific TCR α and β chains were singularly expressed. The two mouse lines were then crossed together giving generation to the Env126 transgenic mouse in which the expression of both transgenes was achieved.

5.1.2. Characterization of Env126 transgenic mouse model

In order to verify the presence of HBs₁₂₆₋₁₃₈ CD4⁺T cells in Env126 transgenic mice, we initially tested and established a tetramer staining protocol with which we were able to detect HBs-sp CD4⁺T cells *ex vivo*. Major histocompatibility complex MHCII-peptide tetramers have recently been proved to represent a powerful technology for the detection of low number Ag-specific CD4⁺T cells (Coss *et al*, 2020; Pastore *et al*, 2019). NIH Tetramer Core Facility provided us with a specific class II fluorescently labelled tetramer loaded with the HBs₁₂₆₋₁₃₈ peptide (I-A_b HBsAg 126-138, RGLYFPAGGSSSG).

With the aim of proving the effective development of transgenic HBs-specific CD4⁺T cells, untreated Env126 mice were sacrificed together with control untreated WT mice to check the presence and the phenotype of HBs-specific CD4⁺T cells (**Fig 12A-C**). With this purpose, the liver together with major primary and secondary lymphoid organs were surgically collected and processed. The resulting cell suspensions were analysed by flow cytometry. In Env126 mice, we found that only 20-30% of total CD4⁺T cell population was expressing the transgenic HBs-specific TCR (**Fig. 12B**). However, out of CD4⁺T cells, HBs Tetramer positive (HBs-Tet⁺) CD4⁺T cells were displaying a resting naïve phenotype in each organ, like untreated WT CD4⁺T cells, as expected (**Fig 12C**).

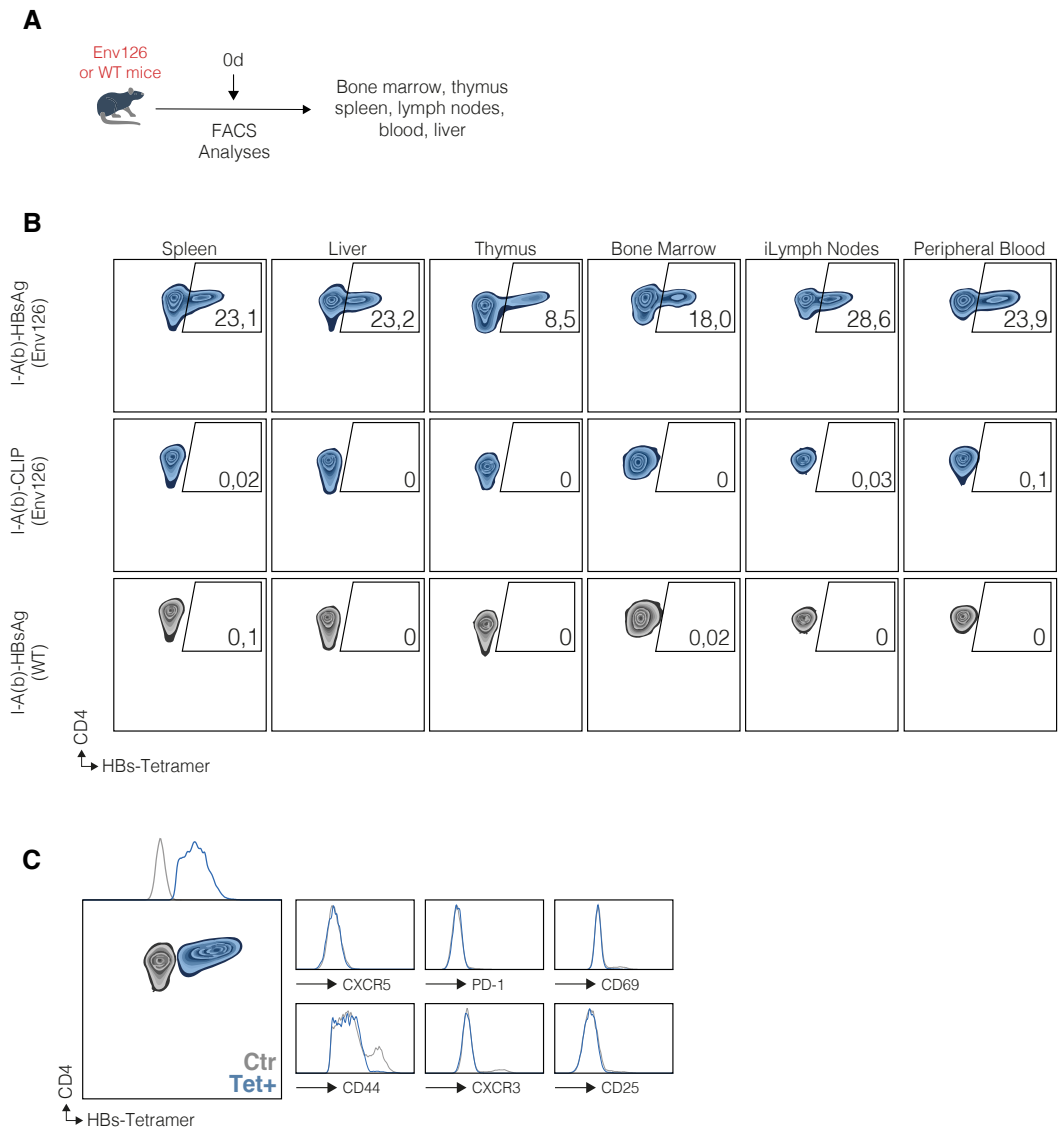


Figure 12 • HBs-sp CD4⁺T cells in Env126 mice.

(A) Experimental design. Untreated WT and Env126 mice were sacrificed, and various organs were surgically collected: spleen, liver, thymus, bone marrow, inguinal lymph nodes, peripheral blood. All organs were processed in accordance to relative protocols, and the obtained cell suspensions were analysed by FACS. (B) Representative flow cytometry plots showing the frequency of HBs-sp CD4⁺T cells in different organs of Env126 (blue, n=10) and control mice (grey, n=5). Cell suspensions of Env126 organs were stained with both HBs₁₂₆₋₁₃₈ peptide loaded tetramer (I-Ab HBsAg, blue, upper plots) and unloaded tetramer as a control (I-Ab CLIP, blue, middle plots) both provided by NIH Tetramer Core Facility. Env126 CD4⁺T cells were identified as Live, CD45⁺, B220⁻CD19⁻ CD8⁻CD3⁺CD4⁺HBs-Tet⁺. (C) Representative FACS plot of total CD4⁺T cells in the spleen of Env126 mice (left, n=10). HBs-Tetramer⁺ CD4⁺T cell population is depicted in blue, control WT CD4⁺ T cells population are coloured in grey; mean fluorescent intensity (MFI) levels of HBs-Tetramer expression are depicted above the plot. (right) MFIs of indicated surface markers on HBs-Tetramer⁺ CD4⁺T cells (blue) and control WT CD4⁺T cells (grey). Env126 CD4⁺T cells were identified as Live, CD45⁺, B220⁻CD19⁻ CD8⁻CD3⁺CD4⁺HBs-

Tet⁺. Data in **(B)** are representative of 3 independent experiments, data in **(C)** are representative of at least 10 independent experiments.

The main purpose of Env126 mice was to be used as a primary source of homogenous HBs-sp CD4⁺T cells donor for *in vivo* adoptive transfer experiments. For this reason, to increase the total HBs-sp CD4⁺T cells numbers and exclude polyclonal endogenous T cell contamination, Env126 mice have been mated with recombination activating gene 1 knock-out mice (Rag1^{-/-} CD45.1, C57BL/6N) (**Fig. 13A**) that do not develop mature T and B cells (Mombaerts *et al*, 1992). This approach, which already proved to be successful in the generation of other CD4⁺T TCR-transgenic mice (Li *et al*, 2001), allowed us to obtain a progeny in which endogenous CD4⁺T cell development was prevented and stringent production of HBs-specific CD4⁺ transgenic T cells is favoured (**Fig. 13B**).

With the expression of a congenic marker, we obtained the definitive Env126 Rag1^{-/-} CD45.1/.2 mouse in which all CD4⁺T cells are able to recognize HBsAg peptide and also carry the differential Ptpc^a pan leukocyte marker, permitting us to specifically and easily track donor and host CD4⁺T cells in adoptive transfer experiments by both flow cytometry and imaging analyses, using anti-mouse CD45.1 and CD45.2 antibodies (**Fig. 13A**). Env126 Rag1^{-/-} mice were in parallel also crossed with Rag1^{-/-} CD45.1 CAG-eGFP mice allowing to directly examine and understand the *ex vivo* and *in vivo* dynamics of Env126 CD4⁺T cells by both static and live imaging techniques (**Fig. 13A**).

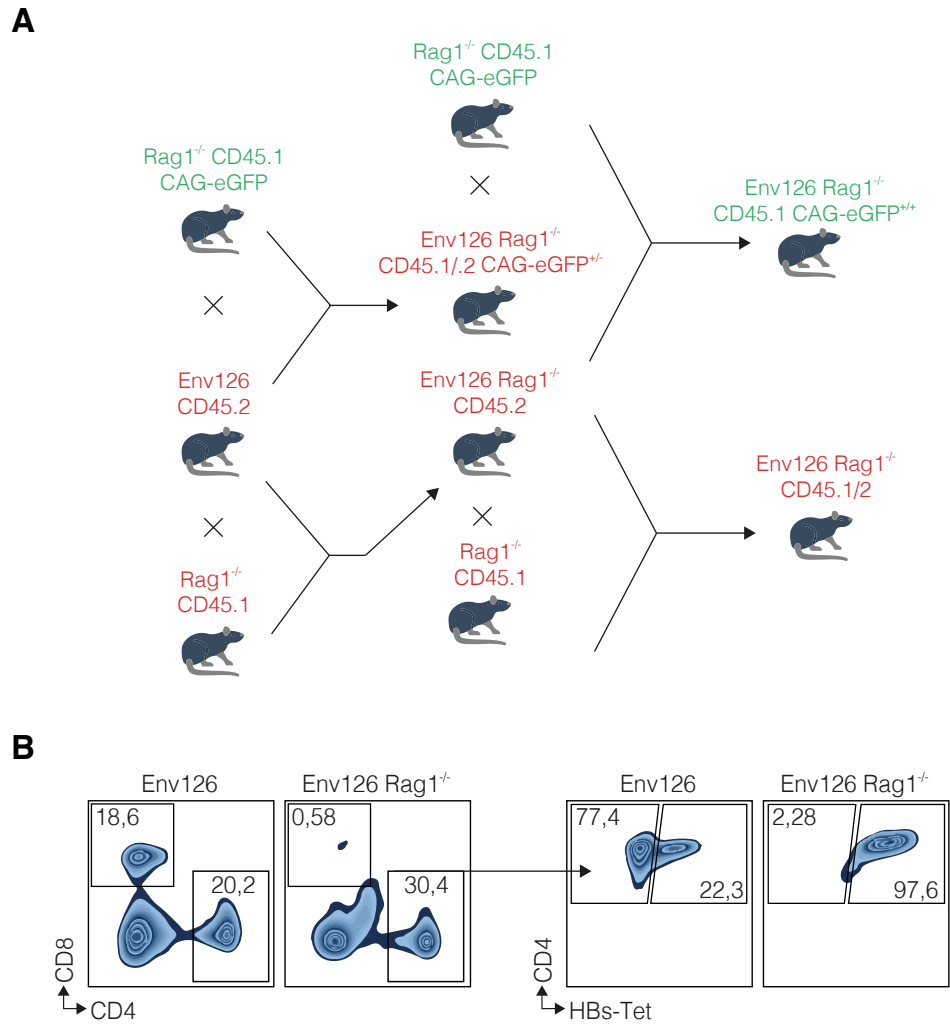


Figure 13 • Env126 Rag1^{-/-} lines generation.

(A) Representative scheme of the crossing strategy used to generate Env126 Rag1^{-/-} CD45.1/2 mice and Env126 Rag1^{-/-} CD45.1 CAGe-GFP mice. Briefly, Env126 Rag1^{-/-} CD45.2 mice were crossed by two generations with Rag1^{-/-} CD45.1 mice to generate Env126 Rag1^{-/-} CD45.2 mice and with Rag1^{-/-} CD45.1 CAGe-GFP mice by two generation to generate Env126 Rag1^{-/-} CD45.1 CAGe-GFP mice. The first final mouse line (bottom right, red) carries the totality of the CD4⁺T cells population specific for the HBs₁₂₆₋₁₃₈ peptide on which the Ptpcr^a pan leukocyte marker is expressed in heterozygosity to allow *ex vivo* tracking by flow cytometry. The second (up right, green) final mouse line carry the totality of the CD4⁺T cells population that is specific for the HBs₁₂₆₋₁₃₈ peptide, express the Ptpcr^a pan leukocyte marker CD45.1 and display CAG-eGFP protein expression in homozygosity, to allow imaging experiments. (B) Representative flow cytometry plots showing the frequency of CD4⁺ T cells (left plots) and HBs-sp CD4⁺T cells (right plots) in the spleen of Env126 mice and Env126 Rag1^{-/-} mice. Env126 CD4⁺T cells were identified as Live, CD45⁺, B220⁻CD19⁻ CD8⁻CD3⁺CD4⁺HBs-Tet⁺. Data in (B) are representative of at least 10 independent experiments.

5.1.3. Functional testing of Env126 transgenic mouse model

After characterizing the presence and the frequency of HBs-sp CD4⁺T cells in Env126 mice, we next assessed their functionality. We showed that under physiological condition transgenic Env126 CD4⁺T cells display a resting naïve phenotype in all analysed organs (**Fig. 12B**). However, their functionality and capability to get activated was still to be investigated. To this purpose, we performed *in vitro* culture experiments in which we tested whether Env126 CD4⁺T cells could get activated under Ag-specific or Ag-independent stimuli.

To this end, we first tested Env126 CD4⁺T cells responsiveness *in vitro* after 4 hours of stimulation followed by intracellular flow cytometry staining with the purpose of detecting produced cytokines (**Fig. 14A-B**). Purified CD4⁺T cells from the spleen of both WT and Env126 mice were cultured with PMA and Ionomycin or HBsAg₁₂₆₋₁₃₈ peptide as Ag-unspecific and Ag-specific stimuli, respectively. After 4 hours *in vitro* stimulation, we observed that PMA and Ionomycin were able to stimulate the production of TNF α in CD4⁺T cells of both WT and Env126 mice (**Fig. 14B**, right plots). On the other hand, the stimulation with the cognate Ag HBs₁₂₆₋₁₃₈ specifically influenced the phenotype of only Env126 CD4⁺T cells, and not WT ones. This initially confirmed both the presence and the responsiveness of the reactive HBs-sp TCR. We also checked at the production of IFN γ cytokine and saw that, if stimulated with unspecific stimuli such as PMA and Ionomycin, both WT and Env126 CD4⁺T were able to produce IFN γ at low levels. However, the HBsAg₁₂₆₋₁₃₈ peptide was not able alone to induce and sustain a detectable IFN γ production in both WT and Env126 CD4⁺T cells (**Fig. 14B**, middle plots).

This observation is consistent with the notion that T cell *in vitro* stimulation by PMA/Ionomycin directly activate PKC and Ca²⁺ mobilization independently of the TCR stimulation, leading to the production of IFN γ down to the NF-kB pathway (Ai *et al*, 2013). On the other hand, the stimulation with the HBsAg₁₂₆₋₁₃₈ peptide alone is not able to provide proper signals to Env126 CD4⁺T that therefore produce only early activation cytokines, such as TNF α (Tuzlak *et al*, 2021).

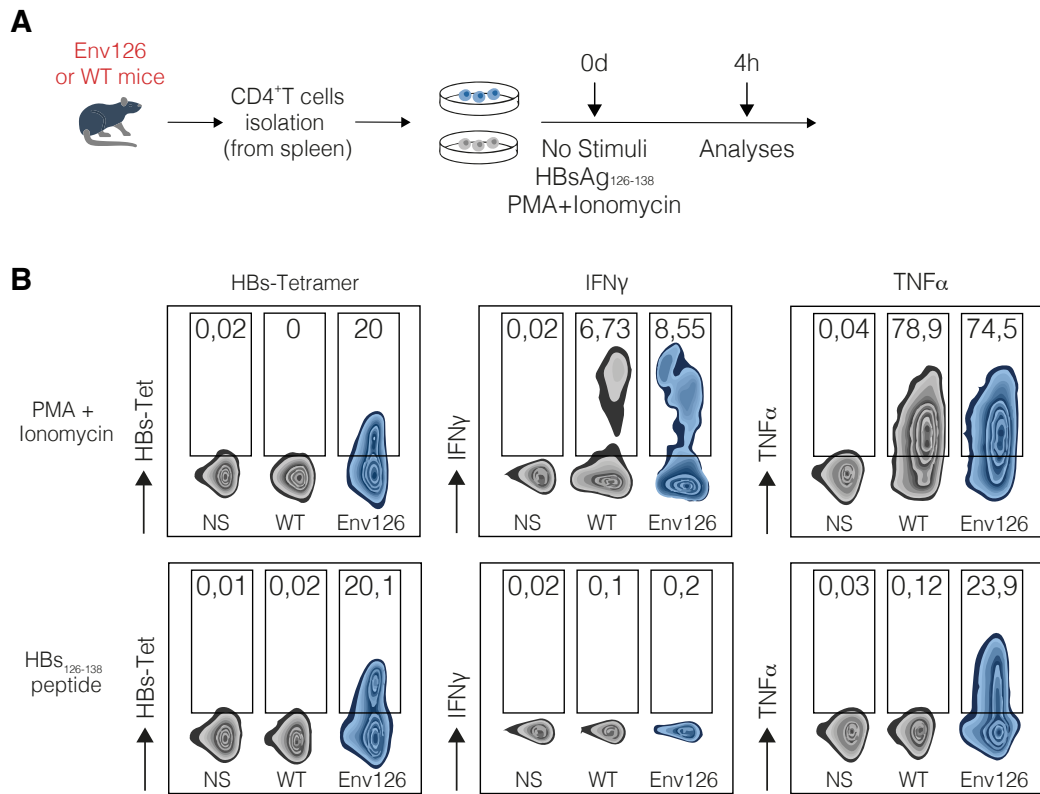


Figure 14 • Env126 CD4⁺T cells get activated *in vitro* after cognate peptide stimulation.

(A) Schematic design of the experimental setup. CD4⁺T cells from untreated WT (grey) and Env126 (blue) transgenic mice were isolated from the spleen and cultured *in vitro* under 4 hours stimulation in three different conditions: no stimuli (medium), HBsAg₁₂₆₋₁₃₈ (1 μ g/mL) or PMA (50 ng/mL) and Ionomycin (1 μ g/mL). After 4 hours, intracellular staining was performed to assess cell cytokines production. (B) Representative flow cytometry plots showing the HBs-Tetramer expression and the IFN γ and TNF α production by NS CD4⁺T cells (unstimulated WT CD4⁺T cells, n=3), stimulated WT CD4⁺T cells (grey, n=3), stimulated Env126 CD4⁺T cells (blue, n=6) under indicated stimulation condition. Upper panels show Tetramer expression and cytokines production after 4 hours stimulation with PMA and Ionomycin; bottom panels show Tetramer expression and cytokines production after 4 hours stimulation with HBsAg₁₂₆₋₁₃₈. WT CD4⁺T cells were identified as Live, CD45⁺, B220⁻CD19⁻CD8⁻CD4⁺; Env126 CD4⁺T cells were identified as Live, CD45⁺, B220⁻CD19⁻CD8⁻CD4⁺HB-Tet⁺. Data are representative of at least 3 independent experiments.

After testing their response after short *in vitro* stimulation, we tested their functionality after 48 hours *in vitro* culture to assess their proliferation capacity and expression of surface markers in different stimulation conditions. To this end, purified CD4⁺T cells from the spleen of both WT and Env126 mice were labelled with Cell Trace Violet (CTV) and put in culture with antiCD3/antiCD28 or HBsAg₁₂₆₋₁₃₈ peptide as Ag-unspecific and

Ag-specific stimuli, respectively (**Fig. 15A-C**). Treatment of T cells with monoclonal anti-CD3 antibodies and anti-CD28 antibodies provide a co-stimulatory signal that engages the TCR, this technique can be used for antigen-induced activation and was compared with the specific Ag stimulation given by cognate Ag of Env126 CD4⁺T cells. After 48 hours, CD4⁺T cells proliferation was evaluated basing on the dilution of CTV, monitored by flow cytometry assay (**Fig. 15B**). While antiCD3/antiCD28 stimulation was able to act as potent mitogen of both WT and Env126 CD4⁺T cells, HBsAg₁₂₆₋₁₃₈ was instead able to exclusively induce the proliferation of Env126 CD4⁺T cells (**Fig. 15B**). *In vitro* HBs-Ag stimulation induced only in Env126 CD4⁺T cells the upregulation of early activation markers CD44 and CD69 as well as CD25; no PD-1 expression was detected (**Fig. 15C**).

Overall, we concluded that Env126 CD4⁺TCR transgenic mice had functional HBs-sp CD4⁺T cells with naïve and resting phenotype under physiological conditions, that can possibly undergo activation upon specific-Ag recognition *in vitro* with the cognate peptide. We concluded that Env126 mice represented a proper primary source for *in vivo* adoptive transfer experiments and were suitable for further studies.

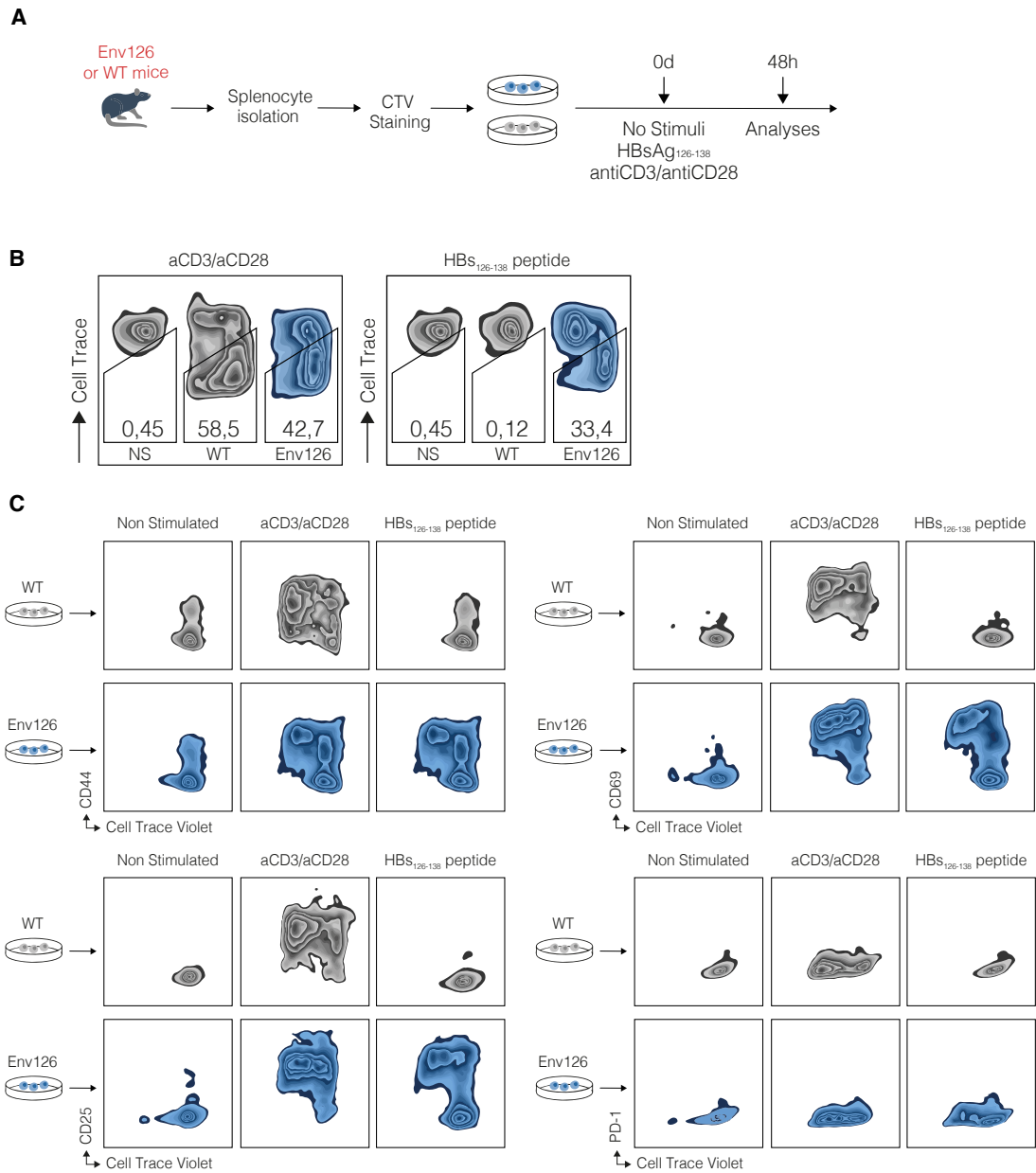


Figure 15 • Env126 CD4⁺T cells proliferate and get activated upon HBsAg recognition *in vitro*.

(A) Schematic representation of the experimental setup. Total splenocytes of WT (gray cells, n=3) or Env126 (blue cells, n=5) mice were isolated and labelled with Cell Trace Violet (CTV). Total splenocytes were *in vitro* cultured for 48 hours under three different conditions: no stimuli (medium), antiCD3/antiCD28 stimulation or HBsAg₁₂₆₋₁₃₈ (1 µg/mL). After 48 hours cells were collected and analyzed by flow cytometry to test their proliferation capacity and expression of activation surface markers. (B) Representative FACS plots showing the CTV expression by WT and Env126 CD4⁺T cells after 48 hours of culture in three different conditions. i) no stimuli (NS, n=3) ii) antiCD3/antiCD28 (left panel, WT in grey n=3, Env126 in blue n=5) or HBsAg₁₂₆₋₁₃₈ peptide (right panel, WT in grey n=3, Env126 in blue n=5). WT and Env126 CD4⁺T cells were identified as Live, CD45⁺, B220⁻CD19⁻CD8⁻CD4⁺ (C) Representative FACS plots showing CTV expression compared with different surface marker expression on total CD4⁺T cells from both

WT (grey plots, n=3) and Env126 (blue plots, n=5) after 48 hours of indicated stimulation conditions. CTV expression is measured on the X axis compared with CD44 (upper left panel), CD69 (upper right panel), CD25 (bottom left panel), PD-1 (bottom right panel) surface expression. WT CD4⁺T cells were identified as Live, CD45⁺, B220⁻CD19⁻ CD8⁻ CD4⁺. Env126 CD4⁺T cells were identified as Live, CD45⁺, B220⁻CD19⁻ CD8⁻ CD4⁺HBs-Tet⁺. Data are representative of at least 3 independent experiments.

5.1.4. Naïve Env126 CD4⁺ T response in HBV-Tg mice

After assessing the *in vitro* specificity and functionality of Env126 CD4⁺T cells, we wanted to evaluate their *in vivo* response. This was done by taking advantage of 1.3.32 transgenic mice, an HBV-replication competent transgenic mouse model already well established in our laboratory (HBV-Tg, lineage 1.3.32). HBV-Tg mice have been used as recipient mice for all the next experiments that will be shown, if not otherwise indicated. In HBV-Tg mice almost the totality (~98%) of hepatocytes expresses all HBV proteins and replicate HBV at high levels without any evidence of cytopathology (Guidotti *et al*, 1995). HBV-Tg mice are immunocompetent mice and completely tolerant at the T cell level (Guidotti *et al*, 1995; Iannacone & Guidotti, 2015).

To understand the *in vivo* response of Env126 CD4⁺T cells, purified naïve Env126 CD4⁺T cells (CD4 T_N Env126) were adoptively transferred into HBV-replication competent transgenic mice (HBV-Tg) and WT mice as a control (**Fig. 16A**). The sALT activity was monitored in the blood of transferred mice at different time points pre- and post-cell transfer. Mice were sacrificed at day 5 post cell transfer and immune composition of liver, spleen, peripheral and draining lymph nodes was analysed by flow cytometry (**Fig. 16A**).

The transfer of 10⁶ naïve Env126 CD4⁺T cells in HBV-Tg mice did not lead to any rise in sALT activity (**Fig. 16B**), indicating the absence of T-cell mediated liver damage. We found that Env126 CD4⁺T cells were detectable in the liver of HBV-Tg mice but not in the liver of WT mice (**Fig. 16C**). However, transferred Env126 CD4⁺ T cells represented only small percentage of total CD4⁺ T cell population (~1-2%). Absolute numbers as well indicate that Env126 CD4⁺T cells do not significantly expand when transferred into HBV-Tg mice (**Fig. 16D**).

Looking at the expression of both surface and transcriptional factors, we could confirm that the phenotype of naïve Env126 CD4⁺T cells is comparable in the liver of WT and HBV-Tg mice (**Fig. 16E**). Indeed, in both conditions Env126 CD4⁺T cells were driven to express levels of master regulator transcription factors as T-bet, Foxp3 or Bcl-6 that were similar to the ones expressed by WT control CD4⁺T cells (**Fig. 16E**, upper left panels); indicating the absence of a precise directed differentiation of Env126 CD4⁺T cells after recognizing cognate Ag in HBV-Tg mice. This was confirmed by the absence of effector cytokines production (**Fig. 16E**, bottom left panels) and the comparable expression levels T cell activation surface markers between Env126 in the two conditions.

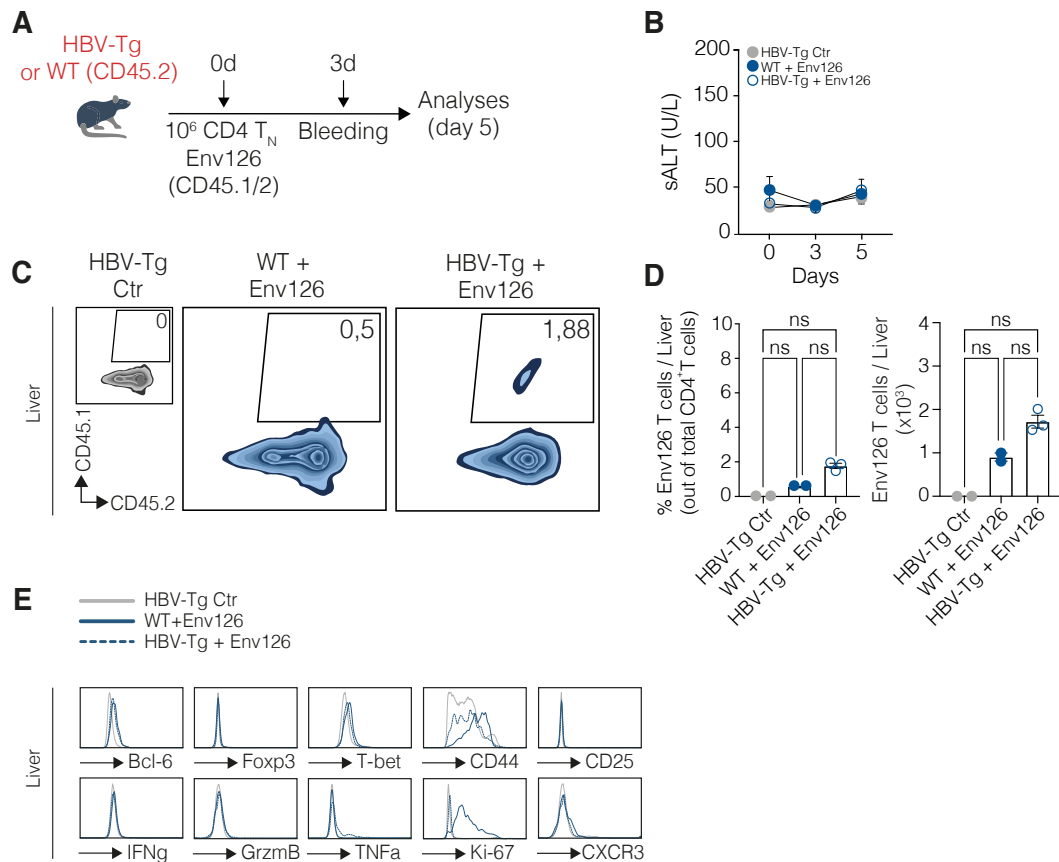


Figure 16 • Naïve Env126 CD4⁺T cells slightly expand and activate but do not differentiate, when transferred into HBV-Tg mice.

(A) Schematic design of the experimental setup: HBV-Tg (CD45.2) mice were injected (intravenously) with 10^6 naïve Env126 CD4⁺T cells (CD4 T_N Env126, CD45.2). As a control, WT mice (CD4 T_N Env126, CD45.2) were as well transferred in parallel with 10^6 naïve Env126 CD4⁺T cells (CD45.1/2); untreated HBV-Tg mice were also included in the experiment as a control. Blood serum was collected immediately before, 3 days after and at day 5 after cell transfer for sALT activity measurement. Mice were sacrificed at day 5 post cell transfer when spleen and liver of untreated control of cell-transferred mice were collected. (B) Serum transaminase activity (sALT) in untreated and WT and HBV-Tg mice transferred with at indicated time points. (C) Representative flow cytometry plots showing the frequency of Env126 CD4⁺T cells in the liver of untreated mice (HBV-Tg Ctr, grey left plot n=2), WT mice transferred with Env126 CD4⁺T cells (WT + Env126, middle blue plot, n=2) and HBV-Tg mice transferred with Env126 CD4⁺T cells (HBV-Tg + Env126, right blue panel n=3). Env126 CD4⁺T cells were defined as Live, CD45⁺, B220⁻CD19⁻, CD8⁻CD4⁺, CD45.1⁺ CD45.2⁺. (D) Env126 T cell frequency out of total CD4⁺T cell population in the liver of indicated groups of mice at day 5 post cell-transfer (left graph); absolute Env126 T cells numbers in the liver of indicated groups of mice at day 5 post cell transfer (right graph). Env126 CD4⁺T cells were defined as Live, CD45⁺, B220⁻CD19⁻, CD8⁻CD4⁺, CD45.1⁺ CD45.2⁺. (E) MFI of indicated surface markers, intranuclear transcriptional factors or proteins, and cytokines, in CD45.1/2⁺ Env126 CD4⁺T cells at day 5 post transfer in the liver of WT (continuous line, blue) and HBV-Tg mice (segmented lines, blue); grey lines

represent MFI levels of indicated markers in endogenous CD45.2⁺CD4⁺T cells in the liver of untreated HBV-Tg mice as a control. Env126 CD4⁺T cells in WT and HBV-Tg mice were defined as Live, CD45⁺, B220⁻CD19⁻, CD8⁻CD4⁺, CD45.1⁺ CD45.2⁺; endogenous control CD4⁺T cells in HBV-Tg untreated mice were identified as Live, CD45⁺, B220⁻CD19⁻, CD8⁻CD4⁺ CD45.1⁻ CD45.2⁺. Data are representative of at least 3 independent experiments. Data are expressed as mean \pm SEM. ns p-value > 0.05, two-way ANOVA with Sidak's multiple comparison test (**B**) Kruskal-Wallis Test (**D**).

However, we found that when transferred into HBV-Tg mice, and not in WT mice, Env126 CD4⁺T cells expression of Ki-67 protein was increased (**Fig. 16E**, bottom right panel). Being Ki-67 a nuclear protein expressed in actively proliferating cells (Sobecki *et al*, 2016), its increased expression in Env126 CD4⁺T cells after transfer in HBV-Tg mice is consistent with the small, but still not significant, absolute number increment we could detect between the two different conditions (**Fig. 16D**).

The observation obtained from the spleen of transferred mice were mostly comparable of those we obtained for the liver (**Fig. 17A-C**). The frequency and absolute number of Env126 CD4⁺T cells in WT and HBV-Tg mice was comparable (**Fig. 17A, Fig. 17B**). Likewise, the phenotype of transferred of Env126 CD4⁺T cells in WT and HBV-Tg mice was comparable based on the MFI levels of expressed surface markers as well as intranuclear transcription factors and produced cytokines (**Fig. 17C**). However, as it was observed in the liver, Env126 CD4⁺T cells expression of Ki-67 marker was increased when transferred into HBV-Tg mice (**Fig. 17C**, bottom right panel), confirming an augmented proliferation capacity of Env126 CD4⁺T cells in the presence of the cognate Ag within HBV-Tg mice.

Of note, we were not able to spot the presence of Env126 T cells in both peripheral inguinal lymph nodes and liver-draining lymph nodes (data not shown).

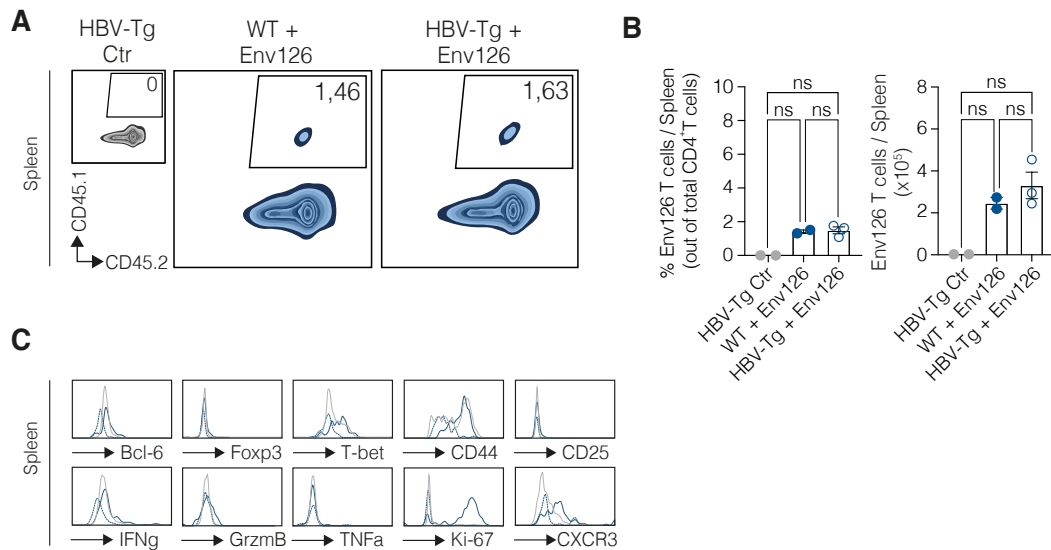


Figure 17 • Naïve Env126 CD4⁺T cells phenotype is comparable in the spleen of WT and HBV-Tg transferred mice.

Experimental setup (Fig. 16A): HBV-Tg (CD45.2) mice were injected (intravenously) with 10^6 naïve Env126 CD4⁺T cells (CD4 T_N Env126, CD45.2). As a control, WT mice (CD4 T_N Env126, CD45.2) were as well transferred in parallel with 10^6 naïve Env126 CD4⁺T cells (CD45.1/2); untreated HBV-Tg mice were also included in the experiment as a control. Blood serum was collected immediately before, 3 days after and at day 5 after cell transfer for sALT activity measurement. Mice were sacrificed at day 5 post cell transfer when spleen and liver of untreated control of cell-transferred mice were collected. (A) Representative flow cytometry plots showing the frequency of Env126 CD4⁺T cells in the spleen of untreated mice (HBV-Tg Ctr, grey left plot n=2), WT mice transferred with Env126 CD4⁺T cells (WT + Env126, middle blue plot, n=2) and HBV-Tg mice transferred with Env126 CD4⁺T cells (HBV-Tg + Env126, right blue panel n=3). Env126 CD4⁺T cells were defined as Live, CD45⁺, B220⁻CD19⁻, CD8⁻CD4⁺, CD45.1⁺ CD45.2⁺. (B) Env126 T cell frequency out of total CD4⁺T cell population in the spleen of indicated groups of mice at day 5 post cell-transfer (left graph); absolute Env126 T cells numbers in the spleen of indicated groups of mice at day 5 post cell transfer (right graph). Env126 CD4⁺T cells were defined as Live, CD45⁺, B220⁻CD19⁻, CD8⁻CD4⁺, CD45.1⁺ CD45.2⁺. (C) MFI of indicated surface markers, intranuclear transcriptional factors or proteins and cytokines in Env126 T cells at day 5 post transfer in the spleen of WT (continuous line, blue) and HBV-Tg mice (segmented lines, blue); grey lines represent MFI levels of indicated markers in endogenous CD4⁺T cells in the spleen of untreated mice as a control. Env126 CD4⁺T cells were defined as Live, CD45⁺, B220⁻CD19⁻, CD8⁻CD4⁺, CD45.1⁺ CD45.2⁺; endogenous CD4⁺T cells from untreated control WT mice were identified as Live, CD45⁺, B220⁻CD19⁻, CD8⁻CD4⁺ CD45.1⁻ CD45.2⁺. Data are representative of at least 3 independent experiments. Data are expressed as mean \pm SEM. ns p-value > 0.05, Kruskal-Wallis Test (B)

From this first experiments we concluded that the adoptive transfer into HBV-Tg mice drives Env126 CD4⁺T cells to slightly expand but is not able to lead to their activation or differentiation into effector CD4⁺T cells. This conclusion is based on the results showing

an increased in Ki-67 expression in hepatic and splenic Env126 CD4⁺T cells when transferred in HBV-Tg mice, but not in WT mice where their specific Ag is not present or expressed. This is in part consistent to what was found recently in our laboratory (Bénéchet et al, 2019) when it was shown how, in a similar pattern, CD8⁺T cells are only able to expand, but not differentiate into effector CD8⁺T cells, when transferred in HBV-Tg mice. However, despite the antigenic stimulation happening as the result of the interaction of the TCR and CD4 co-receptor with antigen-MHCII complexes, the activation and differentiation process of CD4⁺T cells is way more complicated. Indeed, CD4⁺T cells activation and lineage-specific differentiation depends on various factors: cytokine milieu of the microenvironment, concentration of antigens, type of APCs presenting the Ag and presence costimulatory signals (Luckheeram et al, 2012). We concluded that Env126 CD4⁺T cells are not able to get activated when transferred in HBV-Tg mice. Instead, they showed the ability to slightly proliferate without acquiring any T effector features. We hypothesize this could be mainly due to an inefficient priming of Env126 CD4⁺T cells and with future experiments we will focus on understanding where, when and how Env126 CD4⁺T cells are primed in HBV-Tg mice and why this leads to the observed effects.

These results, however, did not exclude a conceivable role of Env126 CD4⁺T cells in the definition, influence, and impact on CD8⁺T cell responses in our model of HBV pathogenesis. We decided then to explore this aspect and the obtained results are shown in the next paragraphs.

5.2. Exploring CD8⁺-CD4⁺ T cell cooperation in HBV pathogenesis

Coordinated cooperation between distinct cell types is a hallmark of successful immune function. Several studies have highlighted that the CD8⁺T cell responses to foreign antigens depend on CD4⁺T cell help in different pathogenic conditions (Ahrends *et al*, 2017; Aubert *et al*, 2011; Laidlaw *et al*, 2016; Novy *et al*, 2007).

Previous observations made in our lab, indicate that hepatocellular priming of HBV-sp CD8⁺ T cells triggers a unique dysfunctional program that does not overlap with that of classical exhausted T cells (Bénéchet *et al*, 2019; Guidotti *et al*, 2015; de Simone *et al*, 2021). Hepatocellular priming of naïve HBV-sp CD8⁺ T cells leads to local activation and proliferation, but lack of differentiation into effector cells; rather, it initiates a differentiation program with progressive accumulation of transcriptional and chromatin changes that ultimately result in a dysregulated T cell phenotype. Consistent with this, HBV-sp CD8⁺ T that encountered the Ag into the liver, do not respond to anti-PD-L1 therapy, but instead can be re-invigorated by IL-2 (de Simone *et al*, 2021; Bénéchet *et al*, 2019).

Our will to study CD4⁺T-CD8⁺T cell cooperation during HBV pathogenesis was then born from the hypothesis that efficient priming of CD8⁺T cells to non-cytolytic pathogens like HBV – which triggers no intrahepatic innate immune responses during the initial phase of infection – may depend on CD4⁺T cell help. This hypothesis is supported by an observation in experimentally infected chimpanzees, where CD4⁺T cell depletion before inoculation of a normally rapidly controlled inoculum precluded CD8⁺T cell priming and caused persistent infection with minimal immunopathology (Asabe *et al*, 2009). Direct evidence on this issue, however, is lacking (HBV infects only humans and chimpanzees where access to tissue specimens is lacking).

By taking advantage of HBV-sp CD8⁺ TCR transgenic mice available in our laboratory, we wanted to characterize the spatiotemporal dynamics of Env126 CD4⁺T cell activation and differentiation and explore the extent to which they can help intrahepatic CD8⁺T cell responses.

5.2.1. Adoptive transfer of naïve Env126 CD4⁺ T cells do not impact on CD8⁺T cell response in HBV-Tg mice

To study the immune mechanisms of CD4⁺T-CD8⁺T cell cooperation in HBV-Tg mice, we took advantage of envelope-specific naïve CD8⁺TCR transgenic T cells (Env28 CD8⁺T_N, Balb/c). In Env28 mice, ~80% of total CD8⁺T cells carry a reactive TCR that is specific for the epitope 28-39 contained in the surface protein of HBV (Isogawa et al, 2013). From already published data, we know that adoptively transferred Env28 CD8⁺T_N into HBV-Tg mice expressing all viral proteins in the hepatocytes, leads to their proliferation but failure in developing IFN γ or cytolytic capacities and this is mainly attributable to hepatocellular Ag presentation (Bénéchet et al, 2019).

We first wanted to understand whether the adoptive transfer of Env126 CD4⁺T cell is able to positively impact on Env28 CD8⁺T differentiation in HBV-Tg mice and we did so performing co-transfer experiments.

As first, we adoptively transfer naïve Env126 CD4⁺T cells together with naïve Env28 CD8⁺T cells in HBV-Tg mice. Briefly, naïve Env126 CD4⁺T cells and naïve Env28 CD8⁺T cells were isolated from the spleen of Env126 and Env28 transgenic mice, respectively. At day of isolation, 10⁶ naïve Env126 CD4⁺T cells (Env126 T_N) were co-transferred with 10⁶ naïve Env28 CD8⁺T cells (Env28 T_N) into HBV-Tg mice. Liver disease was monitored by sALT activity pre-transfer and at day 3 post cell transfer. The livers of co-transferred mice were surgically collected at day 5 post cell transfer and evaluated by flow cytometry and histological analyses (**Fig. 18A**). HBV-Tg mice transferred with Env28 T_N alone were included as a control, as well as untreated HBV-Tg mice.

The sALT activity was comparable between the three conditions, meaning that no T cell-mediated liver immunopathology could be highlighted at day 5 post cell transfer in HBV-Tg mice. This was true whether Env28 T_N were transferred alone or with Env126 T_N cells (**Fig. 18B**). In line with this result, no difference in Env28 T cells numbers was observed in the liver of transferred and co-transferred mice (**Fig. 18C**).

Histological analyses revealed that T cells formed peri-vascular clusters (**Fig. 18D**), a situation that is similar to chronic HBV infection (Krishna, 2021) and that was previously highlighted (Bénéchet et al, 2019). The adoptive transfer of Env126 T_N cells was not able to change this observation, as the same aggregation pattern was observed in the co-transfer condition (**Fig. 18D**).

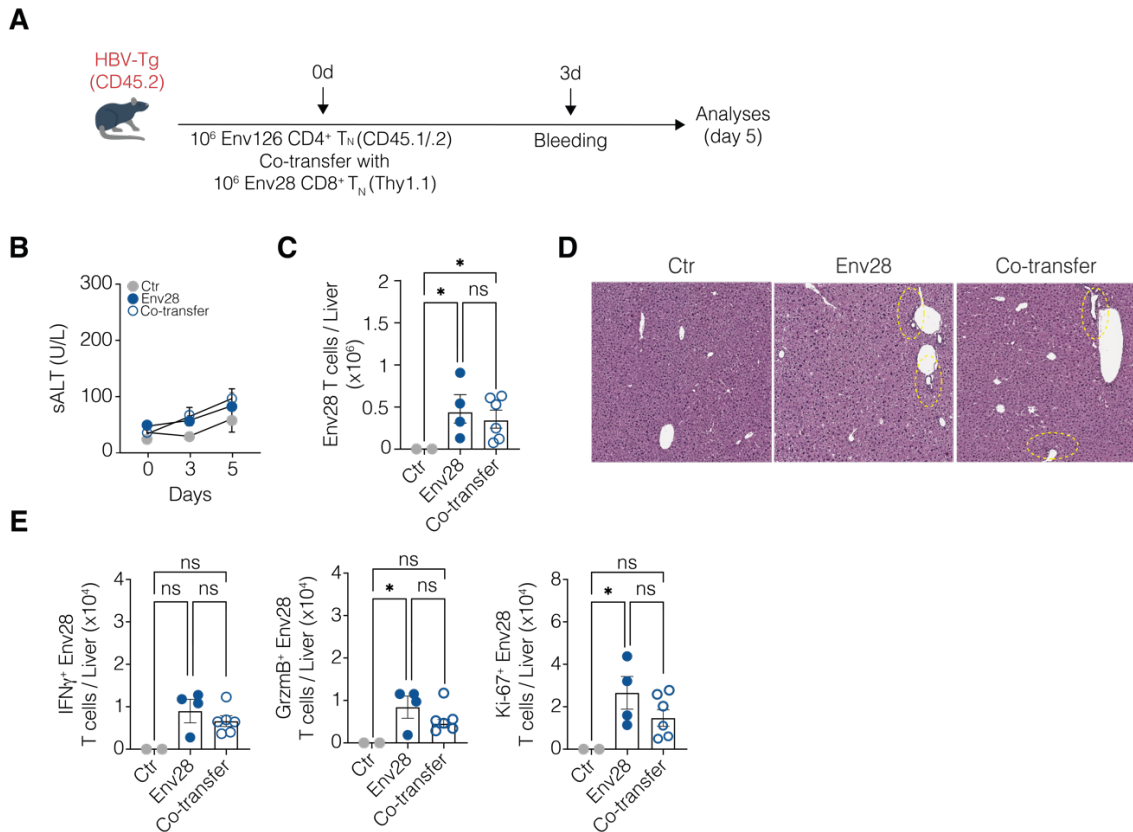


Figure 18 • Adoptive transfer of naive Env126 CD4⁺T cells do not ameliorate Env28 CD8⁺T cell effector functions in HBV-Tg mice.

(A) Experimental design. 10⁶ naïve Env126 CD4⁺T cells (Env126 T_N, CD45.1/2, C57BL/6) were co-transferred with 10⁶ naïve Env28 CD8⁺T cells (Env28 T_N, Thy1.1, Balb/c) into HBV-Tg mice (C57BL/6 x Balb/c hybrid, CD45.2) (n=6). As a control, naïve Env28 CD8⁺T cells were transferred alone in HBV-Tg mice (Env28, n=4) were included in the experiment, as well as untreated HBV-Tg mice (Ctr, n=2). sALT activity was monitored before transfer and at day 3 and 5 post cell transfer, timepoint at which all mice were sacrificed, and liver organs were surgically collected to further analyses. (B) Serum transaminase activity (sALT) in untreated HBV-Tg mice (Ctr, grey dots), HBV-Tg mice transferred with naïve Env28 (Env28, full blue dots) and HBV-Tg mice co-transferred with naïve Env28 T_N and Env126 T_N (Co-transfer, empty blue dots) at indicated time points. (C) Absolute numbers of Env28 CD8⁺T cells in the liver of indicated group of mice at day 5 post cell transfer. (D) Immunohistochemical representative micrographs of liver

sections from the indicated group of mice at day 5 post cell transfer in HBV-Tg mice. Micrographs are showing the H&E staining of liver sections highlighting the distribution of leukocyte infiltrates in the liver parenchyma. Dotted lines denote leukocyte perivascular clusters. Scale bars represent 200 μm . (E) Absolute numbers of IFN γ - (left graph) and GrzmB- (middle graph) producing Env28 CD8⁺T cells in the liver of indicated group of mice at day 5 post cell transfer upon *in vitro* 4 hours peptide restimulation. Absolute number of Ki-67 expressing Env28 CD8⁺T cells in the liver of indicated group of mice at day 5 post cell transfer is shown in the third plot. Env28 CD8⁺T cells were defined as Live, CD45⁺, B220⁻CD19⁻, CD8⁺CD4⁻, CD45.1⁻CD45.2⁻Thy1.1⁺. Data are expressed as mean \pm SEM. Data are representative of at least 3 independent experiments. ns p-value > 0.05, * p-value \leq 0.05, two-way ANOVA with Sidak's multiple comparison test (B), Kruskal-Wallis Test (C, E)

The phenotype of Env28 T cells was not altered. Indeed, the absolute number of Env28 T cells with effector or cytolytic capacities was comparable between the two conditions after *in vitro* peptide restimulation (Fig. 18E). Likewise, the proliferation level of Env28 T cells was comparable whether Env28 T_N were transferred alone or with Env126 T_N cells, as it can be inferred from Ki-67 expression levels (Fig. 18E, right histogram).

Env126 T cells, even if co-transferred with Env28 T cells, displayed the same phenotype and accumulation profile (data not shown) that was previously observed after transfer into HBV-Tg mice (Fig. 16).

With these experiments we concluded that the adoptive transfer of Env126 T_N cells was not able to sustain and/or help the response of Env28 T_N in HBV-Tg mice. We attributed these results to the activation state of Env126 T cells. As we observed that the adoptive transfer of naïve Env126 T cells into HBV-Tg mice leads to their proliferation but not to their activation or differentiation, we hypothesized that Env28 T_N cells could may benefit from activated CD4⁺T cells help, in line with the three-cell-type hypothesis (Wu & Murphy, 2022).

With next experiments, we explored different ways to activate Env126 T cells and understand in which conditions and to which extent they can help HBV-sp CD8⁺T cell immune responses against HBV.

5.2.2. Pre-*in vitro* activated Env126 CD4⁺T cells are not able to sustain CD8⁺T cell response in HBV-Tg mice

We showed that naïve Env126⁺T cell do not impact on HBV-sp CD8⁺T cell responses in HBV-Tg mice. For this reason, we wanted to assess whether *in vitro* activated Env126 T cells could instead act differently with regards to Env28 T cell responses in HBV-Tg mice. Pre-*in vitro* activation has been previously shown to be an efficient way to study the behaviour of activated CD4⁺T cells *in vivo* (Summers *et al*, 2009; Westhorpe *et al*, 2018).

We activated *in vitro* Env126 T cells as follow. Briefly, the splenocytes of Env126 mice were isolated and cultured in complete medium containing HBsAg₁₂₆₋₁₃₈ cognate peptide (1µg/mL). After 24 hours, the cells were washed and supplemented with 2.5% EL-4 supernatant. After 5 days of culture, Env126 were isolated and analysed by flow cytometry (**Fig. 19A**). Env126 T cells that were cultured as indicated were able to produce significant amount of effector cytokine TNFα after 5 days of culture (**Fig. 19B**-left panels). Of note, only small fraction of Env126 T cells was able to produce also IFNγ (**Fig. 19B**-right panels), consistent with the fact that Ag-stimulation alone is not able to drive CD4⁺T cells lineage-specific differentiation (Luckheeram *et al*, 2012). However, Env126 T cells were able to acquire a T activated phenotype as shown by the differential expression of CD44 and CD62L after *in vitro* culture with the peptide (**Fig. 19C**).

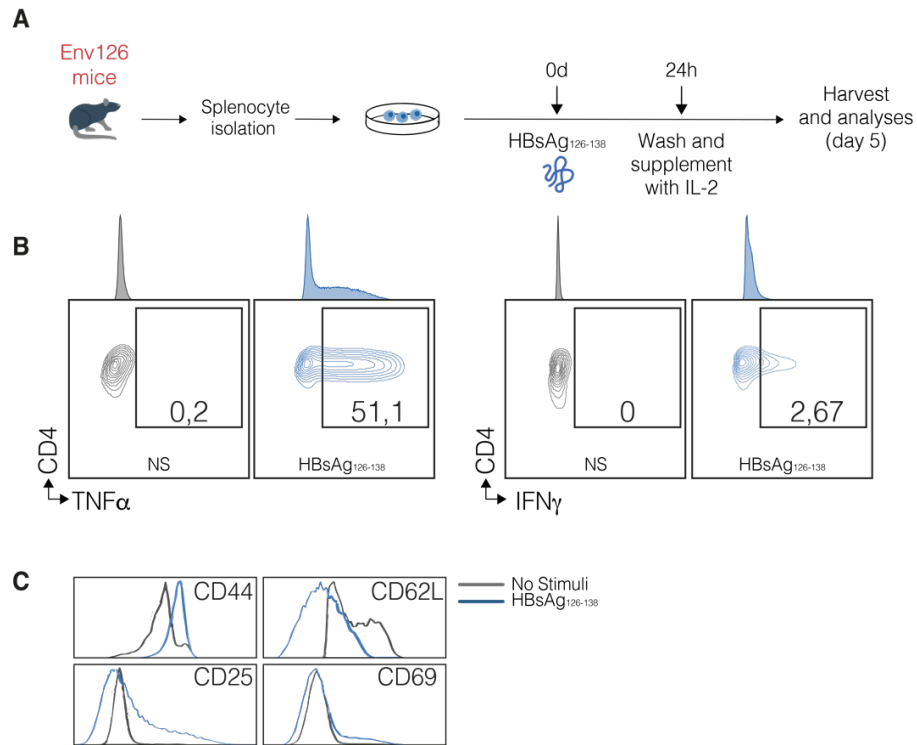


Figure 19 • *Pre-in vitro* activation of Env126 CD4⁺T cells.

(A) Schematic representation of the experimental setup used to pre-activate *in vitro* Env126 CD4⁺T cells. Splenocytes of Env126 mice were isolated and cultured at 1×10^6 cells/mL in complete medium containing HBsAg₁₂₆₋₁₃₈ (1 μ g/mL). Splenocytes of Env126 mice were also cultured with complete medium alone as a control. After 24 hours, cells were washed and supplemented with 2.5% EL-4 supernatant and after two days medium was replaced with fresh medium. After 5 days of culture, Env126 were isolated and analysed by flow cytometry. (A) Representative flow cytometry plots showing the frequency of Env126 CD4⁺T cells producing TNF α (HBsAg₁₂₆₋₁₃₈, left blue plot) or IFN γ (HBsAg₁₂₆₋₁₃₈, right blue plot) after *in vitro* peptide restimulation. Grey plots show the frequency of cytokine production in Env126 that have been not stimulated (NS, not cultured with the peptide) as a control. Upper histogram on each plot shows the MFI modal expression of indicated cytokine on Env126 CD4⁺T cells. Env126 CD4⁺T cells were defined as Live, CD45⁺, CD8⁻CD4⁺, CD45.1⁺ CD45.2⁺. (C) Representative modal MFIs histograms of indicated markers on Env126 CD4⁺T cells at day 5 post culture after peptide pulsing (HBsAg₁₂₆₋₁₃₈, blue lines). MFIs of indicated markers in non-stimulated CD4⁺T cells are shown as a control (NS, grey lines). Env126 CD4⁺T cells were defined as Live, CD45⁺, CD8⁻CD4⁺, CD45.1⁺ CD45.2⁺. Data are representative of at least 2 independent experiments.

We then wanted to understand whether a pre-activated state of Env126 T cells could change their impact on Env28 T cell responses in HBV-Tg mice.

We performed the same *pre-in vitro* activation strategy above shown in order to obtain *pre-in vitro* activated Env126 T cells (Env126 T_A). Briefly, the splenocytes of Env126 mice were isolated and cultured in complete medium containing HBsAg₁₂₆₋₁₃₈ cognate peptide. After 24 hours, the cells were washed and supplemented with 2.5% EL-4 (**Fig. 20A**). After 5 days of culture, Env126 T_A were isolated and co-transferred with naïve Env28 T cells (Env28 T_N) in HBV-Tg mice in a ratio 1:1 (10⁶ Env126 T_A with 10⁶ Env28 T_N). Liver disease was monitored by sALT activity and the liver of experimental mice was analysed in their composition at day 5 post cell transfer by flow cytometry (**Fig. 20A**).

No difference in the sALT activity curves was highlighted between the three conditions, suggesting the absence of any T cell-mediated liver immunopathology at day 5 post cell transfer in HBV-Tg mice (**Fig. 20B**). No effect on Env28 T cell accumulation was observed, as the absolute number of on Env28 T cells was comparable in the presence or absence of Env126 T cells (**Fig. 20C**). Moreover, the effector and cytolytic capacity of Env28 T cells was not positively influenced as shown by the total IFN γ - and GrzmB-producing Env28 T cells at day 5 post cell transfer (**Fig. 20D**). Consistently, histological analyses did not reveal any substantial alteration in the liver parenchyma or T cell clusters pattern: T cells formed perivascular tracts in both conditions, as it was already observed (**Fig. 18D**).

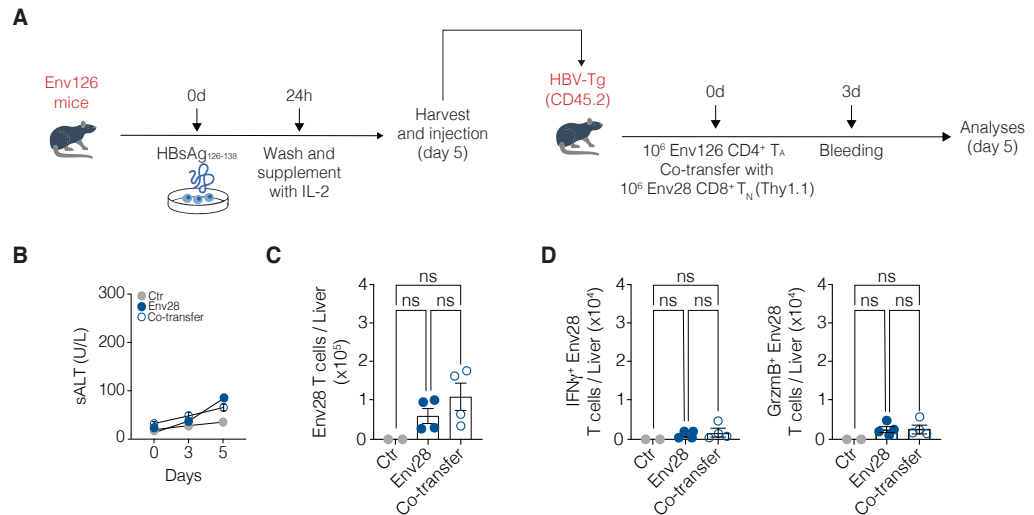


Figure 20 • Adoptive transfer of pre-*in vitro* activated Env126 CD4⁺T_A do not impact on Env28 CD8⁺T cell responses in HBV-Tg mice.

(A) Experimental setup. Splenocytes of Env126 mice were isolated and cultured at 1×10^6 cells/mL in complete medium containing HBsAg₁₂₆₋₁₃₈ ($1 \mu\text{g/mL}$). Splenocytes of Env126 mice were also cultured with complete medium alone as a control. After 24 hours, cells were washed and supplemented with 2.5% EL-4 supernatant and after two days medium was replaced with fresh medium. After 5 days of culture, pre-*in vitro* activated Env126 CD4⁺T cells (Env126 CD4⁺T_A, CD45.1/2) were isolated and 10^6 cells were co-transferred in HBV-Tg mice (C57BL/6 x Balb/c hybrid, CD45.2) with 10^6 naïve Env28 CD8⁺T cells (Env28, Balb/c, Thy1.1) (Co-transfer, $n=4$). As a control, HBV-Tg mice transferred with Env28 CD8⁺T cells alone were included in the experiment (Env28, $n=4$), as well as untreated HBV-Tg mice (Ctr, $n=2$). HBV-Tg mice were monitored in their sALT activity immediately pre-transfer and at day 3 and 5 post transfer, time point at which transferred mice were sacrificed and spleen and liver were analysed. (B) Serum transaminase activity (sALT) in untreated (Ctr, grey dots) HBV-Tg mice, HBV-Tg mice transferred with naïve Env28 (Env28, full blue dots) and HBV-Tg mice co-transferred with naïve Env28 and Env126 CD4⁺T_A (Co-transfer, empty blue dots) at indicated time points. (C) Absolute numbers of Env28 CD8⁺T cells in the liver of indicated group of mice at day 5 post cell transfer. (D) Absolute numbers of IFN γ - (left graph) and GrzmB- (right graph) producing Env28 CD8⁺T cells in the liver of indicated group of mice at day 5 post cell transfer upon *in vitro* 4 hours peptide restimulation. Env126 CD4⁺T cells were defined as Live, CD45⁺, B220⁻CD19⁻, CD8⁻CD4⁺, Thy1.1⁻ CD45.1⁺ CD45.2⁺. Env28 CD8⁺T cells were defined as Live, CD45⁺, B220⁻CD19⁻, CD8⁺CD4⁺, CD45.1⁻CD45.2⁺Thy1.1⁺. Data are expressed as mean \pm SEM. Data are representative of at least 2 independent experiments. ns p-value > 0.05 , two-way ANOVA with Sidak's multiple comparison test (B), Kruskal-Wallis Test (C-D)

With this experiment we concluded that, even if already activated and *in vitro* pulsed, Env126 T cells were not able to sustain and/or help the response of Env28 T_N in HBV-Tg mice. This result was attributed to the fact that pre-*in vitro* pulsed Env126 T cells display an activated phenotype without having acquired a lineage-specific differentiation profile, that instead may be beneficial for Env28 T response. T-helper 1 T cells are known to be the one responsible for driving the help to CTL responses (Borst *et al*, 2018; Laidlaw *et al*, 2016) and for this reason, we cogitated that Th1 Env126 T cells may be required to sustain HBV-sp CD8⁺T cell responses in our model of HBV pathogenesis.

5.2.3. Generation of T_{h1}-like Env126 CD4⁺T cells

In the previous paragraphs, we have shown that both naïve and pre-*in vitro* activated Env126 T cells do not help or rescue the dysfunctional CD8⁺T cell responses in HBV-Tg mice. We hypothesized that this could be probably linked to the fact that Env126 T cells should acquire a proper lineage-specific commitment to drive the help to the CD8⁺T cell compartment.

We therefore attempted to differentiate Env126 T cells into antiviral effector T helper 1 (Th1) CD4⁺T cells with an *in vivo* activation strategy.

We used Rag1^{-/-} mice as recipients in which we transferred 10⁵ Env126 naïve CD4⁺T cells and that we subsequently infected 24 hours later with a recombinant vesicular stomatitis virus encoding for the HBV middle surface envelope glycoprotein (rVSV/s) (Cobleigh *et al*, 2013). Mice were sacrificed at day 7 post infection and the Env126 T cell phenotype was analysed by FACS (**Fig. 21A**).

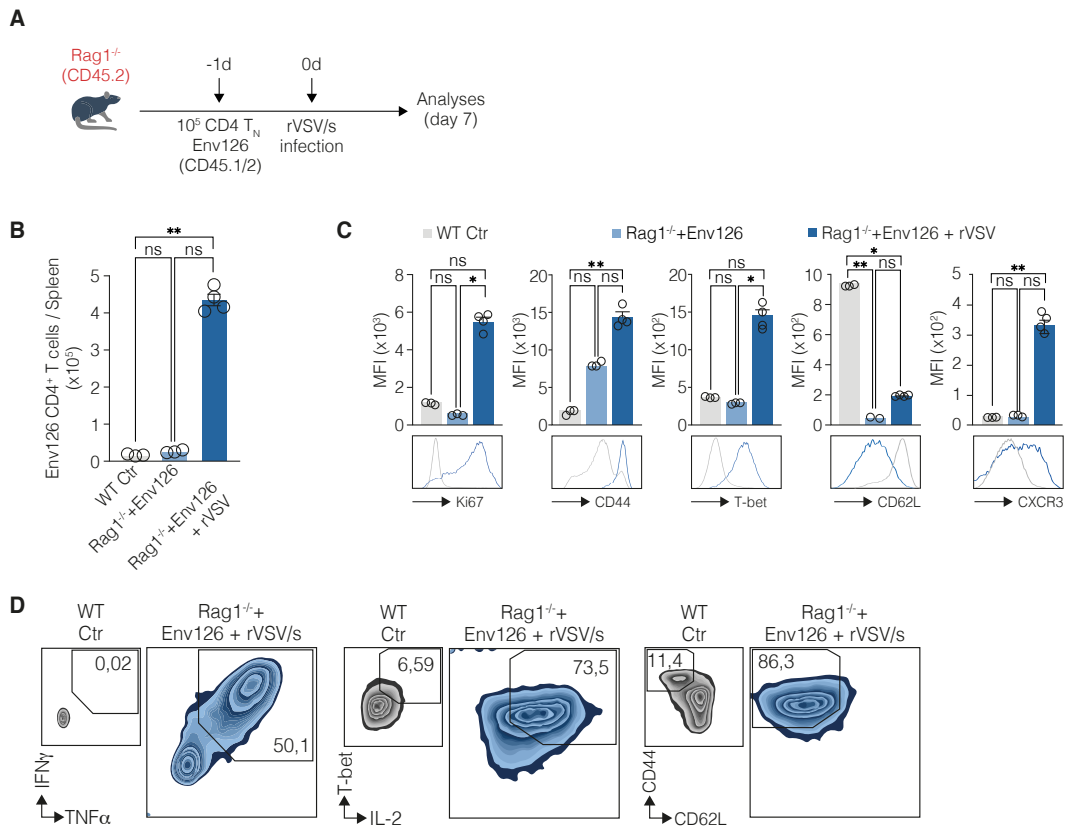


Figure 21 • *In vivo* differentiation of Env126 CD4⁺T transgenic T cells into Th1-like effector CD4⁺T cells.

(A) Schematic design of the experimental setup. Rag1^{-/-} mice (CD45.2, C57BL/6, n=9) were injected intravenously with 10⁵ naïve Env126 transgenic CD4⁺T cells (CD45.1/2). WT untreated mice were included in the experiment as a control (n=3). After 24 hours, a group of Rag1^{-/-} mice (n=6) was infected with rVSV/s. After 7 days, spleens of the three groups of mice were surgically collected and their composition was analysed by flow cytometry. (B) Absolute numbers of Env126 CD4⁺T cells in the spleen of indicated groups of mice at day 7 post infection. (C) Histograms of the MFIs of Ki-67, CD44, T-bet, CD62L and CXCR3 markers on splenic Env126 CD4⁺T cells in indicated group of mice at day 7 post infection (upper histograms). In untreated WT mice, MFIs were calculated on endogenous polyclonal CD4⁺T cells. Under each histogram are depicted representative MFIs of indicated markers on Env126 CD4⁺T cells at day 7 post transfer in the spleen of rVSV/s infected Rag1^{-/-} mice (blue line) and MFIs of indicated markers in endogenous CD4⁺T cells in untreated mice as a control (grey lines). (D) Representative flow cytometry plots showing the frequency of splenic Env126 CD4⁺T cells (blue plots) producing IFN γ and TNF α (left plot), expressing T-bet and producing IL-2 (middle plot) and displaying CD44^{high} and CD62L^{low} phenotype (right plot). Each plot is compared with the same frequencies in endogenous CD4⁺T cells in untreated WT mice (grey plots). Env126 CD4⁺T cells were defined as Live, CD45⁺, B220⁻CD19⁻, CD8⁻CD4⁺, CD45.1⁺ CD45.2⁻; endogenous CD4⁺T cells from untreated WT control were identified as Live, CD45⁺, B220⁻CD19⁻, CD8⁻CD4⁺ CD45.1⁻ CD45.2⁺. Data are expressed as mean \pm SEM. Data are representative of at least 10 independent experiments. ns p-value > 0.05 * p-value \leq 0.05, ** p-value \leq 0.01, Kruskal-Wallis Test (B), one-way ANOVA with Sidak's multiple comparison test (C)

We observed that splenic Env126 T cells significantly expand when Rag1^{-/-} mice underwent rVSV/s infection (**Fig. 21B**). Moreover, not only absolute numbers of Env126 T cells were augmented, but also their phenotype was substantially impacted. Indeed, we saw that following rVSV/s infection, Env126 T cells were expressing effector surface markers, displaying a CD62L^{low}CD44^{high}Ki-67^{high} phenotype (**Fig. 21C-D**), a typical profile that distinguishes effector T cells from their naïve counterparts (Kaech & Cui, 2012). Together with this, Env126 T cells started expressing CXCR3 as a surface marker and the master regulator T-bet (**Fig 21C**), all signatures of T_{h1} commitment (Zhou *et al*, 2009). After 4 hours *in vitro* peptide re-stimulation, we could also highlight that Env126 could produce high quantities of IFN γ , TNF α and IL-2 (**Fig. 21D**). All these observed characteristics were not present if Env126 were transferred into WT mice or in uninfected Rag1^{-/-} mice (**Fig. 21B-D**). Taking all this results together, we concluded that Env126 T cells were able to proliferate, get activated and acquire a T_{h1}-like identity in the abovementioned setup.

As a conclusion, we found a way to *in vivo* pre-activate Env126 T cells into Th1-like effector HBV-sp T cells (**Fig. 21A**). The obtained activated and differentiated CD4⁺T cells population display a typical CD4⁺T_{h1} phenotype that efficiently encountered the cognate-Ag. T_{h1}-like T_E Env126 T cells do also express CXCR3, a G α_j protein-coupled receptor abundantly expressed on activated T lymphocytes and more particularly on T_{h1}CD4⁺T cells (**Fig. 21B**) (Karin, 2020). Moreover, they start expressing T-bet and can produce IFN γ and TNF α after *in vitro* peptide restimulation (**Fig. 21C**). In line with classical T_{h1} phenotype, Env126 T_E produce IL-2 after *in vitro* peptide restimulation, a cytokine that has also recently been described as therapeutic target able to rescue dysfunctional CD8⁺T cells in the context of HBV pathogenesis (Bénéchet *et al*, 2019).

5.2.4. Adoptive transfer of T_{h1}-like Env126 CD4⁺T cells improves Env28 CD8⁺T cell proliferation and effector differentiation in HBV-Tg mice

Since we showed that both naïve and pre-*in vitro* pulsed Env126 T cells are not able to sustain and impact on HBV-sp CD8⁺T cells response in HBV-Tg mice, we wanted then to assess whether T_{h1}-like T_E Env126 T cells were able to sustain HBV-sp CD8⁺T cells response in HBV-Tg mice.

We first generated T_{h1}-like T_E Env126 CD4⁺T cells with the same experimental setup above mentioned (**Fig. 21**). Briefly, we used Rag1^{-/-} mice as recipients in which we transferred 10⁵ Env126 naïve CD4⁺T cells and that we subsequently infected 24 hours later with rVSV/s (Cobleigh *et al*, 2013). Mice were sacrificed at day 7 post infection and T_{h1}-like T_E Env126 T cells (Env126 T_E) were isolated from the spleen of infected mice (**Fig. 22A-left**). At the same time point, 10⁶ Env126 T_E were co-transferred into HBV-Tg with 10⁶ Env28 naïve CD8⁺T cells (Env28 T_N). HBV-Tg mice transferred with 10⁶ Env28 naïve CD8⁺T cells alone were included as a control, as well as untreated HBV-Tg mice. All mice were monitored in their sALT activity immediately before and at day 3 post cell transfer and sacrificed after 5 days. Here, livers of treated and untreated mice were surgically collected and analysed in their composition by flow cytometry (**Fig. 22A-right**).

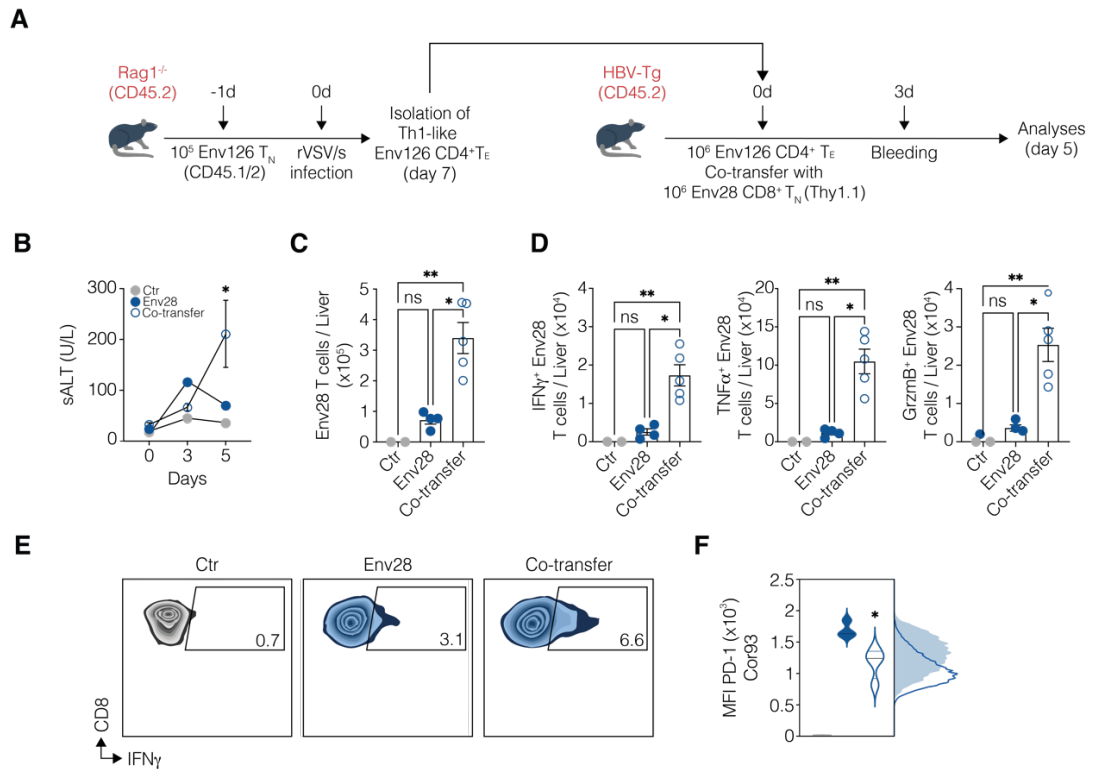


Figure 22 • Adoptive transfer of Th₁-like effector Env126 CD4⁺T cells improves Env28 CD8⁺T cell effector function.

(A) Schematic design of the experimental setup. 10⁵ naïve Env126 CD4⁺T cells (CD45.1/2) were injected intravenously in Rag1^{-/-} mice (CD45.2) which have then been infected with rVSV/s after 24 hours. At day 7 post infection, spleen of injected and infected Rag1^{-/-} mice were surgically collected and Env126 CD4⁺T cells were isolated. At same time point, 10⁶ of the isolated Th1-like T_E Env126 CD4⁺T cells (CD45.1/2) were co-transferred in HBV-Tg mice (C57BL/6 x Balb/c hybrid, CD45.2) with 10⁶ naïve Env28 CD8⁺T cells (Balb/c, Thy1.1) (n=5). As a control, HBV-Tg mice transferred with Env28 CD8⁺T cells alone were included in the experiment (Env28, n=4), as well as untreated HBV-Tg mice (Ctr, n=2). HBV-Tg mice were monitored in their sALT activity immediately pre-transfer and at day 3 and 5 post transfer, time point at which transferred mice were sacrificed and spleen and liver were analyzed. (B) Serum transaminase activity (sALT) in untreated (Ctr, grey dots) HBV-Tg mice, HBV-Tg mice transferred with Env28 (Env28, full blue dots) and HBV-Tg mice co-transferred with Env28 and Env126 (Co-transfer, empty blue dots) at indicated time points. (C) Absolute numbers of Env28 CD8⁺T cells in the liver of indicated group of mice at day 5 post cell transfer. (D) Absolute numbers of IFN γ - (left graph), TNF α - (middle graph) and GrzmB- (right graph) producing Env28 CD8⁺T cells in the liver of indicated group of mice at day 5 post cell transfer, upon *in vitro* 4 hours peptide restimulation. (E) Representative flow cytometry plots showing the frequency of Env28 CD8⁺T cells producing IFN γ in the liver of indicated group of mice at day 5 post cell transfer upon *in vitro* peptide restimulation (blue plots, middle and right). Ctr plot (grey, left) show the frequency of IFN γ producing endogenous CD8⁺T cells in untreated HBV-Tg mice. Env126 CD4⁺T cells were defined as Live, CD45⁺, B220⁻CD19⁻, CD8⁻CD4⁺, Thy1.1⁻CD45.1⁺CD45.2⁺. Env28 CD8⁺T cells were defined as Live, CD45⁺, B220⁻CD19⁻, CD8⁺CD4⁻, CD45.1⁻CD45.2⁺Thy1.1⁺. Endogenous CD8⁺T cells from untreated mice were identified as Live, CD45⁺, B220⁻CD19⁻, CD8⁺CD4⁻, CD45.1⁻CD45.2⁺Thy1.1⁻. (F) Violin plot showing MFI values of PD-1 expression on hepatic Env28 at day 5 post cell transfer in HBV-Tg mice in indicated group of mice (Env28, full blue

violin plot and Co-transfer, empty blue violin plot). In untreated WT mice, MFIs were calculated on endogenous CD8⁺T cells (Ctr, grey violin plot). On right side of the plot are depicted representative MFIs modal curves on Env28 T cells in indicated group of mice (Env28, full light blue curve and Co-transfer, dark blue line). Data are expressed as mean ± SEM. Data are representative of at least 5 independent experiments. ns p-value > 0.05 * p-value ≤ 0.05, ** p-value ≤ 0.01, two-way ANOVA with Sidak's multiple comparison test (**B**) Kruskal-Wallis Test (**C-D**)

At day 5 post cell transfer, a slight rise trend in sALT concentration was observed in HBV-Tg mice that were co-transferred with Env28 T and Env126 T cells (**Fig. 22B**). Interestingly, in the liver of co-transferred mice we observed an increase in the absolute numbers of Env28 T cells, that evidently benefitted from the presence of Env126 T_E cells (**Fig. 22C**).

When co-transferred with Env126 T_E cells, Env28 T cells were not only able to accumulate more in the liver, but also their effector phenotype was ameliorated. Indeed, Env28 T cells were more prone to produce IFN γ , TNF α and GrzmB in the presence of Env126 T_E cells, as the absolute number of IFN γ -, TNF α - and GrzmB- producing Env28 T cells was increased in co-transferred mice after *in vitro* peptide restimulation (**Fig. 22D**). Moreover, the intrinsic capacity of Env28 T cells to produce effector cytokines was as well increased, as shown by the frequency of Env28 T cells producing effector cytokines (**Fig. 22E**). On the other hand, the transfer of Env28 T cells alone in HBV-Tg mice led to their progression into dysfunctional CD8⁺T cells that produce little or no effector and cytolytic capacities upon *in vitro* peptide restimulation, as previously shown (Bénéchet et al, 2019; de Simone et al, 2021). Of note, we observed a significant reduction in PD-1 expression levels on Env28 T cells when they were co-transferred with Env126 T_E cells in HBV-Tg mice (**Fig. 22F**).

In line with the augmented accumulation of Env28 T cells in the liver of co-transferred mice, we noticed a positively effect on Env28 T cells proliferation in the presence of Env126 T_E cells. Indeed, when Env126 T_E cells were present, Env28 T cells presented an increased expression of Ki-67 (**Fig. 23A, B**), indicating an ameliorated proliferation capacity. We also observed a differential Ki-67 expression in Env28 T cells, being able to distinguish between medium- and high- Ki-67 expressing cells (**Fig. 23C**). When co-

transferred with Env126 T_E cells, the frequency of Env28 T cells expressing Ki-67 at high levels was strongly increased (**Fig. 23C, D**). Rather, when Env28 T cells were transferred alone into HBV-Tg mice, the fraction that expressed the protein at medium levels was more prominent (**Fig. 23C**).

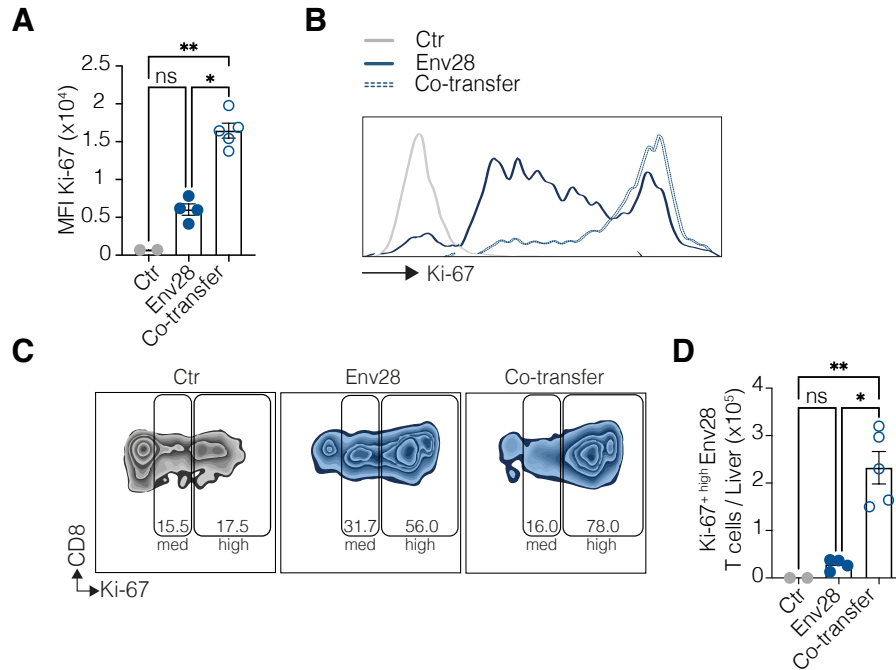


Figure 23 • Adoptive transfer of T_{H1}-like effector Env126 CD4⁺T cells improves Env28 CD8⁺T cell proliferation.

10⁶ naïve Env28 CD8⁺T cells were transferred in HBV-Tg mice with or without 10⁶ Th1-like T_E Env126 CD4⁺T cells (CD45.1/2), HBV-Tg untreated mice were used as a control. Experimental mice were sacrificed 5 days post cell transfer and the liver was analyzed by flow cytometry. (**A**) Histograms of the MFIs of Ki-67 on hepatic Env28 CD8⁺T cells at day 5 post transfer (Env28, full blue dots) or post co-transfer (Co-transfer, empty blue dots) with Env126 CD4⁺T cells in HBV-Tg mice. As a control, Ki-67 MFI was calculated on endogenous CD8⁺T cells of untreated mice (Ctr, grey dots). (**B**) MFI representative modal expression of Ki-67 on hepatic Env28 CD8⁺T cells at day 5 post transfer (continuous blue line), or post co-transfer (segmented blue line) with Env126 CD4⁺T cells in HBV-Tg mice. Grey line represents Ki-67 MFI on CD8⁺T cells in untreated HBV-Tg mice. (**C**) Representative flow cytometry plots showing the frequency of Env28 CD8⁺T cells expressing Ki-67 at medium (med, left gate) and high (high, right gate) levels at day 5 post transfer and co-transfer in HBV-Tg mice (blue plots). Grey plot (Ctr, left panel) represents frequency of CD8⁺T cells expressing Ki-67 at medium (med, left gate) and high (high, right gate) levels in untreated mice. Env28 CD8⁺T cells were defined as Live, CD45⁺, B220⁻CD19⁻, CD8⁺CD4⁺, CD45.1⁻CD45.2⁺Thy1.1⁺. Endogenous CD8⁺T cells from untreated mice were identified as Live, CD45⁺, B220⁻CD19⁻, CD8⁺CD4⁺, CD45.1⁻CD45.2⁺Thy1.1⁺. (**D**) Absolute numbers of Ki-67 high-expressing Env28 CD8⁺T cells in the liver

of indicated group of mice at day 5 post cell transfer. Data are expressed as mean \pm SEM and are representative of at least 5 independent experiments. ns p-value > 0.05 * p-value ≤ 0.05 , ** p-value ≤ 0.01 , two-way ANOVA with Sidak's multiple comparison test (A), Kruskal-Wallis Test (D)

We concluded then that the adoptive transfer of Env126 T_E cells is able to improve Env28 T cells proliferation and also their effector cytolytic capacity. Of note, none of the reported effects were observed neither in the spleen nor in both peripheral or liver-draining lymph nodes.

Looking at Env126 T cells, we observed that at day 5 post cell transfer they were still trackable in the liver of HBV-Tg mice. Of note, almost the totality of Env126 T cells was highlighted in the liver and not in the spleen of co-transferred mice (**Fig. 24A**). The phenotype of T_{h1}-like Env126 T_E cells was maintained at day 5 post transfer in the liver of HBV-Tg mice. Indeed, Env126 T_E cells were still displaying a CD44^{high}CD62L^{low}Tbet^{high}Ki-67^{high} profile (**Fig. 24B, C**) and still were able to produce T_{h1}-cytokines such as TNF α , IFN γ and IL-2 (**Fig. 24C**) upon *in vitro* peptide restimulation. These data indicated that at day 5 post transfer with Env28 T cells in HBV-Tg mice, Env126 T_E cells could preserve their phenotype and accumulated preferentially in the liver.

Of note, it is important to mention that a group in which Env126 T_E cells were transferred alone in HBV-Tg mice was included in the experiments discussed (data not shown). In detail, HBV-Tg mice were transferred with 10⁶ Env126 effector CD4⁺T cells alone and were included as a control in the experiments. When transferred alone, in the absence of Env28 T cells, Env126 T_E cells did not cause any liver immunopathology, assessed by sALT activity and histological analyses (data not shown), that did not reveal any alteration in liver structural and cellular composition. When transferred alone, Env126 T_E cells accumulate in the liver of HBV-Tg mice, in which they maintain their effector phenotype and capacity, as assessed by FACS analyses of surface markers expression and cytokines production after 4 hours *in vitro* peptide restimulation (data not shown).

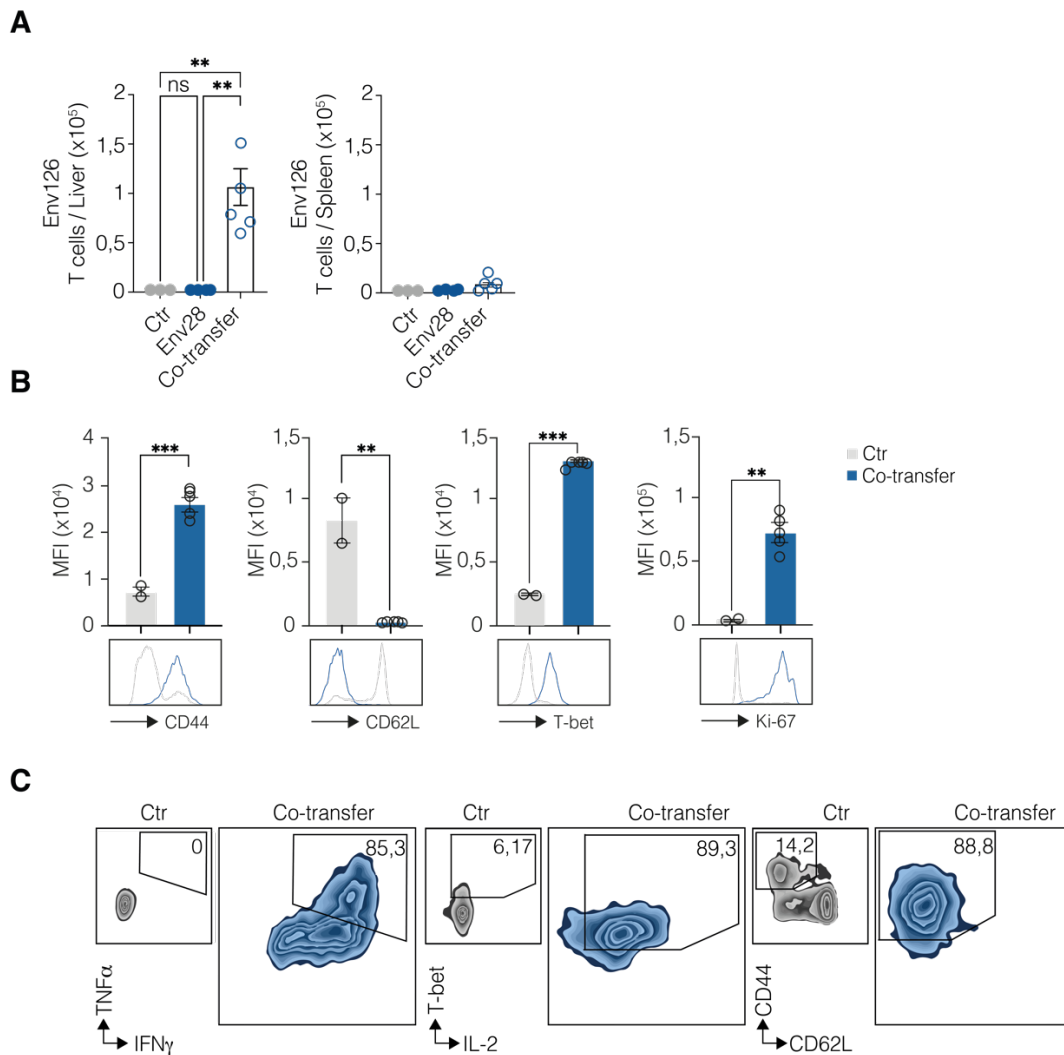


Figure 24 • Env126 preserve their Th₁-like effector phenotype after co-transfer with Env128 in HBV-Tg mice.

10⁶ naïve Env28 CD8⁺T cells were transferred in HBV-Tg mice with or without 10⁶ Th₁-like T_E Env126 CD4⁺T cells (CD45.1/2), HBV-Tg untreated mice were used as a control. Experimental mice were sacrificed 5 days post cell transfer and the liver was analyzed by flow cytometry. **(A)** Absolute numbers of Env126 CD4⁺T cells in the liver of indicated group of mice at day 5 post cell transfer. **(B)** Histograms of the MFIs of CD44, CD62L, T-bet and Ki-67 on hepatic Env126 CD4⁺T cells in indicated group of mice at day 5 post cell transfer. Env126 MFIs post cell transfer in HBV-Tg mice are compared with MFIs of same markers in untreated control mice. In untreated WT mice (Ctrl, grey), MFIs were calculated on endogenous CD4⁺T cells. Under each histogram are depicted representative modal MFIs histograms of indicated markers on Env126 CD4⁺T cells at day 5 post transfer in the liver of HBV-Tg mice co-transferred with Env28 and Env126 T cells (blue line) and MFIs of indicated markers in endogenous CD4⁺T cells in untreated mice as a control (grey lines). **(C)** Representative flow cytometry plots showing the frequency of Env126 CD4⁺T cells (blue plots) producing IFN γ and TNF (left plots), expressing T-bet and producing IL-2 (middle plots) and displaying a CD44^{high}CD62L^{low} phenotype (right

plots) in the liver of indicated group of mice at day 5 post cell transfer upon *in vitro* peptide restimulation. Ctr plot (grey, left of each plot) show the frequency of cytokines production/marker expression on endogenous CD4⁺T cells in untreated HBV-Tg mice. Env126 CD4⁺T cells were defined as Live, CD45⁺, B220⁻CD19⁻, CD8⁻CD4⁺, Thy1.1⁻ CD45.1⁺ CD45.2⁺. Endogenous CD4⁺T cells from untreated mice were identified as Live, CD45⁺, B220⁻CD19⁻, CD8⁻CD4⁺, CD45.1⁻CD45.2⁺Thy1.1⁻. Data are expressed as mean ± SEM. Data are representative of at least 5 independent experiments. ns p-value > 0.05, ** p-value ≤ 0.01, *** p-value ≤ 0.001, Kruskal-Wallis Test (A), two-way ANOVA with Sidak's multiple comparison test (B)

Subsequently, we wanted to spatially visualize the effect of the adoptive transfer of Env126 T_E cells on Env28 T cells inside the liver tissue.

To this end, we repeated the same experiment already described (Fig. 22A) using trackable reporter Env28 T cells expressing the fluorescent DsRed protein (β -actin-DsRed^{+/+} Env28 TCR mice, Balb/c). Briefly, we used Rag1^{-/-} mice as recipients in which we transferred 10⁵ Env126 naïve CD4⁺T cells and that we subsequently infected 24 hours later with rVSV/s (Cobleigh *et al*, 2013). Mice were sacrificed at day 7 post infection and T_{h1}-like T_E Env126 T cells were isolated from the spleen of infected mice (Fig. 25A-left). At same time point, 10⁶ Env126 T_E were co-transferred into HBV-Tg with 10⁶ Env28 DsRed^{+/+} naïve CD8⁺T cells (Env28 T_N DsRed). HBV-Tg mice transferred with 10⁶ Env28 T_N DsRed cells alone were included as a control, as well as untreated HBV-Tg mice. All mice were sacrificed at day 5 post cell transfer when livers of treated and untreated mice were surgically collected and resolved by flow cytometry, confocal and immunohistochemistry analyses (Fig. 25A-right).

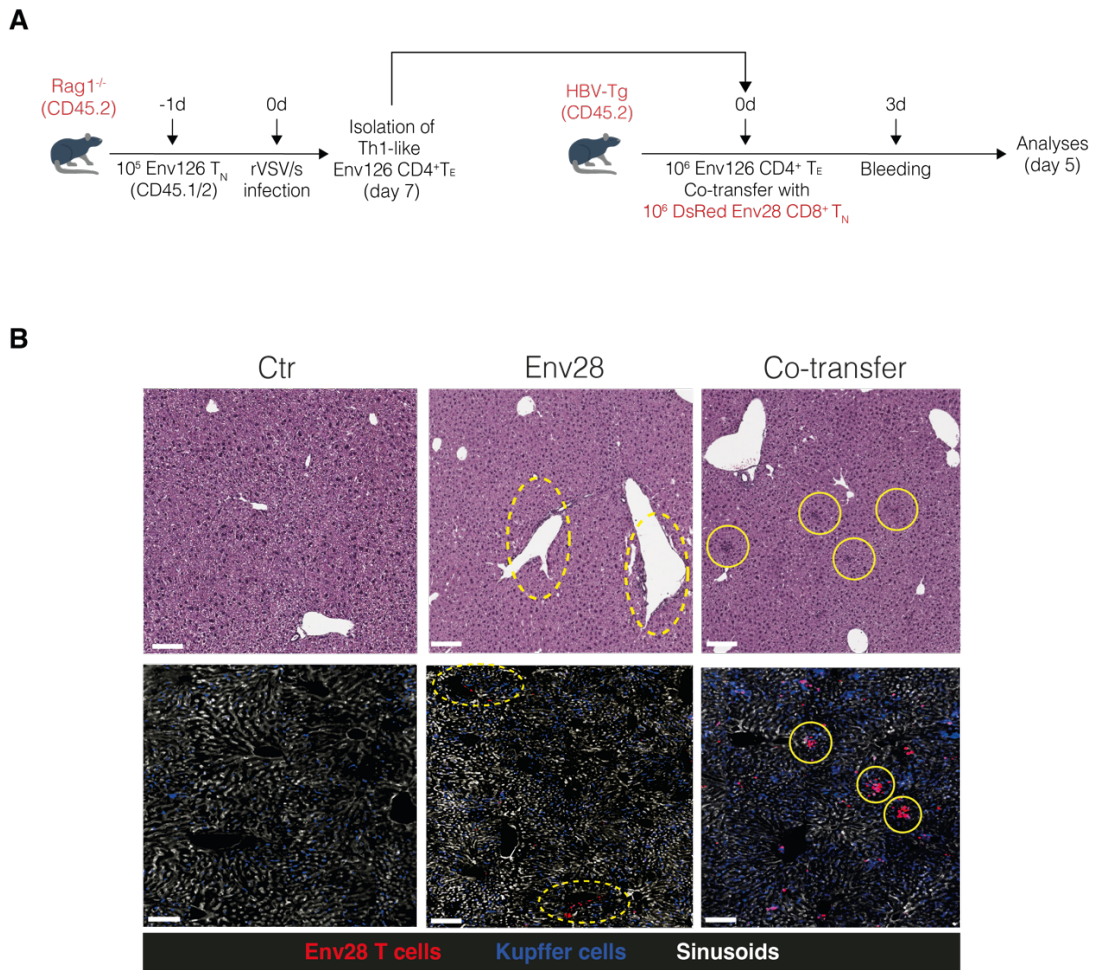


Figure 25 • Env28 CD8⁺T cells form extravascular clusters when co-transferred with Th₁-like CD4⁺T_E Env126.

(A) Schematic design of the experimental setup. 10^5 naïve Env126 CD4⁺T cells (CD45.1/2) were injected intravenously in Rag1^{-/-} mice (CD45.2) which have then been infected with rVSV/s after 24 hours. At day 7 post infection, spleen of injected and infected Rag1^{-/-} mice were surgically collected and Env126 CD4⁺T cells were isolated. At same time point, 10^6 of the isolated Th1-like T_E Env126 CD4⁺T cells (CD45.1/2) were co-transferred in HBV-Tg mice (C57BL/6 x Balb/c hybrid, CD45.2) with 10^6 naïve DsRed^{+/+} Env28 CD8⁺T cells (Balb/c, Thy1.1 DsRed, n=6). As a control, HBV-Tg mice transferred with DsRed^{+/+} Env28 CD8⁺T cells alone were included in the experiment (Env28, n=5), as well as untreated HBV-Tg mice (Ctr, n=3). At day 5 post cell transfer mice were sacrificed and liver lobules were collected to perform histological and confocal analyses. (B) (upper panels) Immunohistochemical representative micrographs of liver sections from the indicated group of mice at day 5 post cell transfer in HBV-Tg mice. Micrographs are showing the H&E staining of liver sections highlighting the distribution of leukocyte infiltrates in the liver parenchyma. Dotted lines denote leukocyte perivascular clusters, continuous lines denote extravascular leukocyte clusters. Scale bars represent 200 μ m. (Lower panels) Confocal immunofluorescence representative micrographs of liver sections from the indicated group of mice at day 5 post cell transfer in HBV-Tg mice. The micrographs show the distribution of DsRed^{+/+} Env28 CD8⁺T cells (red) in liver parenchyma. Sinusoids are highlighted by anti-CD38 Ab (white) and Kupffer cells are highlighted by anti-F4/80 Ab (blue). Scale bars represent 200 μ m. Data are representative of at least 3 independent experiments.

At day 5 post cell transfer, all previously highlighted effects on Env28 T cells proliferation and phenotype were observed (data not shown).

Histological and confocal analyses revealed T cell clusters scattered throughout the liver lobule when Env28 T cells were co-transferred with Env126 T_E cells in HBV-Tg mice (**Fig. 25B**), in a pattern that is reminiscent to that observed during acute self-limited HBV infection (Guidotti L G *et al*, 1999). By contrast, Env28 T cells formed clusters that coalesced around vascular tracts if transferred alone in HBV-Tg mice (**Fig. 25B**), a situation that is similar to chronic HBV infection (Krishna, 2021) and that was previously highlighted (Bénéchet *et al*, 2019).

From these experiments we concluded that, overall, the adoptive transfer of T_{h1}-like Env126 T_E cells can positively impact on Env28 T cells response in HBV-Tg mice, facilitating their differentiation into CTLs with enhanced effector and cytotoxic capacities. The positive effects pertain to different aspects of Env28 T cells activity. Indeed, Env28 display an improved proliferation capacity in the presence of Env126 T_E cells, and this leads to their enhanced accumulation inside the live. This accumulation was combined with a modification in their spatial positioning inside the liver organ: Env28 T cells showed to be capable of forming extravascular clusters when co-transferred with Env126 T_E, despite the uniform expression of viral proteins in the liver of HBV-Tg mice (Guidotti *et al*, 1995). From a functional point of view, Env28 T cells that were co-transferred with Env126 T_E cells gained in effector and cytolytic functions. Indeed, this was clear from their augmented capacity of producing T effector cytokines such as IFN γ and TNF α and the increased production of GrzmB, a protein known to be involved in pathogen-infected cells killing by CD8⁺T cells (Salti *et al*, 2011). We concluded that the efficient priming of CD8⁺T cells response to a non-cytolytic pathogen like HBV, may depend on CD4⁺T cell help.

5.2.5. T_{h1}-like Env126 CD4⁺T cells help is non-cognate specific

We next wondered if TCR affinity and specificity might influence and impact on the potential dependence of HBV-sp CD8⁺T cells from CD4⁺T cell help.

For this reason, we performed the same experiment (**Fig. 22A**) with CD8⁺T cells coming from Cor93 TCR CD8⁺T transgenic mice, in which ~98% of CD8⁺T cells carry a reactive TCR specific for the HBV core protein and therefore carry a different virus Ag specificity. In detail, Cor93 CD8⁺T cells recognize the H^{2b}-restricted epitope comprising the residues 93-100 contained within the HBV core protein, and also display a higher Ag-affinity compared with Env28 CD8⁺T cells (Isogawa *et al*, 2013).

We then repeated the same co-transfer experiment using Cor93 TCR CD8⁺T transgenic mice as HBV-sp CD8⁺T cells donor (**Fig. 26A**).

Briefly, we used Rag1^{-/-} mice as recipients in which we transferred 10⁵ Env126 naïve CD4⁺T cells and that we subsequently infected 24 hours later with rVSV/s. Mice were sacrificed at day 7 post infection and Env126 T cells were isolated (**Fig. 26A**-left). At same time point, 10⁶ Env126 T_E were co-transferred into HBV-Tg with 10⁶ Cor93 naïve T cells (Cor93 T_N). HBV-Tg mice transferred with 10⁶ Cor93 T_N cells alone were included as a control, as well as untreated HBV-Tg mice. All HBV-Tg mice were monitored in their sALT activity at day 3 post transfer and sacrificed at day 5 post cell transfer when livers of treated and untreated mice were surgically collected for flow cytometry and histological analyses (**Fig. 26A**-right).

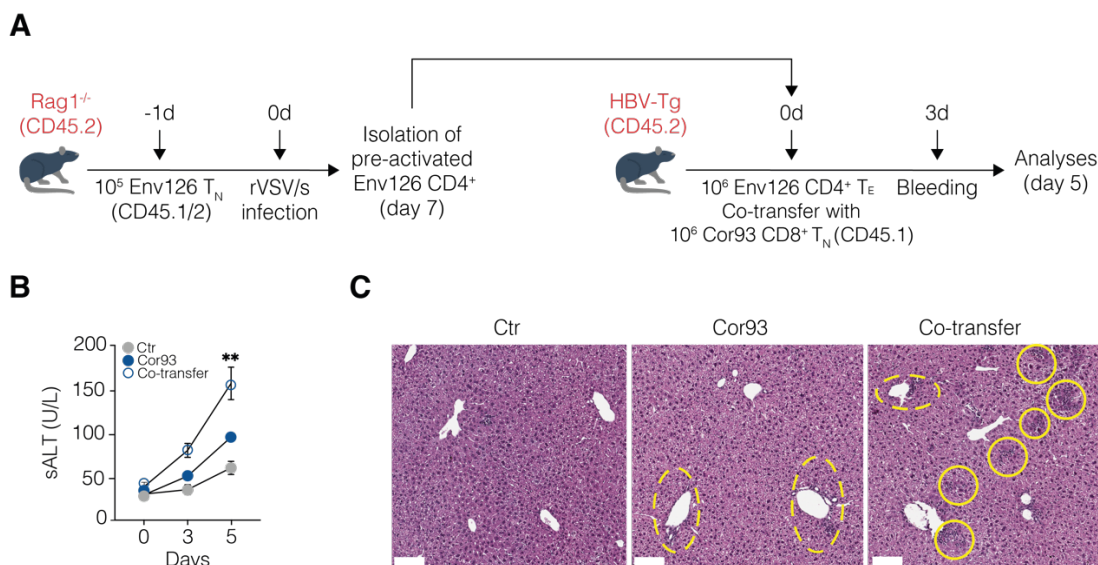


Figure 26 • Adoptive transfer of T_{H1}-like effector Env126 CD4⁺T cells improves Cor93 CD8⁺T cell-mediated liver immunopathology.

(A) Schematic design of the experimental setup. 10⁵ naïve Env126 CD4⁺T cells (CD45.1/2) were injected intravenously in Rag1^{-/-} mice (CD45.2) which have then been infected with rVSV/s after 24 hours. At day 7 post infection, spleens of injected and infected Rag1^{-/-} mice were surgically collected and Env126 CD4⁺T cells were isolated. At same time point, 10⁶ of the isolated T_{H1}-like T_E Env126 CD4⁺T cells (CD45.1/2) were co-transferred in HBV-Tg mice (C57BL/6, CD45.2) with 10⁶ naïve Cor93 CD8⁺T cells (C57BL/6, CD45.1, n=5). As a control, HBV-Tg mice transferred with Cor93 CD8⁺T cells alone were included in the experiment (Cor93, n=4), as well as untreated HBV-Tg mice (Ctr, n=2). HBV-Tg mice were monitored in their sALT activity immediately pre-transfer and at day 3 and 5 post transfer, time point at which transferred mice were sacrificed and the liver was analysed. (B) Serum transaminase activity (sALT) in untreated (Ctr, grey dots) HBV-Tg mice, HBV-Tg mice transferred with Cor93 (Cor93, full blue dots) and HBV-Tg mice co-transferred with Cor93 and Env126 (Co-transfer, empty blue dots) at indicated time points. (C) Immunohistochemical representative micrographs of liver sections from the indicated group of mice at day 5 post cell transfer in HBV-Tg mice. Micrographs are showing the H&E staining of liver sections highlighting the distribution of leukocyte infiltrates in the liver parenchyma. Dotted lines denote leukocyte perivascular clusters, continuous lines denote extravascular leukocyte clusters. Scale bars represent 200 μm. Data are expressed as mean ± SEM. Data are representative of at least 3 independent experiments. ** p-value ≤ 0.01, two-way ANOVA with Sidak's multiple comparison test (B)

The presence of Env126 T_E caused an augmented liver disease, as shown by rise in sALT activity at day 5 post cell transfer (Fig. 26B). The rise in sALT activity was in parallel followed by the same histological features we highlighted in the previously shown experiment (Fig. 26C). Indeed, T cells were able to form clusters scattered

throughout the liver lobule when Cor93 T were co-transferred with Env126 T_E (**Fig. 26C**-right panel) and this was not true if Env126 T_E cells were absent (**Fig. 26C**-middle panel).

As Env28, also Cor93 T cells benefited from Env126 T_E presence as they were numerically increased in the liver of co-transferred mice (**Fig. 27A**). The more prominent accumulation of Cor93 was explained by the rise in the frequency of Ki-67 expressing Cor93 T cells in co-transferred mice (**Fig. 27C**). As previously shown for Env28, Cor93 T cells were ameliorated not only in their proliferation capacity but also in their effector phenotype. Indeed, in the presence of Env126 T_E cells, Cor93 T cells were most likely to produce TNF α IFN γ and GrzmB. This was highlighted by the increase of absolute numbers of TNF α - IFN γ - and GrzmB- producing Cor93 T cells in the liver co-transferred mice (**Fig. 27B**) as well as by the rise in the frequency of total Cor93 T cells that were able to produce effector- and cytolytic-related cytokines (**Fig. 27D**).

From these experiments we concluded that the adoptive transfer of T_{h1}-like Env126 CD4⁺ T_E cells can positively impact also on Cor93 CD8⁺T cells response in HBV-Tg mice. As before, the positive effects impacted on different aspects of Cor93 T cells activity: proliferation capacity, formation of extravascular clusters, and augmented effector and cytolytic functions. The observation of these effects on Cor93 T cells, which carry a different Ag-specificity and TCR affinity compared to Env28 T cells, led us to conclude that the efficient priming of CD8⁺T cells in HBV infection, may depend on CD4⁺T cell help and that this help does not require CD4⁺ and CD8⁺T cells to carry the same Ag-specificity.

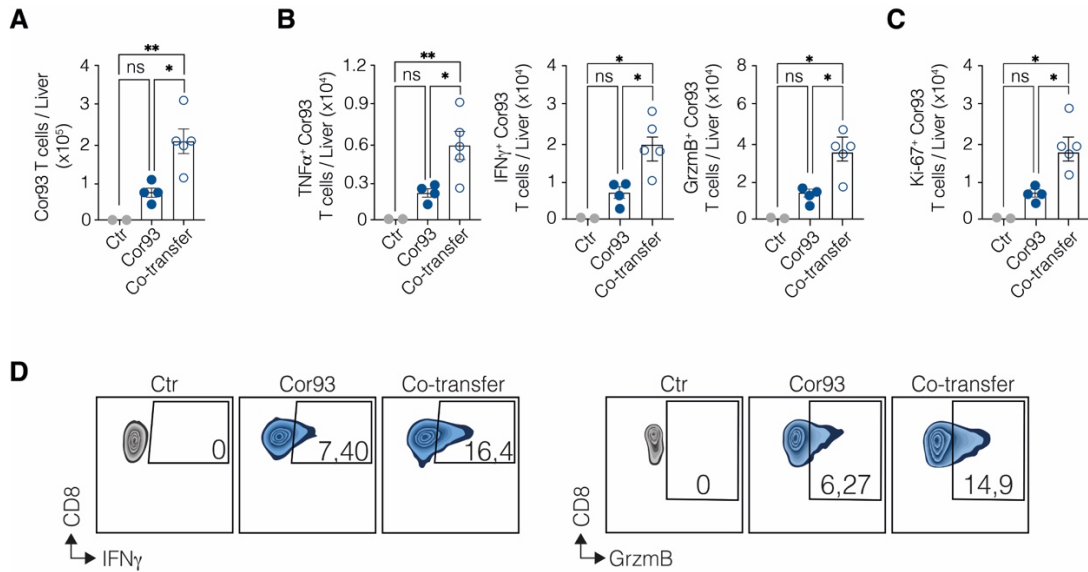


Figure 27 • Adoptive transfer of T_{H1} -like effector Env126 $CD4^+$ T cells improves Cor93 $CD8^+$ T cell effector function.

10^6 naïve Cor93 $CD8^+$ T cells were transferred in HBV-Tg mice with or without 10^6 T_{H1} -like T_E Env126 $CD4^+$ T cells (CD45.1/2), HBV-Tg untreated mice were used as a control. Experimental mice were sacrificed 5 days post cell transfer and the liver was analysed by flow cytometry. **(A)** Absolute numbers of Cor93 $CD8^+$ T cells in the liver of indicated group of mice at day 5 post cell transfer. **(B)** Absolute numbers of TNF α - (left graph), IFN γ - (middle graph) and Grzm β - (right graph) producing Cor93 $CD8^+$ T cells in the liver of indicated group of mice at day 5 post cell transfer upon *in vitro* 4 hours peptide restimulation. **(C)** Absolute numbers of Ki-67 $^+$ Cor93 $CD8^+$ T cells in the liver of indicated group of mice at day 5 post cell transfer. **(D)** Representative flow cytometry plots showing the frequency of Cor93 $CD8^+$ T cells producing IFN γ (left plots) and GrzmB (right plots) at day 5 post transfer and co-transfer in the liver HBV-Tg mice (blue plots). Grey plots (Ctr) represent frequency of $CD8^+$ T cells producing IFN γ and GrzmB in untreated mice as a control. Cor93 $CD8^+$ T cells were defined as Live, CD45 $^+$, B220 $^-$ CD19 $^-$, CD8 $^+$ CD4 $^-$, CD45.1 $^+$ CD45.2 $^-$. Endogenous $CD8^+$ T cells from untreated mice were identified as Live, CD45 $^+$, B220 $^-$ CD19 $^-$, CD8 $^+$ CD4 $^-$, CD45.1 $^-$ CD45.2 $^+$. Data are expressed as mean \pm SEM. Data are representative of at least 3 independent experiments. ns p-value > 0.05 * p-value ≤ 0.05 , ** p-value ≤ 0.01 , Kruskal-Wallis Test (A-C)

5.2.6. Adoptive transfer of T_{h1}-like Env126 CD4⁺T cells improves the cross-presentation capacity of Kupffer cells in HBV-Tg mice

We wanted then to follow up on these observations by attempting to dissect the cellular and molecular mechanism underlying the effects of Env126 T_E cell help to HBV-sp CD8⁺T cells. Previous studies have shown that, for CD4⁺T cells to provide optimal help to CD8⁺T cells, the epitopes recognized by CD4⁺ and CD8⁺T cells have to be linked (Mitchison NA & O'Malley C, 1987), implying that the two T cell types recognize the antigen on the same APC (Borst *et al*, 2018; Wu & Murphy, 2022).

Current accepted model of CD4⁺-CD8⁺ T cell cooperation in viral infections comprehend diverse features. As first, a CD8⁺T cell is primed by an APC which can capture viral components and present their antigens via MHC-I molecules on their surface. The presenting APC can efficiently perform priming activity if “licensed” by CD4⁺ T cells that interact with them by recognizing cognate antigens presented on MHC-II molecule on the same APC (Bevan, 2004).

We thought then to investigate about the myeloid involvement in our experimental setup. Briefly, we used Rag1^{-/-} mice as recipients in which we transferred 10⁵ Env126 naïve CD4⁺T cells and that we subsequently infected 24 hours later with rVSV/s. Mice were sacrificed at day 7 post infection and Env126 CD4⁺T cells were isolated (**Fig. 28A-left**). At same time point, 10⁶ Env126 CD4⁺ T_E (Env126 T_E) were co-transferred into HBV-Tg with 10⁶ Env28 naïve CD8⁺T cells (Env28 T_N). HBV-Tg mice transferred with Env28 T_N cells alone were included as a control, as well as untreated HBV-Tg mice. All mice were monitored in their sALT activity just before cell transfer and at day 3 post transfer. They were sacrificed at day 5 post cell transfer when livers of treated and untreated mice were surgically collected to assess the composition and phenotype of both hepatic DCs and KCs by flow cytometry (**Fig. 28A-right**).

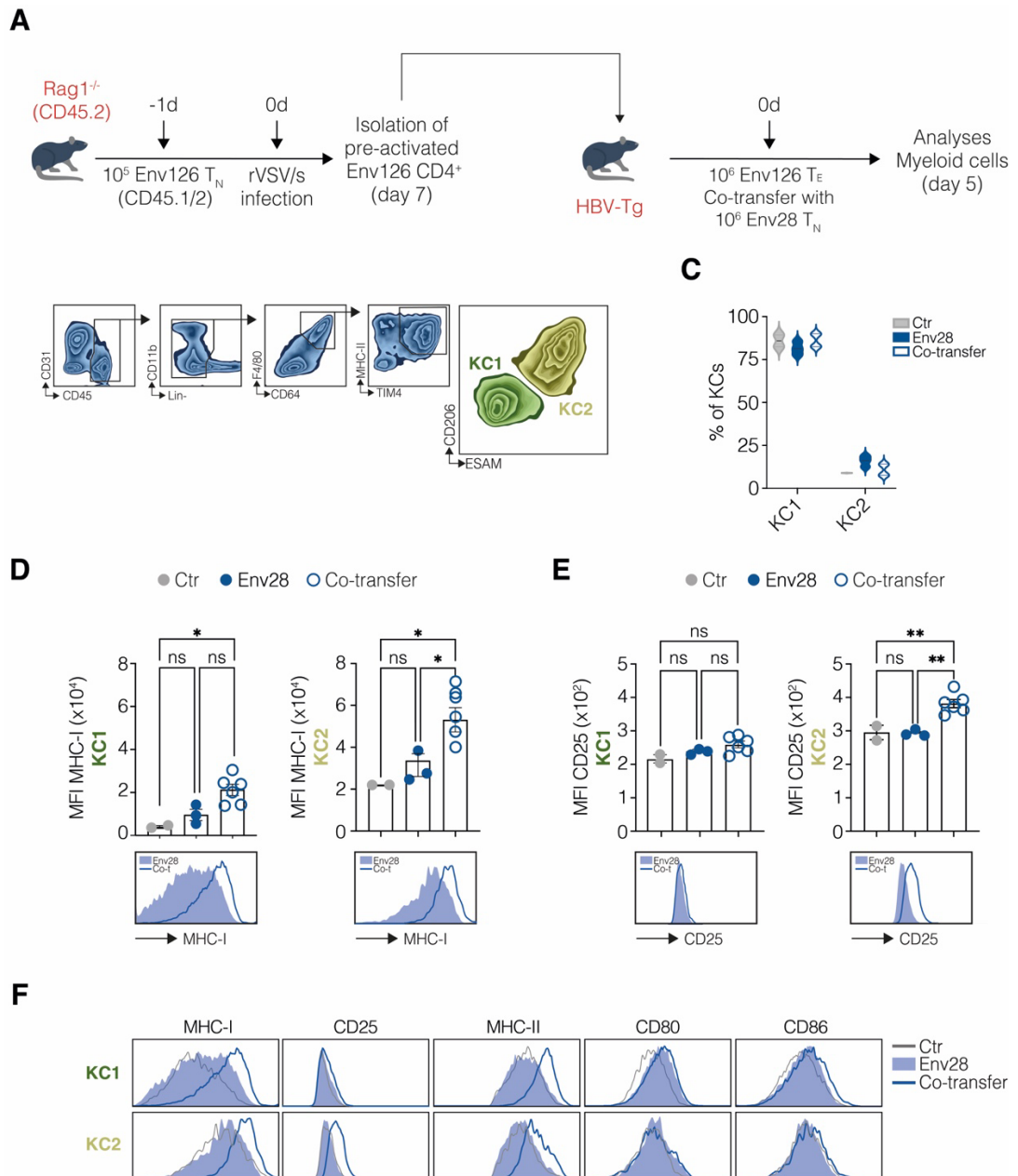


Figure 28 • KCs ameliorate their cross-presenting capacity after adoptive transfer of Env126 T_E cells in the liver HBV-Tg mice.

(A) Schematic design of the experimental setup. 10^5 naïve Env126 CD4⁺T cells (CD45.1/2) were injected intravenously in Rag1^{-/-} mice (CD45.2) which have then been infected with rVSV/s after 24 hours. At day 7 post infection, spleens of injected and infected Rag1^{-/-} mice were surgically collected and Env126 CD4⁺T cells were isolated. At same time point, 10^6 of the isolated Th1-like T_E Env126 CD4⁺T cells (CD45.1/2) were co-transferred in HBV-Tg mice (C57BL/6, CD45.2) with 10^6 naïve Env28 CD8⁺T cells (C57BL/6, CD45.1) (Co-transfer, n=6). As a control, HBV-Tg mice transferred with Env28 CD8⁺T cells alone were included in the experiment (Env28, n=3), as well as untreated HBV-Tg mice (Ctr, n=2). HBV-Tg mice were monitored in their sALT activity immediately pre-transfer and at day 3 and 5 post transfer, time point at which transferred mice were sacrificed and the liver was analysed. (B) Representative flow cytometry plot of KC1 and KC2 gating strategy. KC are identified as Live, CD45⁺CD3⁺CD8⁺CD4⁺CD19⁻B220⁻

CD11b^{int}F4/80⁺CD64⁺MHC-II⁺TIM4⁺ liver non parenchymal cells. KC1 are identified as ESAM⁻CD206⁻ KCs. KC2 are identified as ESAM⁺CD206⁺ KCs. (C) Relative representation of KC1 and KC2 percentages inside KC population in the liver of indicated groups of mice at day 5 post cell transfer. (D) Histograms of the MFIs of MHC-I expression on KC1 (left histogram) and KC2 (right histogram) cells in indicated group of mice at day 5 post cell transfer. Under each histogram are depicted representative modal MFI curves of MHC-I on KC1 and KC2 cells at day 5 post transfer in the liver of co-transferred mice (blue empty curve) and Env28 transferred mice (light blue full curve). (E) Histograms of the MFIs of CD25 on KC1 (left histogram) and KC2 (right histogram) cells in indicated group of mice at day 5 post cell transfer. Under each histogram are depicted representative modal MFI curves of MHC-I expression on KC1 and KC2 cells at day 5 post transfer in the liver of co-transferred mice (blue empty curve) and Env28 single transferred mice (light blue full curve). (F) Representative MFI histograms of MHC-I, CD25, MHC-II, CD80 and CD86 expression on KC1 (upper plots) and KC2 (bottom plots) at day 5 post cell transfer in the indicated groups of mice. Data are expressed as mean \pm SEM. Data are representative of at least 3 independent experiments. ns p-value > 0.05 * p-value \leq 0.05, ** p-value \leq 0.01, two-way ANOVA with Sidak's multiple comparison test (D, E)

We analysed total non-parenchymal liver cells with particular focus on KCs and DCs. In particular, we applied a well-established gate strategy in order to distinguish between the two subpopulations of KCs (Fig. 28B, C), which have been recently discovered to be composed by KC1 and KC2 (de Simone *et al*, 2021; Blériot & Ginhoux, 2019; Blériot *et al*, 2020).

At day 5 post cell transfer, no differences in KCs composition were observed in the liver of treated and untreated mice (Fig. 28C). However, we observed an increase in the expression of MHC-I molecule on both KC1s and KC2s in the liver of mice where Env126 T_E were adoptively transferred (Fig. 28D). Consistent with recent findings showing the requirement of KC2 for the IL-2 mediated restoration of CD8⁺T cell dysfunctionality induced by hepatocellular priming (de Simone *et al*, 2021), we interestingly also observed an augmented expression of CD25 molecule on KC2 cells surface (Fig. 28E). This profile was not observed on KC1s. Besides an increase in MHC-I expression, we also could highlight a parallel increase in the expression of MHC-II molecule on the surface of both subpopulations of KCs. However, these effects were not in parallel followed by any differences in the expression of co-stimulatory molecules CD80 and CD86 on neither KC1 nor KC2 (Fig. 28F).

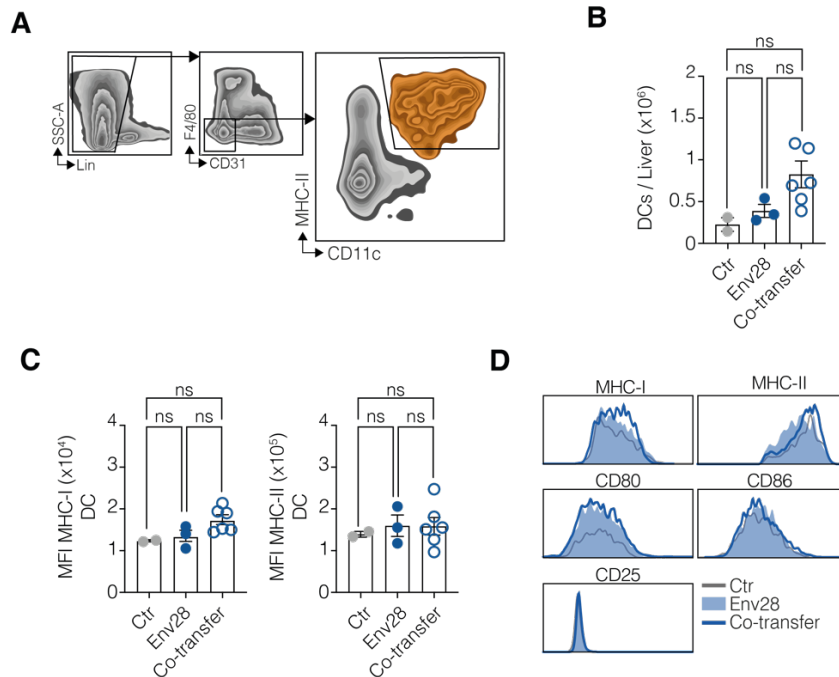


Figure 29 • DCs do not ameliorate cross-presenting capacity after adoptive transfer of Env126 T_E cells in the liver of HBV-Tg mice.

(A) Representative flow cytometry plot of DC gating strategy. DC are identified as Live, CD45⁺CD3⁻CD8⁻CD4⁻CD19⁻B220⁻F4/80⁻CD31⁻MHC-II⁺CD11c⁺ liver non parenchymal cells. (B) Absolute numbers of DCs in the liver of indicated groups of mice at day 5 post cell transfer. (C) Histograms of the MFIs of MHC-I (left histogram) and MHC-II (right histogram) on DCs in indicated group of mice at day 5 post cell transfer. (D) Representative histograms of MFI curves of MHC-I, MHC-II, CD80, CD86 and CD25 expression on DCs at day 5 post cell transfer in the indicated groups of mice. DCs were identified as Live, CD3⁺CD19⁻F4/80⁻CD31⁻MHC-II⁺CD11c⁺. Data are expressed as mean \pm SEM. Data are representative of at least 3 independent experiments. ns p-value > 0.05, Kruskal-Wallis Test (B), two-way ANOVA with Sidak's multiple comparison test (C).

A slight, but not significant, increase trend in DCs absolute numbers was observed in the liver of co-transferred mice at day 5 post cell transfer (Fig. 29A). However, we were not able to mark any variations in the expression of MHC-I or MHC-II on DCs (Fig. 29B). The same was observed for the expression levels of co-stimulatory molecules CD80 and CD86 (Fig. 29C). No expression of CD25 was observed on DCs surface, consistent with what was previously reported (Raeber *et al.*, 2020).

Taken all together, these results suggested that after adoptive transfer of Env126 CD4⁺T_E cells, KCs up-regulate MHC-I cross-presenting machinery inside the liver. In

KC2s, this effect is in parallel followed by the up-regulation of CD25, the α subunit of high-affinity IL-2 receptor (Pol *et al*, 2020), a cytokine that was already ascribed with the potential of reverting T cell dysfunction in HBV context, by pushing the cross-presentation process in KC2s (de Simone *et al*, 2021). On the other hand, we were not able to spot alterations in DCs after the co-transfer of Env126 T_E cells with Env28 T cells in the liver of treated mice in our model of HBV pathogenesis.

5.2.7. Env126 CD4⁺T cells help to HBV-sp CD8⁺T cells is mediated by antigen-presenting cells

Giving the amelioration we observe in HBV-sp CD8⁺ T cell activity and the effects on KCs and DCs that the adoptive transfer Env126 CD4⁺ T_E cells can bring in our HBV-Tg mouse model, we wanted to understand the contribution of APCs on the CD4⁺-CD8⁺ T cell cooperation.

To do so, we took advantage of two additional HBV-Tg mouse models.

In order to understand the requirement of APCs in our experimental observations, we used HBV-Tg mice lacking the expression of MHC-II molecules. In particular, we used HBV-Tg MHC-II^{-/-} mice (1.3.32 MHC-II^{-/-} lineage, C57BL/6): HBV-replication-competent transgenic HBV mice that were crossed with MHC^{-/-} mice in which a specific deletion disrupts class II MHC genes (H2-Ab1, H2-Aa, H2-Eb1, H2-Eb2, H2-Ea) (Madsen *et al*, 1999). In these mice all the hepatocytes can produce and replicate the complete HBV genome and its structural proteins at high levels without any evidence of cytopathology and no APC can express or produce MHC-II molecules. Moreover, we used as recipient animals also MUP-core mice, which express a non-secretable form of the core protein (HBcAg) under the transcriptional control of the liver-specific mouse urinary promoter (MUP promoter) in 100% liver hepatocytes (Guidotti *et al*, 1994).

We performed the same experimental setup previously described co-transferring Cor93 T_N cells and Env126 T_E cells also in HBV-Tg MHC^{-/-} and MUP-core mice (**Fig. 30**). In the first case, we wanted to assess whether the interaction between APC and Env126 T_E cells is essential to drive the help to HBV-sp CD8⁺T cells. In the second condition, where APCs are equipped with MHC-II molecules, but the cognate Env126 specific-Ag is not present, we wanted to understand whether Ag-recognition by Env126 T_E cells is required to permit CD4⁺-CD8⁺T cell cooperation. In both condition the three-cell interaction model was questioned.

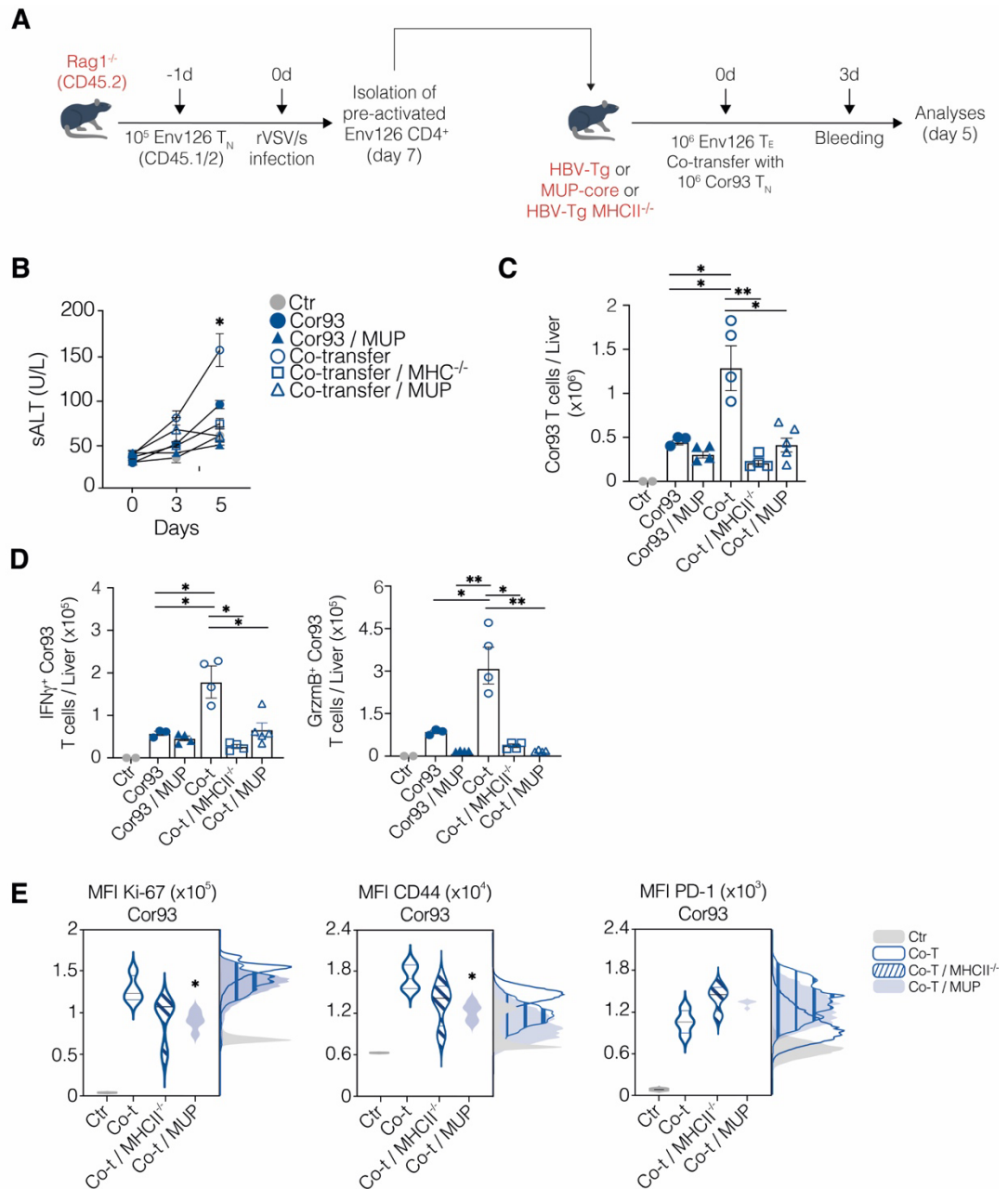


Figure 30 • Env126 and Env28 require APCs to cooperate.

(A) Experimental setup: 10^5 naïve Env126 CD4⁺T cells (CD45.1/2) were injected intravenously in Rag1^{-/-} mice (CD45.2) which have then been infected with rVSV/s after 24 hours. At day 7 post infection, spleens of injected and infected Rag1^{-/-} mice were surgically collected and Env126 CD4⁺T cells were isolated. At same time point, 10^6 of the isolated T_{H1}-like T_E Env126 CD4⁺T cells (CD45.1/2) were co-transferred in HBV-Tg mice (C57BL/6, CD45.2, n=4), MUP-core mice (C57BL/6, CD45.2, n=5) or HBV-Tg MHCII^{-/-} mice (C57BL/6, CD45.2, n=4) with 10^6 naïve Cor93 CD8⁺T cells (C57BL/6, CD45.1). As a control, HBV-Tg (n=3) and MUP-core mice (n=4) transferred with Cor93 CD8⁺T cells alone were included in the experiment, as well as untreated HBV-Tg mice (n=2). All treated and untreated mice were monitored in their sALT activity immediately pre-transfer and at day 3 and 5 post transfer, time point at which mice were sacrificed and the liver analysed by flow cytometry. (B) Serum transaminase activity (sALT) in

untreated (Ctr, grey dots) HBV-Tg mice, HBV-Tg mice transferred with Cor93 (Cor93, full blue dots), MUP-core mice transferred with Cor93 (Cor93/MUP, full blue triangles), HBV-Tg mice co-transferred with Cor93 and Env126 (Co-transfer, empty blue dots), HBV-Tg MHC^{-/-} mice co-transferred with Cor93 and Env126 (Co-t/MHC^{-/-}, empty blue squares) and MUP-core mice co-transferred with Cor93 and Env126 (Co-t/MUP, empty blue triangles). (C) Absolute numbers of Cor93 CD8⁺T cells in the liver of indicated group of mice at day 5 post cell transfer. (D) Absolute numbers of IFN γ - (left graph) and Grzm β - (right graph) producing Cor93 CD8⁺T cells in the liver of indicated group of mice at day 5 post cell transfer upon *in vitro* 4 hours peptide restimulation. (E) Violin plots showing MFI values of Ki-67, CD44 and PD-1 expression on hepatic Cor93 at day 5 post cell transfer in indicated group of mice. In untreated WT mice, MFIs were calculated on endogenous CD8⁺T cells. On right side of the plot are depicted representative MFIs modal curves on Env28 T cells in indicated group of mice. Cor93 CD8⁺T cells were defined as Live, CD45⁺, B220⁻CD19⁻, CD8⁺CD4⁻, CD45.1⁺CD45.2⁻. Endogenous CD8⁺T cells from untreated mice were identified as Live, CD45⁺, B220⁻CD19⁻, CD8⁺CD4⁻, CD45.1⁻CD45.2⁺. Data are expressed as mean \pm SEM. Data are representative of at least 2 independent experiments. ns p-value > 0.05 * p-value \leq 0.05, ** p-value \leq 0.01, two-way ANOVA with Sidak's multiple comparison test (B) Kruskal-Wallis Test (C, D).

Briefly, we transferred 10^5 Env126 naïve CD4⁺T cells into Rag1^{-/-} mice which subsequently infected 24 hours later with rVSV/s. All Rag1^{-/-} mice were sacrificed at day 7 post infection and Env126 T cells were isolated (Fig. 30A-left). At same time point, 10^6 Env126 CD4⁺ T_E (Env126 T_E) were co-transferred with 10^6 Cor93 naïve CD8⁺T cells (Cor93 T_N) into HBV-Tg, HBV-Tg MHC^{-/-} or MUP-core mice. HBV-Tg and MUP-core mice transferred with 10^6 Cor93 T_N cells alone were included as a control, as well as untreated mice. All experimental mice were monitored in their sALT activity immediately before cell transfer and at day 3 post transfer. They were sacrificed at day 5 post cell transfer when livers of all mice were collected and analysed by FACS (Fig. 30A-right).

We observed sALT elevation only if Cor93 and Env126 T_E cells were co-transferred into HBV-Tg mice, meaning that the adoptive transfer of Env126 T_E cells is not able to favour liver T-cell mediated damage in MUP-core or HBV-Tg MHC^{-/-} mice (Fig. 30B). Consistent with this data, Cor93 T cells were able to accumulate and vigorously expand, and thus receive Env126 T_E cell help, only in HBV-Tg mice and not in MUP-core or HBV-Tg MHC^{-/-} mice (Fig. 30C).

Looking at Cor93 T cells phenotype, we could appreciate an ameliorated effector state and cytolytic capacity only in HBV-Tg mice as well (Fig. 30D). Indeed, Env126 T_E cells can sustain Cor93 T cells response, which can better differentiate and acquire cytotoxic

capacities, only in HBV-Tg mice and not in MUP-core or HBV-Tg MHC^{-/-} mice where their interaction with APC is abolished (**Fig. 30D**).

Finally, Cor93 T cell surface markers also indicated that their proliferation and activation were improved, and this was true only when Env126 T_E cells could efficiently interact with APC via Ag-presentation, as indicated by the MFIs of Ki-67, CD44 and -PD-1 on their cell surface (**Fig. 30E**).

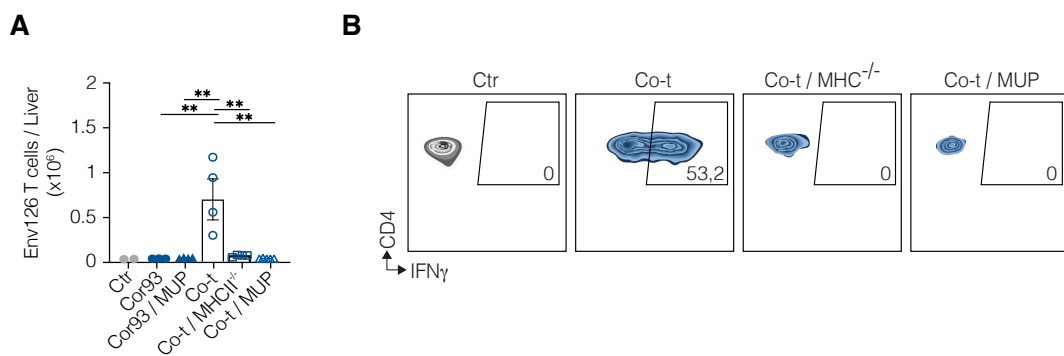


Figure 31 • Env126 T_E cells get activate and expand only after interacting with APCs in HBV-Tg mice.

(A) Absolute numbers of Env126 CD4⁺T cells in the liver of indicated group of mice at day 5 post cell transfer. (B) Representative flow cytometry plots showing the frequency of hepatic Env126 CD4⁺T cells producing IFN γ at day 5 post transfer in the liver of indicated groups of mice after *in vitro* peptide restimulation. Grey plots (Ctr) represent the frequency of CD4⁺T cells producing IFN γ in untreated mice as a control. Env126 CD4⁺T cells were defined as Live, CD45⁺, B220⁻CD19⁻, CD8⁻CD4⁺, CD45.1⁺ CD45.2⁺. Endogenous CD4⁺T cells from untreated mice were identified as Live, CD45⁺, B220⁻CD19⁻, CD8⁻CD4⁺, CD45.1⁻CD45.2⁺. Data are expressed as mean \pm SEM. Data are representative of at least 2 independent experiments. ** p-value \leq 0.01, Kruskal-Wallis Test (A).

Of note, Env126 T_E cells could proliferate and maintain their activation status only if adoptively transferred in HBV-Tg mice, therefore not in HBV-Tg MHC^{-/-} or MUP-core mice (**Fig. 31A, B**), further indicating that the interaction with APCs not only is

fundamental to permit CD4⁺-CD8⁺T cell cooperation but also to sustain the persistence and activity of Env126 T_E cells in HBV-Tg mice.

From these experiments we concluded that Env126 T_E cells cooperation with HBV-sp CD8⁺T cells necessarily requires APCs as a bridge to deliver and drive the CD4⁺T cell help in our HBV mouse model. Future experiments will be aimed at understanding the molecular and cellular mechanisms by which CD8⁺T cell responses depend on CD4⁺T cell help. Together, these will help clarify the mechanism involved in CD4⁺-CD8⁺T cell cooperation in HBV pathogenesis.

6. DISCUSSION

Hepatitis B Virus infection causes both acute and chronic necro-inflammatory liver diseases and is the most common severe liver infection in the world. Its chronic persistence is associated with varying degrees of liver damage that often progresses to liver cirrhosis and eventually hepatocellular carcinoma (Levrero & Zucman-Rossi, 2016; Farazi & DePinho, 2006). Its public health burden becomes clear if we reason with numbers: the latest data show that, almost 300 million people in the world are chronically infected with HBV and 30 million people get newly infected each year (Hepatitis B Foundation Fact Sheets, 2022). Of these, almost 1.5 million die each year from infection complications (Hepatitis B Foundation Fact Sheets, 2022). Taking into considerations these alarming numbers, the WHO has raised HBV infection as a global health problem and added in the “2030 Agenda Goals” specific operations and activities to prevent and overcome HBV disease (Hutin Y *et al*, 2017). While there are mechanisms of prevention (prophylactic vaccination), the available therapeutic approaches to treat persistent infections are still limited and mostly fail to eliminate the virus. Definitely one of the reasons why, is because many of the immune mechanisms that underly its pathogenesis remain obscure. Thus, we are firmly convinced that further advances in the field will strongly depend on additional elucidation of the mechanisms by which HBV chronicity is established and by which interventions it can be immunologically reverted.

Viral clearance during HBV infection is fundamentally dependent on HBV-specific adaptive immune responses which - being HBV a virus that itself does not trigger any intrahepatic innate immune responses - are the main responsible for both disease pathogenesis and virus elimination (Bertoletti & Ferrari, 2016; Chisari & Ferrari, 1995; Guidotti & Chisari, 2006; Chisari *et al*, 2010). Among adaptive immune responses, the one put in place by HBV-specific (HBV-sp) CD8⁺T cells has been found to be, by far, the most crucial. Indeed, as main effectors of optimal viral control, achieved by targeting and eliminating HBV-infected hepatocytes, CD8⁺T cells remain the major direct authors of disease resolution (Thimme *et al*, 2003). However, during chronic HBV pathogenesis dysfunctional, detrimental, and weak virus specific CD8⁺T cells response is unable to

completely clear HBV from infected patients. CD8⁺T cells unresponsiveness and dysfunction has been mainly attributed to hepatocellular priming (Wong *et al*, 2015; Holz *et al*, 2010). Understandably, scientific research has been focused on CD8⁺T cells during the last decades and regrettably left the field with a significant lack of data that does persists with respect to the other important T cell compartment: CD4⁺T cells (Upkar S. Gill & Neil E. McCarthy, 2020). Functionally differentiated CD4⁺T cells are critical components of virus-induced adaptive immune responses in terms of development, maintenance, and control of antiviral CD8⁺T cells: they support their activation, and differentiation, as well as their long-lasting memory establishment (Ahrends *et al*, 2017; Borst *et al*, 2018). Nevertheless, CD4⁺T cells relevance in the design of therapeutic vaccines, antibody-based T cell immunomodulators, and cellular therapies is of already known importance (Amigorena, 2015; Borst *et al*, 2018) and could be much better exploited in CHB treatments conception (Maini & Pallett, 2018; Upkar S. Gill & Neil E. McCarthy, 2020; Buschow & Jansen, 2021).

Despite the insufficient attention received, a critical observation was made in chimpanzees more than one decade ago: animals immunodepleted from CD4⁺T cells prior to infection, are precluded from effective CD8⁺T cell differentiation and develop persistent infection (Asabe *et al*, 2009). This brought us to hypothesize that the efficient priming of CD8⁺T cells to HBV could depend on CD4⁺T cell help. The complete lack of information regarding CD8⁺-CD4⁺T cell cooperation in HBV pathogenesis, together with the urgent need of a detailed understanding of the cellular and molecular immune mechanisms underlying HBV pathogenesis, led us to study the role of virus-specific CD4⁺T cells in an HBV-Tg mouse model.

To pursue this objective, we *ad hoc* developed a new transgenic mouse model in which all CD4⁺T cells can recognize the HBsAg (Section 5.1). Env126 transgenic TCR mice carry both the transgenes encoding for the alpha and beta chain of a reactive TCR that is specific for the residues 126-138 of the HBsAg (**Fig. 11**). These mice are fertile, viable, of normal weight and size and do not present any physical abnormalities. We initially tested the presence of Ag-specific CD4⁺T cells taking advantage of fluorochrome-conjugated tetramers (**Fig. 12**) provided by the NIH Tetramer Core Facility. We observed that Env126 CD4⁺T cells were representing among the 15% and 30 % of the entire CD4⁺T

cell population in Env126 transgenic mice among diverse organs (**Fig. 12B**), indicating that the *knock-in* of TCR chains was accomplished. Moreover, in each of analyzed organs, Env126 CD4⁺T cells were displaying a classical resting naïve phenotype with no evidence of alterations (**Fig. 12C**). However, the low percentages of Env126 T cells obtained among total CD4⁺T cell population indicated also that endogenous TCR genes were still preferentially rearranged and expressed. These observations led us to decide to mate Env126 transgenic mice to Rag1^{-/-} mice to abolish the endogenous T development and favour the maturation of only transgenic Env126 CD4⁺T cells (**Fig. 13A**). This approach allowed us to obtain transgenic Env126 mice in which ~98% of CD4⁺T cells is specific for HBsAg and thus facilitating their use as primary source of CD4⁺T cells for adoptive transfer experiments (**Fig. 13B**).

In the meantime, we tested the functionality and responsiveness of Env126 T cells in *in vitro* under diverse conditions (**Fig. 14 and 15**). Upon cognate Ag-stimulation *in vitro*, we showed that Env126 T cells can get activated and actively produce TNF α (**Fig. 14B**), proliferate (**Fig. 15B**) and express activation surface markers (**Fig. 15C**), indicating that HBsAg stimulation was able to specifically elicit their response, not observed in WT control mice. These first *in vitro* experiments confirmed that Env126 T cells had permanently integrated the two chain transgenes, and the successful integration led to a stable and functional expression of the HBs-specific TCR on their cell surface. Although not being scientifically relevant, this first experimental phase was very important as it proved the efficiency and reliability of Env126 transgenic T cells, thus permitting us to proceed to investigate their dynamics *in vivo*.

We studied the dynamics of Env126 T cell responses in HBV-replication competent transgenic mice (hereafter HBV-Tg), a well-established mouse model in which all HBV genome and proteins are expressed and produced inside the hepatocytes, which are permissive to virus replication and allows viral spread at high levels with no evidence of cytopathology or liver damage (Guidotti *et al*, 1995). HBV-Tg mice are fully immune competent transgenic mice and are completely tolerant at the T cell level. Upon adoptive transfer in HBV-Tg mice, we were able to observe Env126 T cells in both liver and spleen of HBV-Tg mice in comparable percentages (**Fig. 16C,D and 17A,B**). As a control, Env126 T cells were also transferred in WT mice where they were detectable in the spleen

but almost not able to accumulate in the liver (**Fig. 16C**). In both conditions, Env126 T cells did not get activated or started to produce any effector cytokine, as well as expressing any lineage-specific transcriptional factor (**Fig. 16E and 17C**). This was confirmed by the observed non-significant increase in sALT activity, demonstrating that naïve Env126 T cells are not sufficient to cause any T cell mediated liver injury (**Fig. 16B**). However, only when transferred into HBV-Tg mice Env126 T cells displayed an active proliferative state, as we observed Ki-67 expression in both splenic and hepatic Env126 T cells in HBV-Tg mice and not in WT mice, where the HBsAg is completely absent (**Fig. 16E and 17C**). This was the first observation we obtained regarding the dynamics of HBV-sp CD4⁺T cell responses in HBV-Tg mice.

The fact that Env126 T cells cannot get activated or differentiate after adoptive transfer in HBV-Tg mice did seem reasonable to us. Indeed, this was in part overlapping and shared with what was already described for HBV-sp CD8⁺T cells undergoing intrahepatic priming during HBV infection. Alex Bénéchet *et al.* in our lab already showed that HBV-sp CD8⁺T cells, when adoptively transferred into HBV-Tg mice, are able to recognize the antigen and proliferate, without anyway acquiring effector T cell features (Benechet & Iannacone, 2017; Bénéchet *et al.*, 2019). We think that the reported Env126 T cell unresponsiveness in HBV-Tg mice could be due by a suboptimal priming of these cells that results in only low levels of cell division and no signs of specific differentiation or activation. Up to now, there are no studies available describing the spatiotemporal dynamics of Ag-sp CD4⁺T cell undergoing hepatocellular priming during their response against hepatotropic viruses such as HBV. However, their inability to respond to hepato-derived antigens was already in part described in model of adeno-associated mediated Ag delivery into hepatocytes (Wuensch *et al.*, 2010; Derkow *et al.*, 2011), in line with our findings. With ongoing and future experiments, we will follow up on this observation, trying to understand where, when and how Env126 T cells get primed and activated in HBV-Tg mice. It is reasonable to think that the absence of an inflammatory environment, together with the density of non-professional APCs in the liver leads to the failure of Env126 T cells priming and activation. Whether this is due to the amount of antigen present in the liver of HBV-Tg mice, the low levels of MHC-II or the absence co-stimulatory molecules on liver APCs (Crispe, 2011) remains to be clarified and will be further investigated. Our findings then stand only at the beginning of the understanding

of CD4⁺T cells reactivity towards liver-derived antigens, an aspect that we are currently still investigating.

In parallel with the study of naïve Env126 T cell priming and activation dynamics in HBV-Tg mice, we wanted to study their potential cooperation with HBV-specific CD8⁺T cells (Section 5.2).

We know from previous studies that the functional consequence of HBV-sp CD8⁺T cells intrahepatic priming in the early phases of immune responses toward hepatotropic viruses, is the establishment of a dysfunctional phenotype. After recognizing the Ag in the liver, HBV-sp CD8⁺T cells acquire a dysfunctional state, different from the classical exhaustion (Blank *et al*, 2019), by which they proliferate and accumulate around hepatic portal tracts without acquiring efficient effector and cytolytic features (Bénéchet *et al*, 2019; Guidotti *et al*, 2015). We decided then to explore whether En126 T cells could help intrahepatic CD8⁺T cells differentiation and antiviral activity.

It must be said that direct evidence of CD4⁺T-CD8⁺T cell cooperation and a subsequent evaluation of its relevance during HBV pathogenesis is currently lacking. Our will to study this issue was mainly raised from a previous observation in HBV infected chimpanzees. Asabe *et al*. reported how the depletion of CD4⁺T cells before HBV infection carried out with an inoculum that normally leads to a rapid and controlled CD8⁺T antiviral response, results into the establishment of persistent chronic disease (Asabe *et al*, 2009), bringing to light the possibility that an early CD4⁺T response may be necessary to induce CD8⁺T cell antiviral activity and facilitate viral clearance during HBV pathogenesis. However, the importance and cruciality of CD4⁺T-CD8⁺T cell cooperation during the acute phase of hepatotropic viral infections is still considered somehow controversial (Upkar S. Gill & Neil E. McCarthy, 2020). Some studies previously hypothesized the necessity of an early wave of CD4⁺T cell response and therefore help to Ag-specific CD8⁺T cell to reach a successful viral clearance in HCV context (Smyk-Pearson *et al*, 2008; Urbani *et al*, 2006) defending the importance of CD4⁺T cell help during the priming phase of CD8⁺T cells. On the other hand, diverse studies have instead reported that the importance of CD4⁺T cell help mainly lies on the generation of only secondary efficient memory CD8⁺T cell antiviral responses (Janssen

et al, 2003; Sun & Bevan, 2003; Laidlaw *et al*, 2016; Shedlock & Shen, 2003). Nevertheless, some studies also support both possibilities (Novy *et al*, 2007).

We made use of HBV-Tg mice together with HBs-sp CD8⁺ TCR transgenic mouse model to study the CD4⁺T-CD8⁺T cell cooperation in our experimental setup. In detail, we questioned this issue taking advantage of envelope-specific CD8⁺ TCR transgenic mice (hereafter Env28) in which ~80% of total CD8⁺T cells bear a functional TCR that recognize the epitope 28-39 of HBsAg when this is presented on MHC-I molecules (Isogawa *et al*, 2013): Env28 mice were used as primary donor source for HBs-specific CD8⁺T cells (Env28 T cells).

We adoptively transfer naïve Env28 T cells with or without Env126 T cells in HBV-Tg mice in a ratio 1:1 (10⁶ Env28 T cells with or without 10⁶ Env126 T cells). At day 5 post cell transfer, we could not observe any relevant difference of Env28 T cell accumulation and phenotype in the liver of HBV-Tg mice (**Fig. 18C, E**). The absence of any positive impact on Env28 T cell antiviral response was confirmed by both the evaluation of sALT activity in the blood of experimental mice at different time points (**Fig. 18B**) and histological analyses (**Fig. 18D**). In the first case, no elevation in sALT activity was reported when Env126 T cells were adoptively transfer together with Env28 T cells in HBV-Tg mice, that kept sALT activity at physiological levels before and after cell transfer (**Fig. 18B**), indicating the absence of any T-cell mediated liver injury. Indeed, this was further proved by H&E sections obtained from the liver of treated mice at day 5 post cell transfer: T cells remained confined in vascular clusters, and this was true whether Env28 T were transferred alone or along with Env126 T cells in HBV-Tg mice (**Fig. 18D**). In this condition, Env126 T cells also did not benefit from the presence of Env28 T cells (data not shown). Indeed, they displayed the same features and distribution observed when they were transferred alone in HBV-Tg mice (**Fig. 16**). From these results we concluded that the adoptive transfer of naïve Env126 T cells is not able to positively impact on Env28 T cell antiviral responses in HBV-Tg mice.

Our results are in line with previous reported observation (Derkow *et al*, 2011) in which the co-transfer of naïve OT-I and naïve OT-II cells was not able to induce liver damage in mice expressing ovalbumin into hepatocytes. This is consistent to the fact that

with the intrinsic characteristics of liver environment, the absence of proper inflammation and APC licensing, the priming of not only Env28 T cells but also of Env126 T cells can result in their unresponsiveness within the liver not favouring their cooperation. We hypothesized then that, to deliver help to Env28 T cells in early phase of the immune response against the virus, Env126 T cells should first acquire an activation state, in line with the classical and established APCs CD4-mediated licensing model (Castellino & Germain, 2006; Smith *et al*, 2004; Crispe, 2014).

We then implemented an *in vitro* strategy to obtain effector pre-activated Env126 T cells (Section 5.2.2). The rationale of this approach stands in the hypothesis that, if previously activated, Env126 T cells may license APCs in the liver by Ag-MHCII interaction and co-stimulation, allowing APCs to better deliver enhanced signals to Env28 T cells during their intrahepatic priming. We *in vitro* pulsed Env126 T cells for 5 days with the cognate peptide HBS₁₂₆₋₁₃₈ and obtained Env126 T cells capable of producing TNF α and expressing effector surface molecules (**Fig. 19A, B**). After culture, we transferred pre-activated Env126 T_E with Env28 T cells in HBV-Tg mice (**Fig. 20A**). We did not report any sALT elevation (**Fig. 20B**) or liver tissue alterations (data not shown) at day 5 post cell transfer. Indeed, the frequency of differentiated and cytotoxic Env28 T cells was not varying in the presence or absence of Env126 T_E cells (**Fig. 20D**). We concluded that the adoptive transfer of pre-*in vitro* activated Env126 T cells is not able to revert Env28 T cells dysfunction in HBV-Tg mice.

It is known that T-helper CD4⁺T cells are the partners of choice for CD4⁺-CD8⁺ cooperation (Borst *et al*, 2018). For this reason, we attempted to generate fully differentiated antiviral Env126 T cells (Section 5.2.3). We used a pre-*in vivo* activation strategy to generate Th1-like Env126 T cells (**Fig. 21A**): to summarize, we showed that rVSV/s infection - a recombinant vesicular stomatitis virus strain encoding for the HBsAg (Cobleigh *et al*, 2013) – can drive Env126 T cell differentiation into effector Th1-like CD4⁺T cells. In the context of rVSV/s infection, Env126 T cells acquire a CD62L^{low}CD44^{high}T-bet⁺CXCR3⁺ phenotype (**Fig. 21C**) and produce considerable quantities of IFN γ , TNF α and IL-2 (**Fig. 21D**) upon *in vitro* peptide restimulation. The surface features that Env126 displayed were resembling a typical T helper-1 cell lineage commitment (Zhou *et al*, 2009; Krueger *et al*, 2021) and overlapped with the phenotype

of double producers $\text{IFN}\gamma^+\text{TNF}\alpha^+$ CD4^+ T cells that were recently positively correlated with viral clearance in CHB patients (Wang *et al*, 2020).

We then showed that the adoptive transfer of Th1-like Env126 T_E cells (hereafter Env126 T_E) positively impacted on HBV-specific CD8^+ T cell proliferation and differentiation (Section 5.2.4 and 5.2.5) in HBV-Tg mice. This was true whether HBV-sp CD8^+ T cells shared the same antigen specificity of Env126 (Section 5.2.4) or not (Section 5.2.5). Indeed, we showed that the adoptive transfer of Env126 T_E could provide help to both Env28 and Cor93 T cells, which recognize an H2b-restricted epitope of the HBcAg (Isogawa *et al*, 2013).

With the help of Env126 T_E cells, both Env28 and Cor93 showed stronger accumulation in the liver (**Fig. 22C and 27A**) as a consequence of an improved proliferation (**Fig. 23 and 27C**), and they were more prone to acquire an effector differentiated phenotype (**Fig.22D,E and 27B,D**). This betterment led to a rise in sALT activity (**Fig. 22B and 26B**) that reflected the histological appearance of the liver, where we could spot extravascular T cell clusters (**Fig. 25 and 26C**). Help from Env126 T_E cells also led to the downregulation of co-inhibitory receptor PD-1 (**Fig. 22F**), a key feature already imputed to a successful CD4^+ T cell help delivery to CD8^+ T cells in a mouse model of therapeutic anti-cancer vaccination (Ahrends *et al*, 2017). Other *in vivo* studies have suggested the need of help during the early phase of the primary CD8^+ T cells responses in diverse infectious contexts (van Stipdonk *et al*, 2001; Kaech & Ahmed, 2001; Mercado *et al*, 2000; van Stipdonk *et al*, 2003). Our results can initially show that the efficient priming of HBV-specific CD8^+ T cells during HBV pathogenesis could rely on CD4^+ T cell help and more generally, can lead us to hypothesize that this could be linked to the unresponsiveness of HBV-specific CD8^+ T cells observed in CHB patients, where CD4^+ T cell help may be missing. Together with recent data from the clinic (Wang *et al*, 2020; Urbani *et al*, 2006; Tan *et al*, 2018; Urbani *et al*, 2005) in which a possible decisive role for HBV-sp CD4^+ T was cogitated, with these reported results we underpinned the need of a deeper definition of CD4^+ T dynamics in HBV pathogenesis.

A boost in the study of CD4^+ - CD8^+ cooperation came with the understanding of the central role of APCs in mediating such interaction (Bevan, 2004). Indeed, previous

studies have shown that, for CD4⁺ T cells to provide optimal help to CD8⁺ T cells, the epitopes recognized by CD4⁺ and CD8⁺ T cells have to be linked (Mitchison NA & O'Malley C, 1987), suggesting that the same cell presents the epitopes to the two T cell types. Despite the existence of proved APC-independent CD4⁺-CD8⁺ cooperation (Elsaesser *et al*, 2009; Wilson & Livingstone, 2008), we soon wanted to assess the plausible involvement of APCs in our system. At day 5 post cell transfer, we could spot an up-regulation of MHC-II and MHC-I molecules on both KC1 and KC2 (Blériot *et al*, 2020) in the liver of mice that received Env126 T_E cells (**Fig. 28**). This effect was not present on hepatic DC compartment (**Fig. 29**) where only a non-significant increased trend in MHC-I expression was observed. Of note, the phenotype reported in hepatic DCs was the same in the splenic DCs after the adoptive transfer of Env126 T_E cells (data not shown). Kupffer cells are not generally regarded as the main cross-presenting APCs *in vivo*. Instead, type I classical DCs (cDC1s) have been for a long considered the ones doing the job (Bennett *et al*, 1997; John Paul Ridge *et al*, 1998; Hor *et al*, 2015; Ferris *et al*, 2020) mainly inside organ draining lymph nodes (Kitano *et al*, 2016; Laidlaw *et al*, 2014). However, KCs have already been endowed with cross-presenting capacities in multiple context (Muntjewerff *et al*, 2020; Krenkel & Tacke, 2017; de Simone *et al*, 2021).

Without bringing forward any idea on the specific involvement of either KCs or DCs in our experimental setup, we first tried to understand whether APCs in general would at least act as a communication bridge in our system. Indeed, we showed that all the observed “helping” effects were abrogated if Ag-MHCII interaction between Env126 T cells and APCs was abolished (Section 5.2.7). This conditional abrogation was obtained using two additional transgenic mice: HBV replication competent transgenic mice lacking the expression of MHC^{-/-} molecules, and MUP-core mice where MHC-II is normally expressed but there is no presence of Env126 specific cognate Ag (HBsAg) (**Fig. 30A**). We observed that only if both MHC-II and HBsAg were present and produced, Env126 T cells were able to deliver help to Cor93 T cells as explained by the sALT activity levels (**Fig. 30B**) and the absolute numbers of IFN γ ⁺ and GramB⁺ Cor93 T cells in HBV-Tg mice (**Fig. 30D**). These experiments indicated that APCs are essential for CD4⁺-CD8⁺ cooperation, which is not happening if Env126 T cells and APCs are no longer able to interact.

Overall, the gathered data during my PhD serve only as the beginning of the understanding of CD4⁺-CD8⁺ cooperation dynamics in HBV pathogenesis. Still a lot of questions must be answered to elucidate the precise cellular and molecular mechanisms by which Ag-specific CD4⁺T cells help intrahepatic CD8⁺T cell responses against HBV. Where Ag-specific CD4⁺T cells deliver help to CD8⁺T cells? When does this cooperation happen? Through which subtype of APC can CD4⁺ and CD8⁺ T cells communicate with each other? Which specific molecular mechanisms are implicated in their efficient cooperation, and which are their long-term consequences? These are only few of the key points we still need to address. The spatiotemporal dynamics of CD4⁺T-to-CD8⁺T help delivery *in vivo* are still a crackling area of interest and there is still a lot to learn about the timing and positioning of CD4⁺-CD8⁺ cooperation in multiple contexts. It is reasonable to think that Env126-Env28 T cell cooperation takes place at early time points after cell transfer (Pasqual *et al*, 2018), during the priming phase of Env28 T cells. The current accepted model divides T cooperation in two different stages: CD4⁺T and CD8⁺T cells firstly encounter the Ag independently of each other on different types of APCs and only in a second priming phase CD4⁺T and CD8⁺T cells interact with the same APC in a contemporaneous or asynchronized manner (Kitano *et al*, 2016; Gerner *et al*, 2017; Calabro *et al*, 2016). The latter has been the most supported, as not requiring that two rare cells, an Ag-specific CD4⁺T and an Ag-specific CD8⁺T, simultaneously form a three-cells cluster with a single APC, a type of event that would defy probability (Germain *et al*, 2012). We showed that, at day 5 post cell transfer, KCs - and not DCs - in the liver of mice receiving Env126 T_E cells seemed more willing to put in place cross-presenting operations (**Fig. 28**), leading us to provocatively propose that KCs should be taken into consideration as a potential platform for CD4⁺T-to-CD8⁺T help delivery during HBV disease. Future experiments will try to understand which and where is the licensed APC involved in our cooperation system and the timing of its interactions with both CD4⁺T and CD8⁺T cell compartments.

Once identified the APC that orchestrates cooperation, we will explore the precise molecular mechanisms the help signal is proficiently delivered from CD4⁺T cells to CD8⁺T colleagues. Different mechanisms have been proposed to mediate CD4⁺- CD8⁺ cooperation during the last decades that have been recently put together in a tangled commixture of both co-stimulatory and cytokines signals (Borst *et al*, 2018). Signalling

following CD40-CD40L interaction between APCs and CD4⁺T cells is thought to be the main mediator of APC licensing (Bedoui *et al*, 2016). Indeed, in APCs the interaction leads to the upregulation of MHC-I complexes and co-stimulatory molecules such as CD80, CD86 (Prilliman *et al*, 2002) and CD70 (Feau *et al*, 2012; Garris *et al*, 2018), and the production of IL-12, type I IFN (Agarwal *et al*, 2009) and IL-15 (Greyer *et al*, 2016) cytokines; all mechanisms that eventually relay the help signal from APCs to CD8⁺T cells via respective receptors. Beside these above-mentioned helping processes, IL-2 signalling also can drive CD8⁺T cell differentiation and has been reported to have both autocrine and paracrine origins (Peperzak *et al*, 2010). In the first scenario, IL-2 is produced by CTLs themselves, in the latter, CD4⁺T cells-derived IL-2 (Wilson & Livingstone, 2008) could contribute to CD8⁺T cell differentiation, in concert with IL-21 (Elsaesser *et al*, 2009; Li *et al*, 2013). We did not spot any IL-21 production in Env126 T_E cell in any of the reported experiments (data not shown), but we did find IL-2 production among their effector capacities (**Fig. 21D**). Conditional deletions and blocking of some of the listed molecular circuits will help us in understanding which are the precise mechanisms that portray Env126-mediated help to HBV-sp CD8⁺T cells in our experimental HBV model. Indeed, with future experiments will be aimed at understanding the potential molecular mechanisms by which CD8⁺T cells responses depend on the CD4⁺T cell help in our experimental setup. Since signalling via CD40 on the APC is one of the potential mediators of CD4⁺T cell help to CD8⁺T cells, we will assess whether CD40L^{-/-} Env126 T_E cells fail to increase and ameliorate HBV-sp CD8⁺T cell function. Furthermore, we will take advantage of a CRISPR/Cas9-mediated gene knockout protocol to conditionally delete specific cytokines (including IL-2, IFN- γ , and IL-21) in Env126 CD4⁺ T_E cells prior to their transfer to HBV-Tg mice with HBV-sp CD8⁺ T cells. Together, these will help clarify the mechanism involved in CD4⁺-CD8⁺ T cell cooperation in HBV pathogenesis.

Furthermore, the long-term fate of HBV-specific CD8⁺ T cells and Env126 CD4⁺T_E cells will be questioned in our experimental setup with future experiments. It is known that memory CD8⁺T cells are a principal component of immunity against intracellular pathogens such as viruses (Laidlaw *et al*, 2016) and several studies have identified in CD4⁺T cell help a crucial role in defining the development and maintenance of memory CD8⁺T cells in different settings (Cullen *et al*, 2019; Laidlaw *et al*, 2014; Janssen *et al*,

2003; Shedlock *et al*, 2003). It is tempting to speculate that rescued HBV-sp CD8⁺ T cells differentiation into tissue-resident memory (T_{RM}), effector memory (T_{EM}) or central memory (T_{CM}) T cells could be favored following proficient interaction and cooperation with Env126 CD4⁺T_E cells. Since understanding the signals that regulate the development of memory T cells is crucial to efforts to design vaccines capable of eliciting T cell-based immunity and since CD4⁺T cells are known essentials in the formation of protective memory CD8⁺T cells following infection or immunization, future experiments will be also aimed at characterizing the HBV-specific CD8⁺T and CD4⁺T cell response at later time points. In order to understand the mechanisms by which HBV-sp CD4⁺T cells could act to possibly support memory CD8⁺T cell development in HBV-Tg mice, we will perform co-transfer experiments focusing and analyzing the responses of these two populations at different time points in the liver of treated mice after transfer. In particular, we would like to understand the fate and function of HBV-specific CD8⁺ T cells following the reception of Env126 CD4⁺T_E cells help at 14, 21, 28, 42 and 56 days post cell transfer in HBV-Tg mice. This will may provide insight into the role of CD4⁺ T cell help in promoting the maturation of memory CD8⁺T cells following immunization and infection.

Although still many data remain to be collected, and given all recent observations in the field, it is intriguing to hypothesize one of the possible scenarios of CD4⁺-CD8⁺T cell cooperation in our setting. As previously pointed out, our lab recently demonstrated that KC2s can revert the CD8⁺ T cell dysfunction resulting from intrahepatic priming in HBV-Tg mice (de Simone *et al*, 2021). We know that liver anatomy facilitates the interaction between naïve CD8⁺ T cells and hepatocytes which, through the expression of MHC-I molecules, present Ag to circulating CD8⁺ T cells leading to suboptimal CTLs responses (Holz *et al*, 2010; Bénéchet *et al*, 2019). On the other hand, priming of by intrahepatic APCs can favour CD8⁺ T cells differentiation, a scenario that was shown to be achievable by therapeutic administration of exogenous IL-2 that is sensed via high-affinity IL-2R (IL-2 receptor) by KC2s, which ameliorate their cross-presentation capacity, eventually restoring the antiviral potential of CD8⁺ T cells (de Simone *et al*, 2021). It is then tempting to speculate that competent HBV-sp CD8⁺ T cell immune responses during natural HBV infection could require the presence of high local IL-2 concentration, and that a potential natural source of this cytokine might be HBV-sp CD4⁺ T cells. Indeed, effector Ag-sp

CD4⁺ T cells are known great producers of IL-2 upon successful Ag-recognition (Sojka *et al*, 2004), an ability that Env126 T_E cells did show to possess in our setting (**Fig. 21D**) and may be delivered to CD8⁺T cells only with the joint effort of APCs. We can speculate that, after early KC-Env126 interaction and a proper licensing endowment, IL-2 production by Env126 T_E cells may be encouraged, creating a high local IL-2 concentration milieu that on one hand directly pushes CD8⁺T cells differentiation and in parallel equips KCs with enhanced cross-presentation capacities, building an environment that can overall better sustain CD8⁺T cells anti-HBV responses.

EPILOGUE

It is evident that every of these aims and hypotheses must be precisely tested and demonstrated but remains fascinating and exciting being able to consciously make hypothesis and reasoning about possible biological scenarios after a long journey, which is about to end, in the sweet company of adaptive immunity. I believe that many challenges remain in developing efficacious immunotherapies for chronic hepatic infections and liver cancers and that encouraging the advancement in HBV field is necessary in order to find soon, in any way, a solution to this impactful disease, which still makes too many people suffer all over the world. The significance of the data I wanted to present rests in the concept that any further advances in the field will strongly depend on additional elucidation of the mechanisms whereby dysfunctional HBV-sp CD8⁺T cells can be restored in CHB patients. I hope I succeeded in bringing to the light that, to complete this hard task, CD4⁺T cells could definitely be tough, but still helpful, allied companions.

7. MATERIALS AND METHODS

7.1. Mice

C57BL/6 and CD45.1 mice (C57BL/6 inbred) were purchased from Charles River Laboratories. HBV replication competent transgenic mice (1.3.32 lineage, C57BL/6 inbred) have been previously described (Iannacone & Guidotti, 2015; Guidotti *et al*, 1995): these mice express the entire genome of HBV and replicate it in the liver hepatocytes with no evidence of cytopathology and have been used as C57BL/6 x Balb/c H2^{bxd} F1 hybrids. HBV-Tg MHC-II^{-/-} (1.3.32 MHC-II^{-/-} lineage, C57BL/6 inbred) were obtained from the crossing between 1.3.32 lineage and MHC^{-/-} lineage (B6.129S2-H2^{dIAb1-Ea/J}) (Madsen *et al*, 1999). MUP-core mice have been previously described (Guidotti *et al*, 1994): in these mice 100% of hepatocytes can express HBcAg under the transcriptional control of MUP promoter. Rag1^{-/-} mice (B6.129S7-Rag1^{tm1Mom/J}) have been purchased from The Jackson Laboratory (Mombaerts *et al*, 1992). Rag1^{-/-} CD45.1 mice were generated ad hoc for this project.

Env28 TCR transgenic mice (6C2.36 lineage, Thy1.1 Balb/c inbred) have been previously described (Isogawa *et al*, 2013) and carry ~80% of total splenic CD8⁺T cells specific for MHC-I restricted epitope (IPQSLDSWWTSL) located between residues 28 and 39 of the HBsAg. Env28 DsRed TCR transgenic mice were obtained from the crossing of Env28 TCR transgenic mice with CAG-DsRed mice (B6.Cg-Tg(CAG-DsRed*MST)1Nagy/j). Cor93 TCR transgenic mice (BC10.3 lineage, CD45.1 C57BL/6 inbred) display ~98% of splenic CD8⁺T cells specific for MHC-I restricted epitope (MGLKFRQL) comprised between residues 93 and 100 of HBcAg and have been previously described (Isogawa *et al*, 2013). Env126 TCR transgenic mice (Rag1^{-/-} CD45.2 C57BL/6 inbred), in which all CD4⁺T cells recognize an MHC-II restricted epitope located between residues 126 and 138 of HBsAg, were generated ad hoc for this project.

For imaging purposes, Env126 mice (Rag1^{-/-} CD45.2 C57BL/6 inbred) were crossed with CAG-eGFP mice (Rag1^{-/-} CD45.1 C57BL/6 inbred). Env28 and Cor93 TCR transgenic mice were crossed with CAG-DsRed mice (inbred Balb/c and C57BL/6

respectively). In all presented experiments mice were matched for sex, age and HBeAg serum concentrations (concerning 1.3.32 mice) and involved in experiments between 8 and 10 weeks of age. All mice were housed in specific pathogen-free conditions and all experimental procedures have been approved by San Raffaele Scientific Institute's Institutional Animal Committee.

7.2. Viral vectors

Replication non-competent recombinant VSV vector expressing HBsAg (rVSV/s) have been produced, characterized, and used as previously described (Moshkani *et al*, 2019; Bénéchet *et al*, 2019). Infected mice were injected intravenously (i.v.) with 10^6 plaque-forming units of rVSV/s vector 24 hours after Env126 CD4⁺T cells injection. All infectious work has been performed in designated BSL-3 workspaces, in accordance with institutional, national and international guidelines.

7.3. Naïve T Cells isolation

Isolation of CD8⁺T cells from spleens of Cor93 and Env28 mice and CD4⁺T cells from spleens of Env126 transgenic mice have been performed as previously described (Bénéchet *et al*, 2019). Env126 CD4⁺T cells isolation was performed by negative immunomagnetic selection taking advantage of the EasySep[™] Mouse CD4⁺ T Cell Isolation Kit (Negative selection, StemCell Technologies, Cat #19852) which targets non-CD4⁺T cells for their removal by the binding of biotinylated antibodies and streptavidin-coated magnetic particles, that are separated from wanted cells using the EasySep[™] Magnet (StemCell Technologies, Cat #18000). Briefly, spleens of donor mice were disrupted in PBS or HBSS and resuspended at 10^8 cells/mL in indicated medium; Rat Serum (StemCell Technologies, Catalog #19852) was added to the sample at 50 μ L/mL. After incubation, Isolation Cocktail was added to the sample, which was mixed and incubated at RT for 10 min. RapidSpheres[™] (StemCell Technologies, Cat #19852RF) were then added to the samples and 2.5 min incubation was performed at RT. After that,

the tube was placed into EasySep™ Magnet allowing the labelling and discard of unwanted cells.

7.4. Organ processing

7.4.1. Peripheral blood

Peripheral blood leucocytes (PBLs) were obtained by blood retro-orbital sinus withdrawal of anesthetized mice with sodium heparin-coated haematocrit capillaries. Blood samples were twiced treated with ammonium chloride (ACK) lysis buffer in order to lyse all red blood cells, washed twice with PBS and then resuspended in FACS buffer for the analyses. Processing of blood samples was performed as already described(Iannacone *et al*, 2005).

7.4.2. Spleen

Spleen of experimental mice was processed with PBS or HBSS (Hanks' Balanced Salt Solution). The organs were smashed into petri plate through 70µm strainer. The obtained cellular suspension was then centrifuged and pellet was resuspended in ACK lysing buffer, then washed and resuspended for subsequent analyses. Spleen processing has been already described (Bénéchet *et al*, 2019).

7.4.3. Liver

Single-cells suspension of IHL (Intrahepatic Leucocytes) was obtained as previously described (Bénéchet *et al*, 2019). Briefly, experimental mice were perfused at time of autopsy with 10mL of PBS through inferior vena cava. After the surgical removal, the liver organ was smashed into a petri plate through a 70µm strainer. The obtained cell suspension was then incubated and digested at 37°C for 40' into 10mL of RPMI 1640 (Life Technologies) at 0.02% of Collagenase IV (Sigma-Aldrich Cat #C5138) and 0.002% of DNase I (Sigma-Aldrich Cat #11284932001). After that, the sample was

processed in order to discard all the connective tissue and the leucocytes fraction was isolated following 40% Percoll (Sigma Aldrich, Cat #P1644) density gradient centrifugation. If analysis of cytokine production was planned, cell suspension of the liver organ was obtained as described above except for the addition of 1µg/mL of Brefeldin A (Sigma Aldrich, Cat #B5936) in the digestion buffer.

Cell suspensions of LNPCs (liver non parenchymal cells) (5.2.6 and 5.2.7) were obtained as follow. Mice were perfused at time of autopsy by inferior vena cava with 5 mL of PBS. Liver pieces were placed into a 35mm culture dish and cut in small pieces. Liver pieces were dispersed into 10 mL collagenase solution with 200µg/mL Collagenase IV (Sigma-Aldrich) and 0,5 mg/mL of DNase I (Sigma-Aldrich) and incubated for 20 minutes at 37°C. Subsequently, 18G needle-syringes were used to homogenize gently the liver pieces of each sample that were then filtered using a 70µm filter in order to remove all undigested tissue. Cell sediments containing mainly LNPCs were collected with different centrifugation cycles and as a final step RBC (Red Blood Cells) were lysed with 2mL ACK. Cell suspensions were then resuspended in RPMI and ready for further analyses.

7.4.4. Bone marrow

Bone marrow of experimental mice was processed by flushing with a syringe, using PBS or RPMI 1640, directly into the bone. The obtained cellular suspension was centrifuged, and the supernatant was discarded. The cells were resuspended in ACK lysing buffer to eliminate RBC, then washed and resuspended for analyses.

7.4.5. Lymph nodes

Lymph nodes of experimental mice were processed by smashing into 5 mL tube through a 70µm strainer, using PBS or RPMI 1640. The obtained cellular suspension was centrifugate and the pellet was washed and resuspended for analyses. Processing protocol was performed as already described (De Giovanni *et al*, 2020).

7.4.6. Thymus

Thymuses of experimental mice were processed by smashing into through a 70µm strainer into a petri plate using PBS or RPMI 1640. The obtained cellular suspension was centrifugate and the pellet was washed and resuspended for analyses.

7.5. *In vivo* treatments and adoptive transfers

In shown experiments, HBV-Tg mice were injected intravenously with 10^6 Env126 naïve CD4⁺T cells which were isolated from the spleen of untreated Env126 transgenic donor mice (5.1.4. and 5.2.1). In indicated experiments, Rag1^{-/-} mice were injected intravenously with 10^5 Env126 naïve CD4⁺T cells which were isolated from the spleen of untreated Env126 transgenic donor mice (5.2.3-5.2.7). In experiments comprehending *in vivo* activation of Env126 transgenic donor mice, HBV-Tg mice were injected intravenously with 10^6 Env126 CD4⁺T effector cells. In co-transfer experiments, Env126 naïve or effector CD4⁺T cells were injected intravenously with 10^6 naïve Env28 or Cor93 CD8⁺T cells, as previously described (Bénéchet *et al*, 2019) in cited combinations.

7.6. *In vitro* cell activation

In indicated experiments (5.1.3) Env126 CD4⁺T cells were cultured *in vitro* under 4 hours stimulation in lymphocytes complete medium: RPMI 1640, penicillin + streptomycin (100 IU/mL and 100µg/mL, Corning, Cat. #30-002-CI), 2mM L-glutamine (Corning, Cat. #25-005-CI), 50 µM 2-mercaptoethanol (Sigma-Aldrich, Cat. #M6250), HEPES 10mM (Corning, Cat. #25-060-CI), NEAA (non-essential amino acids, Corning, Cat. #25-025-CI) at 100µM. HBsAg₁₂₆₋₁₃₈ was used at 1µg/mL concentration. Ionomycin calcium salt (Sigma Aldrich, Cat #I3909), was used at 1µg/mL concentration in combination with Phorbol-12-myristate-13-acetate (PMA, Sigma Aldrich, Cat #524400) at 50ng/mL concentration. In section 5.1.3, Env126 CD4⁺T cells were cultured *in vitro* for 48 hours in complete medium with HBsAg₁₂₆₋₁₃₈ peptide (1µg/mL) or with Dynaneads™ Mouse T-Activator CD3/CD28 (ThermoFisher Scientific, Cat #11456D) following manufacturer instructions.

If for *ex vivo* intracellular staining to assess cytokine production before FACS analyses, cell suspensions were incubated for 4 hours at 37°C in complete medium, with HBsAg₁₂₆₋₁₃₈, HBsAg₂₈₋₃₉ or HBcAg₉₃₋₁₀₀ at 2 µg/mL with BFA (1 µg/mL, , Carlo Ebra Reagents S.r.l.) and Monensin (Biolegend, Cat #420701) according to manufacturer instructions.

7.7. *In vitro* cell labelling

In indicated experiments (5.1.3) WT or Env126 CD4⁺T cells were labelled with CellTrace™ Violet Cell Proliferation Kit (Cat #C34571) following all manufacturer protocol. Briefly, WT or Env126 CD4⁺T cells were isolated, washed and resuspended in PBS at 10⁶ cells/mL concentration in the working dye solution for 20 minutes at 37°C. After the incubation, complete medium was added to the cell suspension that was rested at room temperature for 5 minutes in order to dilute and remove free remaining dye. Labelled cells were then resuspended in complete medium ready to be cultured.

7.8. Flow cytometry staining and analyses

All the flow cytometry staining of both surface-expressed and intracellular molecules have been performed as was already described (de Giovanni *et al*, 2020; Bénéchet *et al*, 2019). Flow Cytometry staining of intranuclear transcriptional factors was performed with the eBioscience™ Foxp3/Transcription Factor Staining Buffer Set (eBioscience, Cat #00-5523-00) according to manufacturer protocol and instructions. All used antibodies are listed in **Table 1**. When indicated, frequency of Env28⁺ or Cor93⁺ T cells was assessed by dimer staining, as described (Iannacone *et al*, 2005): two different fusions proteins were used in order to identify Env28⁺ or Cor93⁺ T cells. Dimeric H-2Kb:Ig or H-2Ld:Ig fusion proteins (BD Biosciences, Cat #550750 and Cat #550751) were complexed with HBc₉₃₋₁₀₀ peptide (Cor93-100, MGLKFRQL, Primm) or HBs₂₈₋₃₉ peptide (Env28-39, IPQSLDSWWTLS, Primm) respectively.

Env126 Class-II Tetramer was provided by NIH Tetramer Core Facility as both peptide HBs₁₂₆₋₁₃₈ loaded tetramer (I-Ab HBsAg) and unloaded tetramer as a control (I-Ab CLIP). Tetramer staining was performed incubating cell suspensions at 37°C for 1 hour according to manufacturer instructions. Cell viability was assessed taking advantage of ViabilityTM 405/520 fixable dye staining (Miltenyi, Cat #130-130-404) or LIVE/DEADTM Fixable Aqua Dead Cell Stain Kit (ThermoFisher Scientific, Cat #L34957), or Zombie NIRTM Fixable Viability Kit (Biolegend, Cat #423105) following manufacturer protocols.

All flow cytometry analyses have been performed in FACS buffer composed by PBS with 2mM EDTA and 2% FBS (Corning, Cat. #35-079-CV). FACS analyses have been done on BD FACSCantoTM Clinical Flow Cytometry System, BD FACSymphonyTM A5 Cell Analyzer or Cytex[®] Aurora. Flow cytometry data were analyzed with FlowJo Software (Treestar). The list below includes all the antibodies used.

Table 1 • Used Antibodies for flow cytometry

CD45	30-F11	Biolegend Cat#103111
CD45.1	A20	BD Biosciences Cat#565212 Biolegend Cat#110743 Biolegend Cat#110718
CD45.2	104	Biolegend Cat#109807 BD Biosciences Cat#564616 BD Pharmingen Cat#560697 Biolegend Cat#109841
Thy1.1	OX-7	BD Biosciences Cat#740917 Biolegend Cat#202506 BD Pharmingen Cat#554898
CD4	RM4-5	eBioscience Cat#48-0042 BD Biosciences Cat#740208 BD Biosciences Cat#741461 BD Biosciences Cat#741912 Biolegend Cat#100548
CD8	53-6.7	BD Biosciences Cat#612898 Pharmingen Cat#558106 Biolegend Cat#100759 BD Biosciences #747134

B220	RA3-6B2	Biolegend Cat#103277 BD Biosciences Cat#564662
CD19	1D3	Biolegend Cat#156527 BD Biosciences Cat#749027 BD Pharmingen Cat#562291
CD3	145-2C11	Pharmingen Cat#552774 Biolegend Cat#100330 BD Biosciences Cat#564661
CD44	IM7	BD Biosciences Cat#741227
CD62L	MEL-14	Biolegend Cat#104438 Biolegend Cat#104453 Biolegend #161205
CD69	H1.2F3	BD Biosciences Cat#612793 Biolegend Cat#104537 Pharmingen Cat#552879 Biolegend Cat#104525
PD-1	J43	BD Biosciences Cat#744549
CD25	PC61	BioLegend Cat#102022 BD Biosciences Cat#564023
CD80	16-10A1	Biolegend Cat#104738
CD86	GL1	BD Biosciences Cat#564199 BD Bioscience Cat#741737
IA-IE	M5/114.15.2	BD Biosciences Cat#748846
H2-kB	AF6-88.5	BD Biosciences Cat#742861
F4/80	BM8	Invitrogen Cat#MF48021 Biolegend Cat#123117 Biolegend Cat#123131 Biolegend Cat#123110
TIM4	21H12	BD Biosciences Cat#742774
CD64	X54-5/7.1	BD OptiBuild Cat#740622 Biolegend Cat#139311
CD11c	N418	Biolegend Cat#117319 Biolegend Cat#117308
ESAM	1G8/ESAM	Biolegend Cat#136203
CD206	C068C2	Biolegend Cat#141719 Biolegend Cat#141710
CD11b	M1/70	BD Biosciences Cat#562317 Pharmingen Cat#552850 BD Pharmingen Cat#557960
CXCR3	CXCR3-173	BD Biosciences Cat#741895
CXCR5	L138D7	Biolegend Cat#145532 Biolegend Cat#145512
Bcl-6	K112-91	BD Biosciences Cat#562401

Foxp3	FJK-16s	Invitrogen Cat#53577382
T-bet	4b10	Invitrogen Cat#25582580
Ki-67	SolA15	eBioscience Cat#56569882
IFN γ	XMG1.2	Biologend Cat#505830
TNF α	MP6-XT22	BD Biosciences #563943
GrzmB	GB11	Biologend Cat#515406
IL-2	JES6-5H4	Biologend Cat#503837

7.9. Confocal Immunofluorescence and histochemistry

At time of autopsy, mice livers were perfused by inferior vena cava with 10 mL of PBS as liver pieces were surgically removed and instantly fixed in paraformaldehyde at 4% concentration for 16-20 hours. The solutions were then dehydrated in 30% sucrose prior to their embedding into OCT freezing media (Bio-Optica). Liver sections were obtained with CM1520 Cryostat Leica (20 μ m per section). Then, liver sections were stained as was already described x. Antibodies used comprehend: anti-F4/80 Alexa Fluor 647 (Invitrogen, Cat #MF48021), anti-CD38 Brilliant Violet 421 (Biologend, Cat #102732). All images were acquired by Mavig Confocal (Mavig RS-G4 Confocal).

For all the immuno-histochemical staining, liver pieces were harvested in Zinc-Formalin and transferred into 70% Ethanol solutions 24 hours later. All the tissues were then paraffin embedded and stained as previously described (Sitia *et al*, 2011).

7.10. Biochemical analyses

The extent of hepatocellular injury was monitored by the measuring of sALT activity at different and multiple time points after experimental manipulation and cell transfer, as already described (Iannacone & Guidotti, 2015). ALT glutamic pyruvic transaminase (GPT) liquid (#0018257440) was used in order to quantify sALT levels that were

quantified with ILab650 chemical analyser (Instrumentation Laboratory) by International Federation of Clinical Chemistry and Laboratory Medicine–optimized kinetic ultraviolet (UV) method. Quality controls: SeraChem Control Level 1 and Level 2 (#0018162412 and #0018162512). Normal intervals of sALT activity are comprised between 20 and 80 U/L.

7.11. Statistical analyses

Detailed descriptions of all statistical analyses are cited in each figure legend. All the results are expressed as mean \pm SEM. All statistical analyses were performed in GraphPad Prim Software 9. Two-way ANOVA with Sidak's multiple comparison post-test was used to compare two or more groups undergoing different treatments in different timepoints. Kruskal-Wallis Test was used as non-parametric test to compare three or more unpaired groups. The n indicates the number of individual mice analysed per each experiment. Significance is enlisted as follow: ns p-value > 0.05 *, p-value ≤ 0.05 , ** p-value ≤ 0.01 , *** p-value ≤ 0.001 . All experiments were independently performed at least in duplicate if non otherwise indicated.

8. REFERENCES

- Agarwal P, Raghavan A, Nandiwada SL, Curtsinger JM, Bohjanen PR, Mueller DL & Mescher MF (2009) Gene Regulation and Chromatin Remodeling by IL-12 and Type I IFN in Programming for CD8 T Cell Effector Function and Memory. *The Journal of Immunology* 183: 1695–1704
- Ahrends T, Spanjaard A, Pilzecker B, Bąbała N, Bovens A, Xiao Y, Jacobs H & Borst J (2017) CD4+ T Cell Help Confers a Cytotoxic T Cell Effector Program Including Coinhibitory Receptor Downregulation and Increased Tissue Invasiveness. *Immunity* 47: 848-861.e5
- Ai W, Li H, Song N, Li L & Chen H (2013) Optimal method to stimulate cytokine production and its use in immunotoxicity assessment. *Int J Environ Res Public Health* 10: 3834–3842
- Aliabadi E, Urbanek-Quaing M, Maasoumy B, Bremer B, Grasshoff M, Li Y, Niehaus CE, Wedemeyer H, Kraft ARM & Cornberg M (2021) Impact of HBsAg and HBcrAg levels on phenotype and function of HBV-specific T cells in patients with chronic hepatitis B virus infection. *Gut*: gutjnl-2021-324646
- Amigorena S (2015) Helping the Help for CD8+ T Cell Responses. *Cell* 162(6):1210-2
- Ando K, Guidotti LG, Wirth S I, shikawa T, Missale G, Moriyama T, Schreiber RD, Schlicht HJ, Huang SN & Chisari FV (1994) Class I-restricted cytotoxic T lymphocytes are directly cytopathic for their target cells in vivo. *J Immunol*
- Asabe S, Wieland SF, Chattopadhyay PK, Roederer M, Engle RE, Purcell RH & Chisari FV (2009) The Size of the Viral Inoculum Contributes to the Outcome of Hepatitis B Virus Infection. *J Virol* 83: 9652–9662
- Aubert RD, Kamphorst AO, Sarkar S, Vezys V, Ha SJ, Barber DL, Ye L, Sharpe AH, Freeman GJ & Ahmed R (2011) Antigen-specific CD4 T-cell help rescues exhausted

- CD8 T cells during chronic viral infection. *Proc Natl Acad Sci U S A* 108: 21182–21187
- Bamboatz ZM, Stableford JA, Plitas G, Burt BM, Nguyen HM, Welles AP, Gonen M, Young JW & DeMatteo RP (2009) Human Liver Dendritic Cells Promote T Cell Hyporesponsiveness. *The Journal of Immunology* 182: 1901–1911
- Bedoui S, Heath WR & Mueller SN (2016) CD4⁺ T-cell help amplifies innate signals for primary CD8⁺ T-cell immunity. *Immunol Rev* 272: 52–64 doi:10.1111/imr.12426
- Benechet AP & Iannacone M (2017) Determinants of hepatic effector CD8(+) T cell dynamics. *J Hepatol* 66: 228–233
- Bénéchet AP, de Simone G, di Lucia P, Cilenti F, Barbiera G, le Bert N, Fumagalli V, Lusito E, Moalli F, Bianchessi V, Andreatta F, Zordan P, Bono E, Giustini L, Bonilla WV, Bleriot C, Kunasegaran K, Gonzalez-Aseguinolaza G, Pinschewer DD, Kennedy PTF, Naldini L, Kuka M, Ginhoux F, Cantore A, Bertoletti A, Ostuni R, Guidotti LG, Iannacone M (2019) Dynamics and genomic landscape of CD8⁺ T cells undergoing hepatic priming. *Nature* 574: 200–205
- Ben-Moshe S & Itzkovitz S (2019) Spatial heterogeneity in the mammalian liver. *Nat Rev Gastroenterol Hepatol* 16: 395–410 doi:10.1038/s41575-019-0134-x
- Bennett SRM, Carbone FR, Karamalis F, Jacques, Miller FAP & Heath WR (1997) Induction of a CD8⁺ Cytotoxic T Lymphocyte Response by Cross-priming Requires Cognate CD4⁺T Cell Help. *J Exp Med* 186(1):65-70
- le Bert N, Gill US, Hong M, Kunasegaran K, Tan DZM, Ahmad R, Cheng Y, Dutertre CA, Heinecke A, Rivino L, Tan A, Hansi NK, Zhang M, Xi S, Chong Y, Pflanz S, Newell EW, Kennedy PTF, Bertoletti A (2020) Effects of Hepatitis B Surface Antigen on Virus-Specific and Global T Cells in Patients With Chronic Hepatitis B Virus infection. *Gastroenterology* 159: 652–664
- Bertoletti A & Ferrari C (2016) Adaptive immunity in HBV infection. *J Hepatol* 64: S71–S83

- Bertolino P, Bowen DG, McCaughan GW & Fazekas de St. Groth B (2001) Antigen-Specific Primary Activation of CD8+ T Cells Within the Liver. *The Journal of Immunology* 166: 5430–5438
- Bertolino P, Heath WR, Hardy CL, Morahan G & Miller JFAP (1995) Peripheral deletion of autoreactive CD8+ T cells in transgenic mice expressing H-2Kb in the liver. *Eur J Immunol* 25: 1932–1942
- Bevan MJ (2004) Helping the CD8+ T-cell response. *Nat Rev Immunol* 4: 595–602
- Blank CU, Haining WN, Held W, Hogan PG, Kallies A, Lugli E, Lynn RC, Philip M, Rao A, Restifo NP, Schietinger A, Schumacher TN, Schwartzberg PL, Sharpe AH, Speiser DE, Wherry EJ, Youngblood BA, Zehn D (2019) Defining ‘T cell exhaustion’. *Nat Rev Immunol* 19: 665–674
- Blériot C, Chakarov S & Ginhoux F (2020) Determinants of Resident Tissue Macrophage Identity and Function. *Immunity* 52: 957–970
- Blériot C & Ginhoux F (2019) Understanding the Heterogeneity of Resident Liver Macrophages. *Front Immunol* 10:2694
- Borst J, Ahrends T, Bąbała N, Melief CJM & Kastenmüller W (2018) CD4+ T cell help in cancer immunology and immunotherapy. *Nat Rev Immunol* 18:635–647
- Bowen DG, Zen M, Holz L, Davis T, McCaughan GW & Bertolino P (2004) The site of primary T cell activation is a determinant of the balance between intrahepatic tolerance and immunity. *Journal of Clinical Investigation* 114: 701–712
- Buschow SI & Jansen DTSL (2021) CD4+ T cells in chronic hepatitis b and t cell-directed immunotherapy. *Cells* 10(5):1114
- Calabro S, Liu D, Gallman A, Nascimento MSL, Yu Z, Zhang Ting, Chen P, Zhang B, Xu L, Gowthaman U, Krishnaswamy JK, Haberman AM, Williams A, Eisenbarth SC (2016) Differential Intrasplenic Migration of Dendritic Cell Subsets Tailors Adaptive Immunity. *Cell Rep* 16: 2472–2485

- Callery MP, Kamei T & Flye MW (1989) Kupffer cell blockade inhibits induction of tolerance by the portal venous route. *Transplantation* 47(6):1092-4
- Calne RY, Sells RA, Pena JR, Davis DR, Millard PR, Herbertson BM, Binns RM, Davies DA (1969) Induction of Immunological Tolerance by Porcine Liver Allografts. *Nature* 223(5205):472-6
- Castellino F & Germain RN (2006) Cooperation between CD4+ and CD8+ T cells: When, where, and how. *Annu Rev Immunol* 24:519–540
- Chisari F v & Ferrari C (1995) Hepatitis B Virus Immunopathogenesis. *Annu Rev Immunol* 13:29-60
- Chisari FV, Isogawa M & Wieland S (2010) Pathogenesis of hepatitis B virus infection. *Pathologie Biologie* 58: 258–266
- Cobleigh MA, Wei X & Robek MD (2013) A Vesicular Stomatitis Virus-Based Therapeutic Vaccine Generates a Functional CD8 T Cell Response to Hepatitis B Virus in Transgenic Mice. *J Virol* 87: 2969–2973
- Cohen IR, Lajtha INSA, Paoletti R & Lambris JD (2014) Overview of orchestration of CD4+ T cell subsets in immune responses. *Adv Exp Med Biol* 841:1-13
- Coss SL, Torres-Cornejo A, Prasad MR, Moore-Clingenpeel M, Grakoui A, Lauer GM, Walker CM & Honegger JR (2020) CD4+ T cell restoration and control of hepatitis C virus replication after childbirth. *J Clin Invest* 130(2):748-753
- De Creus A, Abe M, Lau AH, Hackstein H, Raimondi G & Thomson AW (2005) Low TLR4 Expression by Liver Dendritic Cells Correlates with Reduced Capacity to Activate Allogeneic T Cells in Response to Endotoxin. *The Journal of Immunology* 174: 2037–2045
- Crispe IN (2003) Hepatic T cells and liver tolerance. *Nat Rev Immunol* 3: 51–62
- Crispe IN (2011) Liver antigen-presenting cells. *J Hepatol* 54: 357–365

- Crispe IN (2014) APC licensing and CD4+T cell help in liver-stage malaria. *Front Microbiol* 5: 617
- Crispe IN & Mehal WZ (1996) Strange brew: T cells in the liver. *Immunol Today* 17(11):522-5
- Dandri M & Lütgehetmann M (2014) Mouse models of hepatitis B and delta virus infection. *J Immunol Methods* 410:39-49
- Decorsière A, Mueller H, van Breugel PC, Abdul F, Gerossier L, Beran RK, Livingston CM, Niu C, Fletcher SP, Hantz O, Strubin M (2016) Hepatitis B virus X protein identifies the Smc5/6 complex as a host restriction factor. *Nature* 531: 386–389
- Derkow K, Müller A, Eickmeier I, Seidel D, Moreira MV, Kruse N, Klugewitz K, Mintern J, Wiedenmann B & Schott E (2011) Failure of CD4 T-cells to respond to liver-derived antigen and to provide help to CD8 T-cells. *PLoS One* 6(7):e21847
- Elsaesser H, Sauer K & Brooks DG (2009) IL-21 is required to control chronic viral infection. *Science* 324: 1569–1572
- Farazi PA & DePinho RA (2006) Hepatocellular carcinoma pathogenesis: from genes to environment. *Nat Rev Cancer* 6: 674–687
- Feau S, Garcia Z, Arens R, Yagita H, Borst J & Schoenberger SP (2012) The CD4+ T-cell help signal is transmitted from APC to CD8 + T-cells via CD27-CD70 interactions. *Nat Commun* 3:948
- Ferrari C (2015) HBV and the immune response. *Liver International* 35: 121–128
- Ferrari C, Penna A, Bertoletti A, Valli A, Antoni AD, Giuberti T, Cavalli A, Petit MA & Fiaccadori F (1990) Cellular immune response to hepatitis B virus-encoded antigens in acute and chronic hepatitis B virus infection. *The Journal of Immunology* 145: 3442 LP – 3449
- Ferris ST, Durai V, Wu R, Theisen DJ, Ward JP, Bern MD, Davidson JT, Bagadia P, Liu T, Briseño CG, Li L, Gillanders WE, Wu GF, Yokoyama WM, Murphy TL,

- Schreiber RD, Murphy KM (2020) cDC1 prime and are licensed by CD4⁺ T cells to induce anti-tumour immunity. *Nature* 584: 624–629
- Ficht X & Iannacone M (2020) Immune surveillance of the liver by T cells. *Sci Immunol* 5(51):eaba2351
- Fumagalli V, Lucia P di, Venzin V, Bono EB, Jordan R, Frey CR, Delaney W, Chisari F v., Guidotti LG & Iannacone M (2020) Serum HBsAg clearance has minimal impact on CD8⁺ T cell responses in mouse models of HBV infection. *Journal of Experimental Medicine* 217(11):e20200298
- Garris CS, Arlauckas SP, Kohler RH, Trefny MP, Garren S, Piot C, Engblom C, Pfirschke C, Siwicki M, Gungabeesoon J, Freeman GJ, Warren SE, Ong S, Browning E, Twitty CG, Pierce RH, Le MH, Algazi AP, Daud AI, Pai SI, Zippelius A, Weissleder R, Pittet MJ (2018) Successful Anti-PD-1 Cancer Immunotherapy Requires T Cell-Dendritic Cell Crosstalk Involving the Cytokines IFN- γ and IL-12. *Immunity* 49: 1148-1161.e7
- Germain RN, Robey EA & Cahalan MD (2012) A Decade of imaging cellular motility and interaction dynamics in the immune system. *Science* 336: 1676–81
- Gerner MY, Casey KA, Kastenmuller W & Germain RN (2017) Dendritic cell and antigen dispersal landscapes regulate T cell immunity. *Journal of Experimental Medicine* 214: 3105–3122
- Gershwin, M. Eric, John M. Vierling and MPM (2007) Liver Immunology: Principles and Practice 6th Edition. *Humana Press*
- Gill US & McCarthy NE (2020) CD4 T cells in hepatitis B virus: “You don’t have to be cytotoxic to work here and help”. *J Hepatol* 72: 9–11
- De Giovanni M, Cutillo V, Giladi A, Sala E, Maganuco CG, Medaglia C, di Lucia P, Bono E, Cristofani C, Consolo E, Giustini L, Fiore A, Eickhoff S, Kastenmüller W, Amit I, Kuka M, Iannacone M (2020) Spatiotemporal regulation of type I interferon

- expression determines the antiviral polarization of CD4⁺ T cells. *Nat Immunol* 21: 321–330
- Goddard S, Youster J, Morgan E & Adams DH (2004) Interleukin-10 Secretion Differentiates Dendritic Cells from Human Liver and Skin. *Am J Pathol* 164(2):511
- Gomez Perdiguero E, Klapproth K, Schulz C, Busch K, Azzoni E, Crozet L, Garner H, Trouillet C, de Bruijn MF, Geissmann F, Rodewald HR (2015) Tissue-resident macrophages originate from yolk-sac-derived erythro-myeloid progenitors. *Nature* 518: 547–551
- Greyer M, Whitney PG, Stock AT, Davey GM, Tebartz C, Bachem A, Mintern JD, Strugnell RA, Turner SJ, Gebhardt T, O'Keeffe M, Heath WR, Bedoui S (2016) T Cell Help Amplifies Innate Signals in CD8⁺ DCs for Optimal CD8⁺ T Cell Priming. *Cell Rep* 14: 586–597
- Guidotti L G, Rochford R, Chung J, Shapiro M, Purcell R & Chisari V F (1999) Viral Clearance Without Destruction of Infected Cells During Acute HBV Infection. *Science* 284(5415):825-9
- Guidotti LG & Chisari F v. (2006) Immunobiology and Pathogenesis of Viral Hepatitis. *Annual Review of Pathology: Mechanisms of Disease* 1: 23–61
- Guidotti LG, Inverso D, Sironi L, di Lucia P, Fioravanti J, Ganzer L, Fiocchi A, Vacca M, Aiolfi R, Sammiceli S, Mainetti M, Cataudella T, Raimondi A, Gonzalez-Aseguinolaza G, Protzer U, Ruggeri ZM, Chisari FV, Isogawa M, Sitia G, Iannaccone M (2015) Immunosurveillance of the liver by intravascular effector CD8⁺ T cells. *Cell* 161: 486–500
- Guidotti LG, Martinez V, Lor Y-T, Rogler CE & Chisari FV (1994) Hepatitis B Virus Nucleocapsid Particles Do Not Cross the Hepatocyte Nuclear Membrane in Transgenic Mice. *J Virol* 68(9):5469-75
- Guidotti LG, Matzke B, Schaller H & Chisari FV (1995) High-level hepatitis B virus replication in transgenic mice. *J Virol* 69: 6158–69

- Herkel J, Jagemann B, Wiegand C, Garcia Lazaro JF, Lueth S, Kanzler S, Blessing M, Schmitt E & Lohse AW (2003) MHC class II-expressing hepatocytes function as antigen-presenting cells and activate specific CD4 T lymphocytes. *Hepatology* 37: 1079–1085
- Holz LE, Warren A, le Couteur DG, Bowen DG & Bertolino P (2010) CD8+ T cell tolerance following antigen recognition on hepatocytes. *J Autoimmun* 34(1):15-22
- Hor JL, Whitney PG, Zaid A, Brooks AG, Heath WR & Mueller SN (2015) Spatiotemporally Distinct Interactions with Dendritic Cell Subsets Facilitates CD4+ and CD8+ T Cell Activation to Localized Viral Infection. *Immunity* 43: 554–565
- Hutin Y, Low-Beer D, Bergeri I, Hess S, Garcia-Calleja JM, Hayashi C, Mozalevskis A, Rinder Stengaard A, Sabin K, Harmanci H, Bulterys M (2017) Viral Hepatitis Strategic Information to Achieve Elimination by 2030: Key Elements for HIV Program Managers. *MIR Public Health Surveill*
- Iannacone M, Andreato F & Guidotti LG (2022) Immunological insights in the treatment of chronic hepatitis B. *Curr Opin Immunol* 77:102207
- Iannacone M & Guidotti LG (2015) Mouse Models of Hepatitis B Virus Pathogenesis. *Cold Spring Harb Perspect Med* 5(11):a021477
- Iannacone M & Guidotti LG (2022) Immunobiology and pathogenesis of hepatitis B virus infection. *Nat Rev Immunol* 22(1):19-32
- Iannacone M, Sitia G, Isogawa M, Marchese P, Castro MG, Lowenstein PR, Chisari FV, Ruggeri ZM & Guidotti LG (2005) Platelets mediate cytotoxic T lymphocyte–induced liver damage. *Nat Med* 11: 1167–1169
- Inverso D & Iannacone M (2016) Spatiotemporal dynamics of effector CD8+ T cell responses within the liver. *J Leukoc Biol* 99: 51–55

- Isogawa M, Chung J, Murata Y, Kakimi K & Chisari F v. (2013) CD40 Activation Rescues Antiviral CD8⁺ T Cells from PD-1-Mediated Exhaustion. *PLoS Pathog* 9(7):e1003490
- Isser A, Silver AB, Pruitt HC, Mass M, Elias EH, Aihara G, Kang S-S, Bachmann N, Chen YY, Leonard EK, Bieler JG, Chaisawangwong W, Choy J, Shannon SR, Gerecht S, Weber JS, Spangler JB, Schneck JP (2022) Nanoparticle-based modulation of CD4⁺ T cell effector and helper functions enhances adoptive immunotherapy. *Nat Commun* 13: 6086
- Janssen EM, Lemmens EE, Wolfe T, Christen U, von Herrath MG & Schoenberger SP (2003) CD4⁺ T cells are required for secondary expansion and memory in CD8⁺ T lymphocytes. *Nature* 421: 852–856
- Jefferies M, Rauff B, Rashid H, Lam T & Rafiq S (2018) Update on global epidemiology of viral hepatitis and preventive strategies. *World J Clin Cases* 6: 589–599
- John Paul Ridge, Francesca Di Rosa & Polly Matzinger (1998) A conditioned dendritic cell can be a temporal bridge between a CD4⁺T-helper and a T-killer cell. *Nature* 393(6684):474-8
- Jung M-C, Diepolder HM, Spengler U, Wierenga EA, Zachoval R, Hoffmann RM, Eichenlaub D, Frosner G, Will H & Pape GR (1995) Activation of a Heterogeneous Hepatitis B (HB) Core and e Antigen-Specific CD4 T-Cell Population during Seroconversion to Anti-HBe and Anti-HBs in Hepatitis B Virus Infection. *J Virol* 69(6):3358-68
- Kaech SM & Ahmed R (2001) Memory CD8⁺ T cell differentiation: Initial antigen encounter triggers a developmental program in naïve cells. *Nat Immunol* 2: 415–422
- Kaech SM & Cui W (2012) Transcriptional control of effector and memory CD8⁺ T cell differentiation. *Nat Rev Immunol* 12(11):749-61
- Karin N (2020) CXCR3 Ligands in Cancer and Autoimmunity, Chemoattraction of Effector T Cells, and Beyond. *Front Immunol* 11:976

- Kiner E, Willie E, Vijaykumar B, Chowdhary K, Schmutz H, Chandler J, Schnell A, Thakore PI, LeGros G, Mostafavi S, Mathis D, Benoist C (2021) Gut CD4⁺ T cell phenotypes are a continuum molded by microbes, not by TH archetypes. *Nat Immunol* 22: 216–228
- Kitano M, Yamazaki C, Takumi A, Ikeno T, Hemmi H, Takahashi N, Shimizu K, Fraser SE, Hoshino K, Kaisho T, Okada T (2016) Imaging of the cross-presenting dendritic cell subsets in the skin-draining lymph node. *Proc Natl Acad Sci U S A* 113: 1044–1049
- Klein I & Crispe IN (2006) Complete differentiation of CD8⁺ T cells activated locally within the transplanted liver. *Journal of Experimental Medicine* 203: 437–447
- Knipe DM & Howley PM (2013) Fields of Virology, 6th Edition *Lippincott Williams & Wilkins*
- Knolle P, Schlaak J, Uhrig A, Kempf P, Meyer Zum Btischenfelde K-H & Gerken G (1995) Human Kupffer cells secrete IL-10 in response to lipopolysaccharide (LPS) challenge. *J Hepatol* 22(2):226-9
- Knolle PA (2014) The liver as a lymphoid organ. *Liver Immunology: Principles and Practice*: 55–64
- Knolle PA, Schmitt E, Jin S, Germann T, Duchmann R, Hegenbarth S, Gerken G & Lohse AW (1999) Induction of Cytokine Production in Naive CD4 T Cells by Antigen-Presenting Murine Liver Sinusoidal Endothelial Cells but Failure to Induce Differentiation Toward T_H1 Cells. *Gastroenterology* 116(6):1428-40
- Ko C, Chakraborty A, Chou WM, Hasreiter J, Wettengel JM, Stadler D, Bester R, Asen T, Zhang K, Wisskirchen K, McKeating JA, Ryu WS, Protzer U (2018) Hepatitis B virus genome recycling and de novo secondary infection events maintain stable cccDNA levels. *J Hepatol* 69: 1231–1241

- Kouskoff V, Signorelli K, Benoist C & Mathis D (1995) Cassette vectors directing expression of T transgenic mice cell receptor genes in transgenic mice. *J Immunol Methods* 180(2):273-80
- Krenkel O & Tacke F (2017) Liver macrophages in tissue homeostasis and disease. *Nat Rev Immunol* 17(5):306-321
- Krishna M (2021) Histological Grading and Staging of Chronic Hepatitis. *Clin Liver Dis (Hoboken)* 17(4):222-226
- Krueger PD, Goldberg MF, Hong SW, Osum KC, Langlois RA, Kotov DI, Dileepan T & Jenkins MK (2021) Two sequential activation modules control the differentiation of protective T helper-1 (Th1) cells. *Immunity* 54: 687-701.e4
- Kruepunga N, Hakvoort TBM, Hikspoors JPJM, Köhler SE & Lamers WH (2019) Anatomy of rodent and human livers: What are the differences? *Biochim Biophys Acta Mol Basis Dis* 1865(5):869-878
- Kudo S, Matsuno K, Ezaki T & Ogawa M (1997) A Novel Migration Pathway for Rat Dendritic Cells from the Blood: Hepatic Sinusoids-Lymph Translocation. *J Exp Med* 185(4):777-84
- Laidlaw BJ, Craft JE & Kaech SM (2016) The multifaceted role of CD4⁺ T cells in CD8⁺ T cell memory. *Nat Rev Immunol* 16(2):102-11
- Laidlaw BJ, Zhang N, Marshall HD, Staron MM, Guan T, Hu Y, Cauley LS, Craft J & Kaech SM (2014) CD4⁺ T Cell Help Guides Formation of CD103⁺ Lung-Resident Memory CD8⁺ T Cells during Influenza Viral Infection. *Immunity* 41: 633–645
- Lampertico P, Agarwal K, Berg T, Buti M, Janssen HLA, Papatheodoridis G, Zoulim F & Tacke F (2017) EASL 2017 Clinical Practice Guidelines on the management of hepatitis B virus infection. *J Hepatol* 67: 370–398
- Lee HW, Lee JS & Ahn SH (2021) Hepatitis B virus cure: Targets and future therapies. *Int J Mol Sci* 22(1):213

- Lee YC, Lu L, Fu F, Li W, Thomson AW, Fung JJ & Qian S (1999) Hepatocytes and Liver Nonparenchymal Cells Induce Apoptosis in Activated T Cells. *Transplant Proc* 31(1-2):784
- Levrero M & Zucman-Rossi J (2016) Mechanisms of HBV-induced hepatocellular carcinoma. *J Hepatol* 64: S84–S101
- Li L, Liu M, Cheng LW, Gao XY, Fu JJ, Kong G, Feng X & Pan XC (2013) HBcAg-Specific IL-21-Producing CD4⁺ T Cells are Associated with Relative Viral Control in Patients with Chronic Hepatitis B. *Scand J Immunol* 78: 439–446
- Li M, Davey GM, Sutherland RM, Kurts C, Lew AM, Hirst C, Carbone FR & Heath WR (2001) Cell-Associated Ovalbumin Is Cross-Presented Much More Efficiently than Soluble Ovalbumin In Vivo. *The Journal of Immunology* 166: 6099–6103
- Limmer A, Ohl J, Kurts C, Ljunggren H-G, Reiss Y, Groettrup M, Momburg F, Arnold B & Knolle PA (2000) Efficient presentation of exogenous antigen by liver endothelial cells to CD8⁺ T cells results in antigen-specific T-cell tolerance. *Nat Med* 6: 1348–1354
- Lohse AW, Knolle PA, Bilo K, Uhrig A, Waldmann C, Ibe M, Schmitt E, Gerken G, Meyer Zum Büschenfelde KH (1996) Antigen-Presenting Function and B7 Expression of Murine Sinusoidal Endothelial Cells and Kupffer Cells. *Gastroenterology* 110(4):1175-81
- Lucas M, Kallies A & Klenerman P (2017) The immune system of the liver: 50 years of strangeness. *Clin Transl Immunology* 6: e164
- Luckheeram RV, Zhou R, Verma AD & Xia B (2012) CD4⁺T cells: Differentiation and functions. *Clin Dev Immunol* 2012:925135
- Madsen L, Labrecque N, Engberg J, Dierich A, Svejgaard A, Benoist C, Mathis D & Fugger L (1999) Mice lacking all conventional MHC class II genes. *Proc Natl Acad Sci USA* 96(18):10338-43

- Maini MK & Pallett LJ (2018) Defective T-cell immunity in hepatitis B virus infection: why therapeutic vaccination needs a helping hand. *Lancet Gastroenterol Hepatol* 3: 192–202
- Mancini M, Hadchouel M, Tiollais P & Michel M-L (1998) T Cells After DNA-Based Immunization-Secreting γ Transgenic Mouse Model by IFN-Expression in a Hepatitis B Surface Antigen Regulation of Hepatitis B Virus mRNA expression in a hepatitis B surface antigen transgenic mouse model by IFN-gamma-secreting T cells after DNA-based immunization. *J Immunol* 161(10):5564-70
- Melssen M & Slingluff CL (2017) Vaccines targeting helper T cells for cancer immunotherapy. *Curr Opin Immunol* 47:85-92
- Mercado R, Vijh S, Allen SE, Kerksiek K, Pilip IM & Pamer EG (2000) Early Programming of T Cell Populations Responding to Bacterial Infection. *The Journal of Immunology* 165: 6833–6839
- Mitchison NA & O'Malley C (1987) Three-cell-type clusters of T cells with antigen-presenting cells best explain the epitope linkage and noncognate requirements of the in vivo cytolytic response. *Eur J Immunol* 17(11):1579-83
- Mombaerts P, Iacomini J, Johnson RS, Herrup K, Tonegawa S & Papaioannou VE (1992) RAG-1-deficient mice have no mature B and T lymphocytes. *Cell* 68: 869–877
- Moshkani S, Chiale C, Lang SM, Rose JK, Robek MD & Ou J-HJ (2019) A Highly Attenuated Vesicular Stomatitis Virus-Based Vaccine Platform Controls Hepatitis B Virus Replication in Mouse Models of Hepatitis B. *Journal of Virology* 93(5):e01586-18
- Mueller SN & Ahmed R High antigen levels are the cause of T cell exhaustion during chronic viral infection. *Proc Natl Acad Sci U S A* 106(21):8623-8
- Mühlbauer M, Fleck M, Schütz C, Weiss T, Froh M, Blank C, Schölmerich J & Hellerbrand C (2006) PD-L1 is induced in hepatocytes by viral infection and by interferon and mediates T cell apoptosis. *J Hepatol* 45: 520–528

- Muntjewerff EM, Meesters LD & van den Bogaart G (2020) Antigen Cross-Presentation by Macrophages. *Front Immunol* 11:1276
- Naggie S & Lok AS (2021) New Therapeutics for Hepatitis B: The Road to Cure. *Annu Rev Med* 72:93-105
- Ni Y, Lempp FA, Mehrle S, Nkongolo S, Kaufman C, Fälth M, Stindt J, Königer C, Nassal M, Kubitz R, Sülthmann H, Urban S (2014) Hepatitis B and D viruses exploit sodium taurocholate co-transporting polypeptide for species-specific entry into hepatocytes. *Gastroenterology* 146: 1070–1083
- Novy P, Quigley M, Huang X & Yang Y (2007) CD4 T Cells Are Required for CD8 T Cell Survival during Both Primary and Memory Recall Responses. *The Journal of Immunology* 179: 8243–8251
- Palacios R (1982) Concanavalin A triggers T lymphocytes by directly interacting with their receptors for activation. *J Immunol* 128(1):337-42
- Pasqual G, Chudnovskiy A, Tas JMJ, Agudelo M, Schweitzer LD, Cui A, Hacohen N & Victora GD (2018) Monitoring T cell-dendritic cell interactions *in vivo* by intercellular enzymatic labelling. *Nature* 553: 496–500
- Pastore G, Carraro M, Pettini E, Nolfi E, Medaglini D & Ciabattini A (2019) Optimized Protocol for the Detection of Multifunctional Epitope-Specific CD4(+) T Cells Combining MHC-II Tetramer and Intracellular Cytokine Staining Technologies. *Front Immunol* 10: 2304
- Penna A, Artini M, Cavalli A, Levrero M, Bertoletti A, Pilli M, Chisari F v., Rehermann B, del Prete G, Fiaccadori F, Ferrari C (1996) Long-lasting memory T cell responses following self-limited acute hepatitis B. *Journal of Clinical Investigation* 98: 1185–1194
- Penna A, del Prete G, Cavalli A, Bertoletti A, D’Elios MM, Sorrentino R, D’Amato M, Boni C, Pilli M, Fiaccadori F, Ferrari C (1997) Predominant T-helper 1 cytokine

- profile of hepatitis B virus nucleocapsid-specific T cells in acute self-limited hepatitis B. *Hepatology* 25: 1022–1027
- Peperzak V, Xiao Y, Veraar EAM & Borst J (2010) CD27 sustains survival of CTLs in virus-infected nonlymphoid tissue in mice by inducing autocrine IL-2 production. *Journal of Clinical Investigation* 120: 168–178
- Piergiovanni M, Bianchi E, Capitani G, Li Piani I, Ganzer L, Guidotti LG, Iannacone M & Dubini G (2017) Microcirculation in the murine liver: a computational fluid dynamic model based on 3D reconstruction from in vivo microscopy. *J Biomech* 63: 125–134
- Pishesha N, Harmand TJ & Ploegh HL (2022) A guide to antigen processing and presentation. *Nat Rev Immunol* 22(12):751-764
- Pol JG, Caudana P, Paillet J, Piaggio E & Kroemer G (2020) Effects of interleukin-2 in immunostimulation and immunosuppression. *Journal of Experimental Medicine* 217(1):e20191247
- Prilliman KR, Lemmens EE, Palioungas G, Wolfe TG, Allison JP, Sharpe AH & Schoenberger SP (2002) Cutting Edge: A Crucial Role for B7-CD28 in Transmitting T Help from APC to CTL. *The Journal of Immunology* 169: 4094–4097
- Racanelli V & Rehermann B (2006) The liver as an immunological organ. *Hepatology* 3(2 Suppl 1):S54-62
- Raeber ME, Rosalia RA, Schmid D, Karakus U & Boyman O (2020) Interleukin-2 signals converge in a lymphoid-dendritic cell pathway that promotes anticancer immunity. *Sci Trans Med* 12(561):eaba5464
- Salti SM, Hammelev EM, Grewal JL, Reddy ST, Zemple SJ, Grossman WJ, Grayson MH & Verbsky JW (2011) Granzyme B Regulates Antiviral CD8 + T Cell Responses . *The Journal of Immunology* 187: 6301–6309

- Scott CL, Zheng F, De Baetselier P, Martens L, Saeys Y, De Prijck S, Lippens S, Abels C, Schoonoghe S, Raes G, Devoogdt N, Lambrecht BN, Beschin A, Williams M (2016) Bone marrow-derived monocytes give rise to self-renewing and fully differentiated Kupffer cells. *Nat Commun* 7:10321
- Seeger C & Mason WS (2015) Molecular biology of hepatitis B virus infection. *Virology* 479-480:672-86
- Sharma S, Carballo M, Feld JJ & Janssen HLA Immigration and viral hepatitis. *J Hepatol* 63(2):515-22
- Shedlock DJ & Shen H (2003) Requirement for CD4 T cell help in generating functional CD8 T cell memory. *Science (1979)* 300: 337–339
- Shi YH & Shi CH (2009) Molecular characteristics and stages of chronic hepatitis B virus infection. *World J Gastroenterol* 15(25):3099-105
- Shigwang Qian C, Demetris AJ, Murase N, Rao AS, Fung JJ & Starzl TE Murine Liver Allograft Transplantation: Tolerance and Donor Cell Chimerism. *Hepatology* 19(4):916-24
- Shuai Z, Leung MWY, He X, Zhang W, Yang G, Leung PSC & Gershwin ME (2016) Adaptive immunity in the liver. *Cell Mol Immunol* 13: 354–368
- De Simone G, Andreato F, Bleriot C, Fumagalli V, Laura C, Garcia-Manteiga JM, Di Lucia P, Gilotto S, Ficht X, De Ponti FF, Bono EB, Giustini L, Ambrosi G, Mainetti M, Zordan P, Bénéchet AP, Ravà M, Chakarov S, Moalli F, Bajenoff M, Guidotti LG, Ginhoux F, Iannacone M (2021) Identification of a Kupffer cell subset capable of reverting the T cell dysfunction induced by hepatocellular priming. *Immunity* 54: 2089-2100.e8
- Sitia G, Iannacone M, Aiolfi R, Isogawa M, van Rooijen N, Scozzesi C, Bianchi ME, von Andrian UH, Chisari F v. & Guidotti LG (2011) Kupffer cells hasten resolution of liver immunopathology in mouse models of viral hepatitis. *PLoS Pathog* 7(6):e1002061

- Smith CM, Wilson NS, Waithman J, Villadangos JA, Carbone FR, Heath WR & Belz GT (2004) Cognate CD4⁺ T cell licensing of dendritic cells in CD8⁺ T cell immunity. *Nat Immunol* 5: 1143–1148
- Smyk-Pearson S, Tester IA, Klarquist J, Palmer BE, Pawlotsky J-M, Golden-Mason L & Rosen HR (2008) Spontaneous Recovery in Acute Human Hepatitis C Virus Infection: Functional T-Cell Thresholds and Relative Importance of CD4 Help. *J Virol* 82: 1827–1837
- Sobecki M, Mrouj K, Camasses A, Parisis N, Nicolas E, Llères D, Gerbe F, Prieto S, Krasinska L, David A, Eguren M, Birling MC, Urbach S, Hem S, Déjardin J, Malumbres M, Jay P, Dulic V, Lafontaine DLj, Feil R, Fisher D (2016) The cell proliferation antigen Ki-67 organises heterochromatin. *Elife* 5:e13722
- Sojka DK, Bruniquel D, Schwartz RH & Singh NJ (2004) IL-2 Secretion by CD4⁺ T Cells In Vivo Is Rapid, Transient, and Influenced by TCR-Specific Competition. *The Journal of Immunology* 172: 6136–6143
- Steffan A-M, Gendrault J-L, Mccuskey RS, Mccuskey PA & Kim A (1986) Phagocytosis, An Unrecognized Property of Murine Endothelial Liver Cells. *Hepatology* 6(5):830-6
- Van Stipdonk MJB, Hardenberg G, Bijker MS, Lemmens EE, Droin NM, Green DR & Schoenberger SP (2003) Dynamic programming of CD8⁺ lymphocyte responses. *Nat Immunol* 4: 361–365
- Van Stipdonk MJB, Lemmens EE & Schoenberger SP (2001) Naïve CTLs require a single brief period of antigenic stimulation for clonal expansion and differentiation. *Nat Immunol* 2(5):423-9
- Summers SA, Steinmetz OM, Li M, Kausman JY, Semple T, Edgton KL, Borza DB, Braley H, Holdsworth SR & Kitching AR (2009) Th1 and Th17 cells induce proliferative glomerulonephritis. *Journal of the American Society of Nephrology* 20: 2518–2524

- Sun JC & Bevan MJ (2003) Defective CD8 T cell memory following acute infection without CD4 T cell help. *Science (1979)* 300: 339–342
- Suslov A, Boldanova T, Wang X, Wieland S & Heim MH (2018) Hepatitis B Virus Does Not Interfere With Innate Immune Responses in the Human Liver. *Gastroenterology* 154: 1778–1790
- T Jake L (2009) Hepatitis B: The Virus and Disease. *Hepatology* 49: S13–S21
- Tan W, Xia J, Dan Y, Li M, Lin S, Pan X, Wang H, Tang Y, Liu N, Tan S, *et al* (2018) Genome-wide association study identifies HLA-DR variants conferring risk of HBV-related acute-on-chronic liver failure. *Gut* 67: 757 LP – 766
- Thimme R, Wieland S, Steiger C, Ghayeb J, Reimann KA, Purcell RH & Chisari F v (2003) CD8(+) T cells mediate viral clearance and disease pathogenesis during acute hepatitis B virus infection. *J Virol* 77: 68–76
- Tiegs G & Lohse AW (2010) Immune tolerance: What is unique about the liver. *J Autoimmun* 34: 1–6
- Tuzlak S, Dejean AS, Iannaccone M, Quintana FJ, Waisman A, Ginhoux F, Korn T & Becher B (2021) Repositioning TH cell polarization from single cytokines to complex help. *Nat Immunol* 22(10):1210-1217
- Upkar S. Gill & Neil E. McCarthy (2020) CD4 T cells in hepatitis B virus: ““You don’t have to be cytotoxic to work here and help””. *J Hepatol* 72: 9–11
- Urbani S, Amadei B, Fisicaro P, Tola D, Orlandini A, Sacchelli L, Mori C, Missale G & Ferrari C (2006) Outcome of acute hepatitis C is related to virus-specific CD4 function and maturation of antiviral memory CD8 responses. *Hepatology* 44: 126–139
- Urbani S, Boni C, Amadei B, Fisicaro P, Cerioni S, Valli MA, Missale G & Ferrari C (2005) Acute phase HBV-specific T cell responses associated with HBV persistence after HBV/HCV coinfection. *Hepatology* 41: 826–831

- Venkatakrishnan B & Zlotnick A (2016) The Structural Biology of Hepatitis B Virus: Form and Function. *Annu Rev Virol* 3: 429–451
- Volker Benseler (2007) The liver: a special case in transplantation tolerance. *Semin Liver Dis* 27(2):194-213
- Wang H, Luo H, Wan X, Fu X, Mao Q, Xiang X, Zhou Y, He W, Zhang J, Guo Y, *et al* (2020) TNF- α /IFN- γ profile of HBV-specific CD4 T cells is associated with liver damage and viral clearance in chronic HBV infection. *J Hepatol* 72: 45–56
- Warren A, le Couteur DG, Fraser R, Bowen DG, McCaughan GW & Bertolino P (2006) T lymphocytes interact with hepatocytes through fenestrations in murine liver sinusoidal endothelial cells. *Hepatology* 44: 1182–1190
- Westhorpe CLV, Ursula Norman M, Hall P, Snelgrove SL, Finsterbusch M, Li A, Lo C, Tan ZH, Li S, Nilsson SK, Kitching AR, Hickey MJ (2018) Effector CD4⁺ T cells recognize intravascular antigen presented by patrolling monocytes. *Nat Commun* 9(1):747
- Wilson EB & Livingstone AM (2008) Cutting Edge: CD4 + T Cell-Derived IL-2 Is Essential for Help-Dependent Primary CD8 + T Cell Responses . *The Journal of Immunology* 181: 7445–7448
- Wong YC, Tay SS, Mccaughan GW, Bowen DG & Bertolino P (2015) Immune outcomes in the liver: Is CD8 T cell fate determined by the environment? *J Hepatol* 63(4):1005-14
- Wu R & Murphy KM (2022) DCs at the center of help: Origins and evolution of the three-cell-type hypothesis. *Journal of Experimental Medicine* 219(7):e20211519
- Wuensch SA, Spahn J & Crispe IN (2010) Direct, help-independent priming of CD8⁺ T cells by adeno-associated virus-transduced hepatocytes. *Hepatology* 52: 1068–1077

- Yan H, Zhong G, Xu G, He W, Jing Z, Gao Z, Huang Y, Qi Y, Peng B, Wang H, *et al* (2012) Sodium taurocholate cotransporting polypeptide is a functional receptor for human hepatitis B and D virus. *Elife* 1: 1–28
- Yang PL, Althage A, Chung J, Maier H, Wieland S, Isogawa M & Chisari FV (2010) Immune effectors required for hepatitis B virus clearance. *Proc Natl Acad Sci U S A* 107: 798–802
- You Q, Cheng L, Kedl RM & Ju C (2008) Mechanism of T cell tolerance induction by murine hepatic Kupffer cells. *Hepatology* 48: 978–990
- Yuen MF, Chen DS, Dusheiko GM, Janssen HLA, Lau DTY, Locarnini SA, Peters MG & Lai CL (2018) Hepatitis B virus infection. *Nat Rev Dis Primers* 4:18035
- Zhou L, Chong MMW & Littman DR (2009) Plasticity of CD4+ T Cell Lineage Differentiation. *Immunity* 30(5):646-55
- Zhou Z, Xu MJ & Gao B (2016) Hepatocytes: A key cell type for innate immunity. *Cell Mol Immunol* 13: 301–315
- Zhu J, Yamane H & Paul WE (2010) Differentiation of Effector CD4 T Cell Populations. *Annu Rev Immunol* 28: 445–489

